Dissertation

submitted to the

Combined Faculties for the Natural Sciences and for Mathematics

of the Ruperto-Carola University of Heidelberg, Germany

for the degree of

Doctor of Natural Sciences

presented by

Aleksandar Stojic, dipl. biolog

born in Uzice, Serbia

Oral Examination:

10.03.2016.

Characterisation of axonal degeneration during autoimmune optic neuritis

Referees: **Dr. Anne Régnier-Vigouroux**

Prof. Dr. Ricarda Diem

Acknowledgements

First of all I would like to express my deepest gratitude to Prof. Dr. Ricarda Diem for giving me the opportunity to perform my thesis work in her lab. I would like to thank her for providing excellent working conditions and for her continuous support and encouragement during past years.

I would like to thank the following people for their contribution to this thesis:

Prof. Dr. Anne Régnier-Vigouroux for her support and constructive comments regarding my thesis both as my official supervisor and as a member of my thesis advisory committee. I would also like to thank Prof. Dr. med. Andreas Draguhn for being a part of my advisory committee and for his useful comments regarding my thesis.

Dr. Sarah Williams and Dr. Richard Fairless for numerous scientific discussions and their valuable advice regarding experimental designs.

Dr. Dorit Hoffmann, for being a great friend and invaluable colleague; for helping me to fit in and showing me the ropes; for our lengthy scientific discussions and, of course, amazing cycling tours.

Marika Dienes for her excellent technical assistance; for helping me to adapt to life in Germany and for numerous German to English translations and mostly, for being a great company in the lab.

To all the people with whom I have interacted during my thesis work, both in Homburg and in Heidelberg. I would particularly like to thank Dr. Claudia Pitzer and Barbara Kurpiers from the Interdisciplinary Neurobehavioral Core in Heidelberg for their support in the animal work.

To all my friends and family who have always supported me throughout my studies.

To Jovana Bojcevski, for being *"sve šta đaku treba"*.

Abstract

The model of experimental autoimmune encephalomyelitis (EAE) is the most common model for studying pathological processes in multiple sclerosis (MS). In a variant of this model, induced by immunisation of Brown Norway rats with myelin oligodendrocyte glycoprotein (MOG), pathological mechanisms reflects many aspects of MS, observed by the activation of adaptive, innate and humoral immune response (Fairless et al., 2012). In addition to "the classical EAE pathology" characterised by inflammatory demyelination of the spinal cord, these animals also develop autoimmune optic neuritis (AON). The dynamics of the pathological events in AON are similar to those observed in acute optic neuritis in patients, a common early manifestation of MS. Taking this into consideration, the aim of this study was to provide a detailed characterisation of the optic nerve pathology during the course of AON in order to gain further insight into mechanisms of axonal injury and visual dysfunction associated with optic neuritis.

Testing of visual functions by recording of visual evoked potentials (VEPs) revealed a decrease in visual acuity already during the induction phase of AON. During this phase, major pathological changes (such as inflammatory demyelination and axonal loss) in the optic nerve were still absent. However detailed examination of the optic nerve revealed that the observed visual impairment is timed with disruptions in axonal domains involved in saltatory conduction of action potentials (nodes of Ranvier and paranodes). Further evidence of stress was detected in both compartments of paranodal axon-glia junctions observed by alternation in the axonal neurofilament cytoskeleton and increased production of alpha B-crystallin (cryαB), a heat shock protein involved in oligodendrocyte stress response. Observed signs of stress were more prominent in the optic nerve head (ONH), the area which was also characterised by increased numbers of activated microglia and the deposition of autoantibodies. Following the onset of the clinical disease phase animals were characterised with greater impairments in visual functions and with the presence of inflammatory demyelination and increasing signs of axonal injury in optic nerves. In addition to increased expression of cryαB, a portion of oligodendrocytes associated with inflammatory lesions underwent the process of apoptosis.

In order to investigate the origins of observed axonal and oligodendroglial stress and their contribution to disrupted axon-glia paranodal junction in the late induction phase, two different approaches were made. Firstly, the oligodendrocyte compartment was targeted by auto-antibodies through the transfer of sera from MOG-immunised into naïve animals. This led to deposition of auto-antibodies and the presence of oligodendrocyte stress in the ONH, in a similar manner to that observed in the late induction phase. Secondly, a model of primary retinal injury by intravitreal

injection of glutamate was performed and successfully mimicked aspects of the retinal pathology characteristic of the early induction phase. This led to the presence of axonal stress in optic nerves in the similar extent to one observed in the late induction phase of AON. In both instances, the observed signs of stress did not translate across the paranodal axon-glia junction to the other compartment. This suggests that axons and oligodendrocytes could be targeted independently during the induction phase of AON by mechanisms involving a primary retinal insult and the actions of the humoral immune response.

Collectively, the pathological image observed in the induction phase of AON shares great similarities with the pathology of normal-appearing white matter in MS, in terms of both axonal and oligodendroglial stress, further suggesting that the model of AON is useful for studying early degenerative processes in MS. Observed disruptions of axonal domains in the induction phase of AON could serves as a structural correlate of impairment of visual functions. These findings could be relevant for human studies, particularly in a sub-set of MS patients which are characterised by impaired visual functions in the absence of clinically-defined optic neuritis.

Zusammenfassung

Experimentelle autoimmune Enzephalomyelitis (EAE) ist das am häufigsten verwendete Tiermodell zur Untersuchung pathologischer Prozesse in Multipler Sklerose (MS). Eine Variante dieses Modells ist die Immunisierung von braunen Norweger Ratten mit Myelin Oligodendrozyten Glykoprotein (MOG). Die pathologischen Mechanismen der MOG induzierten EAE spiegeln viele Aspekte der MS wieder, unter anderem die Aktivierung der adaptiven, angeborenen und humoralen Immunantwort (Fairless et al., 2012). Zusätzlich zur “klassischen EAE Pathologie”, die durch inflammatorische Demyelinisierung des Rückenmarks gekennzeichnet ist, einwickeln die Tiere außerdem autoimmune Optikusneuritis (AON). Die pathologischen Ereignisse der AON sind denen der akuten Optikusneuritis ähnlich, einer häufigen initialen klinischen Manifestation von MS. Ziel dieser Studie war daher die detailierte Charakterisierung der pathologischen Veränderungen des optischen Nervs im Verlauf der AON um weitergehende Einblicke in die Mechanismen der axonalen Verletzung und visuellen Dysfunktion, die mit der Optikusneuritis assoziiert sind, zu gewinnen.

Die Untersuchung der Funktionsfähigkeit des visuellen Systems mittels Ableitung visuell evozierter Potentiale (VEP) zeigte, dass die Sehschärfe bereits in der Induktionsphase der AON reduziert war. In dieser Phase konnten weder Inflammation noch Demyeliniserung des optischen Nervs beobachtet werden. Detailierte Untersuchungen des optischen Nervs zeigten allerdings, dass die Abnahme der

Sehschärfe zeitlich mit Veränderungen der Ranvier'schen Schnürringe und paranodalen Bereiche korrelierte. Diese Bereiche sind in die saltatorische Erregungsleitung von Aktionspotentialen entlang der Axone involviert. Weitere Anzeichen für Stress konnten in beiden Kompartimenten der paranodalen axo-glialen Verbindungen beobachtet werden: Veränderungen des neurofilamentösen Zytoskeletts in den Axonen und erhöhte Produktion von alpha B-crystallin (cryαB) , einem Hitzeschockprotein das in die Stressantwort von Oligodendrozyten involviert ist. Am Sehnervenkopf, der durch erhöhte Aktivierung von Mikroglia und Ablagerung von Autoantikörpern charakterisiert ist, waren die oben beschriebenen Veränderungen deutlicher ausgeprägt als im restlichen optischen Nerv.

In der klinischen Phase der EAE war die Funktionsfähigkeit des visuellen Systems deutlicher stärker eingeschränkt und inflammatorische Demyelinisierung sowie erhöhte Anzeichen axonaler Verletzungen konnten im optischen Nerv beobachtet werden. Zusätzlich zur erhöhten Expression von cryαB konnte auch Apoptose von Oligodendrozyten im Bereich der inflammatorischen Läsionen nachgewiesen werden.

Um die Ursprünge des beobachteten axonalen und oligodendroglialen Stresses und ihren Beitrag zu den gestörten paranodalen axo-glialen Verbindungen in der späten Induktionsphase genauer zu untersuchen, wurden zwei verschiedene Herangehensweisen ausgewählt. Zum einen wurden das Oligodendrozyten Kompartiment mittels Serumtransfer aus MOG-immunisierten in naive Tiere mit Autoantikörpern gezielt anvisiert. Dies führte zur Ablagerung von Autoantikörpern und Stress der Oligodendrozyten im Sehnervenkopf, wie er auch in der späten Induktionsphase beobachtet werden konnte. Zum Anderen wurde ein Modell gewählt in dem eine primäre, retinale Verletzung durch intravitreale Injektion von Glutamat ausgelöst wurde. Mit diesem Modell konnte eine retinale Pathologie ausgelöst werden, die Aspekte der Pathologie in der frühen Induktionsphase nachahmte. Dies führte zu axonalem Stress im optischen Nerv, der im Umfang mit dem in der späten Induktionsphase der AON vergleichbar war.

In beiden Fällen konnte keine Beeinträchtigung des jeweils anderen Kompartiments beobachtet werden. Dies deutet darauf hin, dass Axone und Oligodendrozyten in der Induktionphase der AON möglicherweise unabhängig voneinander Ziel verschiedener Mechanismen sind in denen primäre retinale Schädigung und die humoralen Immunantwort eine Rolle spielen.

Zusammenfassend lässt sich sagen, dass die pathologischen Vorgänge, die in der Induktionsphase der AON beobachtet werden konnten, viele Gemeinsamkeiten mit Veränderungen in der normal erscheinenden weißen Substanz in MS haben. Dies betrifft sowohl axonalen wie auch oligodendroglialen Stress und legt nahe, dass das vorliegende Tiermodell hilfreich sein kann frühe

neurodegenerative Veränderungen in MS zu untersuchen. Die beobachtete Schädigung der axonalen Domänen in der Induktionsphase der AON könnte als strukturelles Korrelat für die reduzierte Funktionsfähigkeit des visuellen Systems dienen. Diese Erkenntnis könnte auch in Humanstudien von Bedeutung sein, insbesondere in einer Untergruppe von MS Patienten die durch reduzierte visuelle Funktion in Abwesenheit einer klinisch definierten Optikusneuritis charakterisiert ist.

List of publications

Fairless R., Williams S.K., Hoffmann D.B., Stojic A., Hochmeister S., Schmitz F., Storch M.K. and Diem R. (2012) Preclinical retinal neurodegeneration in a model of multiple sclerosis. J Neurosci. 32(16):5585-97.

Not related to the thesis:

Williams S.K., Maier O., Fischer R., Fairless R., Hochmeister S., Stojic A., Pick L., Haar D., Musiol S., Storch M.K., Pfizenmaier K. and Diem R. (2014) Antibody-mediated inhibition of TNFR1 attenuates disease in a mouse model of multiple sclerosis. PLoS One 9(2):e90117.

Table of contents

1 Introduction

1.1 Multiple sclerosis

Multiple sclerosis (MS) is a chronic inflammatory disease of the central nervous system (CNS). It is considered to be the leading non-traumatic cause of neurologic disability in young adults in the western world with an average disease onset between the ages of 20 and 40 (Hauser and Oksenberg, 2006). The disease presents with a complex pathology including inflammatory demyelination of the white and grey matter accompanied by axonal loss and neurodegeneration.

Historically, MS was first described as a distinct disease of the CNS in the 19th century by a French neurologist Jean-Martin Charcot (Charcot M., 1868). He characterised plaque-like lesions in a post-mortem brain of a young woman and termed them *"la sclerose en plaques"*. He was also the first physician to diagnose MS in a living patient using a diagnostic criteria consisting of nystagmus, intention tremor, and scanning speech (Pearce JMS., 2005).

Although there has been significant scientific progress in the field of MS research and management, especially in the last three decades, there are still many unanswered questions when it comes to determining the cause and the mechanisms underlying the pathology of MS. Neurodegeneration is an important component of the pathology correlating with the decline in cognitive and neurological abilities in patients. It is also recognized to be an early event in the disease course starting already during the initial, clinically silent, phase. This highlights the importance of discovering the causality and mechanisms of neurodegeneration, particularly within the early stages of the disease, which could lead to development of neuroprotective and regenerative strategies for better management of MS.

1.2 Epidemiology and genetics of MS

There are approximately 2.3 million people living with MS across the planet (Atlas of MS, 2008). Results from epidemiological studies show an uneven world-wide geographical distribution. Areas with the highest prevalence and incidence of MS are found in the northern hemisphere, mainly in North America and northern Europe (Figure 1.1).

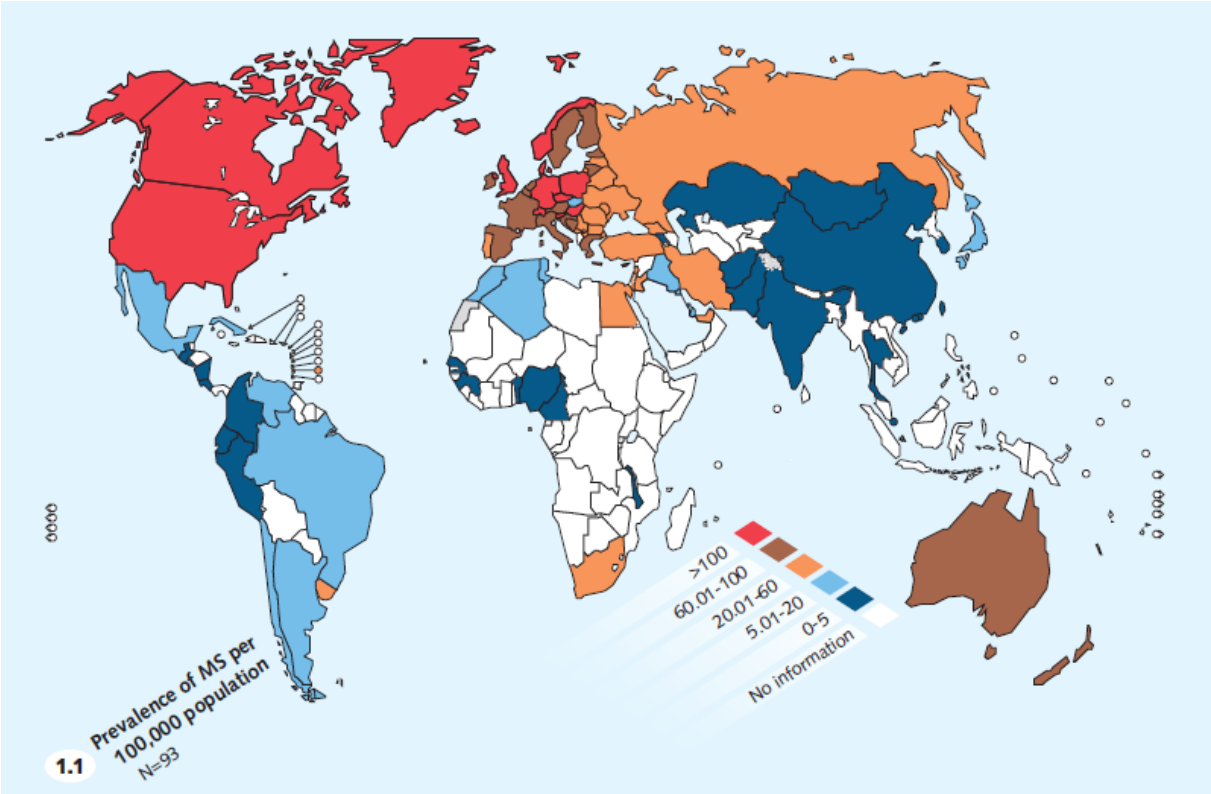

Figure 1.1 Distribution of MS prevalence. This map of MS prevalence was created based on date collected from more than 100 countries in a study led by the World Health Organization (WHO) and Multiple Sclerosis International Federation (MSIF). Image taken from Atlas: Multiple Sclerosis Resources in the World 2008.

There is also an uneven distribution of the disease between the genders. The overall incidence rate for females is 3.6 cases per 100,000 people per year and 2 cases per 100,000 people per year in males (Alonso and Hernan 2008).

The evidence for a genetic component of MS comes from prevalence studies in different ethnic groups and familial occurrence. It is recognized that the risk for developing the disease rises with the increase of genetic material shared between family members. The risk for developing MS in adopted relatives is at the general population level (0% genetic identity, 0.2% risk). The risk found in siblings of MS patients is estimated to be between 3-5% and is the same for dizygotic twins and in cases of one parent being affected with the disease (in all cases there is 50% genetic sharing). The risk rises to 6-10% if both parents were affected with the disease (50% sharing of genetic material with each parent). The highest risk is found in studies with monozygotic twins (100% genetic sharing) where the recurrence risk for MS is estimated at 34% (Ebers et al., 2000; Dyment et al., 2004).

When it comes to ethnicity, it has been observed that people of northern European ancestry have an increased risk for developing MS when compared to other ethnic groups residing at the same latitude

(Pugliatti et al., 2002; Koch-Henriksen and Sørensen, 2010). This phenomenon is also reflected in migration studies. It was shown that in ethnic groups with a low risk for MS, the risk level remains low even after migration to an area with high risk (Detels et al., 1977; Gale and Martyn, 1995; O' Gorman et al., 2012).

The majority of specific genetic variants associated with an increased risk for MS are found to be related to inflammatory pathways with the strongest association being identified in the human leukocyte antigen (HLA) class II domain (Sawcer et al., 2011). The presence of the HLA-DRB1*1501 haplotype in the HLA class II domain, identified by Sawcer et al. as the strongest risk correlate, correlated with more severe inflammation and pathology of the spinal cord when compared with the post mortem tissue from MS patients negative for this haplotype (DeLuca et al., 2013). Other genetic variants with strong MS susceptibility were found in genes encoding for the interleukin-2 receptor α (IL2RA) and interleukin-7 receptor α (IL7RA; Hafler et al., 2007 The International Multiple Sclerosis Genetics Consortium).

The environment also plays a significant role in the prevalence of MS. Interestingly, migration studies, previously used to strengthen the hypothesis of genetics on MS susceptibility, can also be applied when examining the effect of the environment. A decrease in the rate of disease was found in migrants coming from an area with an overall larger risk for MS to an area of lower risk (Gale and Martyn, 1995). This illustrates the complexity of the disease aetiology pointing to interplay between different genetic and environmental factors. The strongest environmental factors implicated in MS susceptibility are found to be vitamin D (Munger et al., 2006; Soilu-Hanninen et al., 2005), smoking (Hedstorm et al., 2009) and Epstein Bar virus (EBV) infection (Haahr et al., 2004; Lucas et al., 2011; Sundqvist et al., 2012).

1.3 Clinical course of MS

Patients suffering from MS present with a variety of neurological symptoms indicative of pathology in various regions of the CNS including cerebrum, cerebellum, the optic nerve, brainstem and the spinal cord (Compston and Coles, 2008). These symptoms vary in their severity, duration and frequency creating different sub-populations between patients. To ensure a proper diagnosis and disease management, a universally applicable classification of different disease subtypes is needed. In 1996 a committee of experts from the US National Multiple Sclerosis Society (NMSS) suggested a classification of the disease course into four different types based on the recurrence and progression of neurological symptoms (Lublin et al., 1996):

- Relapsing-remitting (RRMS)
- Secondary progressive (SPMS)
- Primary progressive (PPMS) and
- Progressive-relapsing MS (PRMS).

In 2013, this committee, now joined by The European Committee of Treatment and Research in MS and The MS Phenotype Group, revisited the original classification, taking into consideration advances in research, diagnosis and management of MS. The progressive-relapsing subtype was dropped due to its overlap with other disease course subtypes, and two additional subtypes were introduced: clinically isolated syndrome (CIS) and radiologically isolated syndrome (RIS; Lublin et al., 2014).

CIS is the first presentation of the disease. It is characterised by a single clinical episode which presents symptoms indicative of inflammatory demyelination. For CIS to be recognized as clinically defined MS (CDMS) it has to fulfil the McDonald criteria for diagnosis of MS which are dissemination in time and space (Polman et al., 2011). The conversion rate from CIS to CDMS is at 60-70% within 20 years following the initial attack (Fisniku et al., 2008; Miller et al., 2012). A recent large, multi-centre study was performed by Kuhle and colleagues, examining the effect of clinical and biochemical marker status on the prediction of conversion from CIS to CDMS. They found an association between the oligoclonal bands status, magnetic resonance imaging (MRI) lesion load, the age of the patients, vitamin D levels and the conversion rate risks (Kuhle et al., 2015).

Radiologically isolated syndrome presents as a demyelinated lesion in the white matter which has no manifestation of neurological symptoms (Okuda et al., 2009; Lublin et al., 2014). These, usually accidental, findings can be indicative of an early disease onset and such patients should be monitored for the possible appearance of first clinical signs of MS.

Relapsing-remitting MS is the most common form of the disease. Approximately 85% of MS patients start the disease with this course with a mean age of onset at 30 years (Trapp and Nave, 2008). Patients are presented with episodes of neurological disability with periods of remission in-between. Neurological symptoms develop rapidly, within hours or days, and recede within weeks from their onset (Miller and Leary, 2007; Trapp and Nave, 2008). In the initial stage of the disease, remissions are usually complete – i.e. neurological symptoms fully resolve. Relapses are unpredictable with an average rate of approximately 1.5 per year (Compston and Coles, 2008). As the disease progresses, the remission phase shortens, relapses become more frequent, full recovery is impaired and patients advance into secondary progressive MS. Within 25 years, 90% of the patients with RRMS typically

advance to SPMS (Image 1.2). This phase is characterised as a steady increase in progression of irreversible neurological disability (Noseworthey et al., 2000; Trapp and Nave, 2008).

Around 15% of patients are characterised with a progressive form of MS (PPMS) from the onset of the disease, with rare events of incomplete remissions (Image 2). The average onset of the disease in these patients is at 40 years, 10 years later than in ones diagnosed with RRMS. Neurological symptoms in PPMS tend to develop slower over time and are connected with impaired motor control rather than with sensory responses (Miller and Leary, 2007). Therefore, PPMS is characterised more as a spinal disease, although symptoms pointing to the involvement of other CNS compartments can also occur (Compston and Coles, 2008). While in RRMS patients the female to male ratio is 2-3:1, reflecting the general gender ratio in all MS patients, in patients with PPMS the distribution of the disease between genders is even (Tremlett et al., 2005; Miller and Leary, 2007).

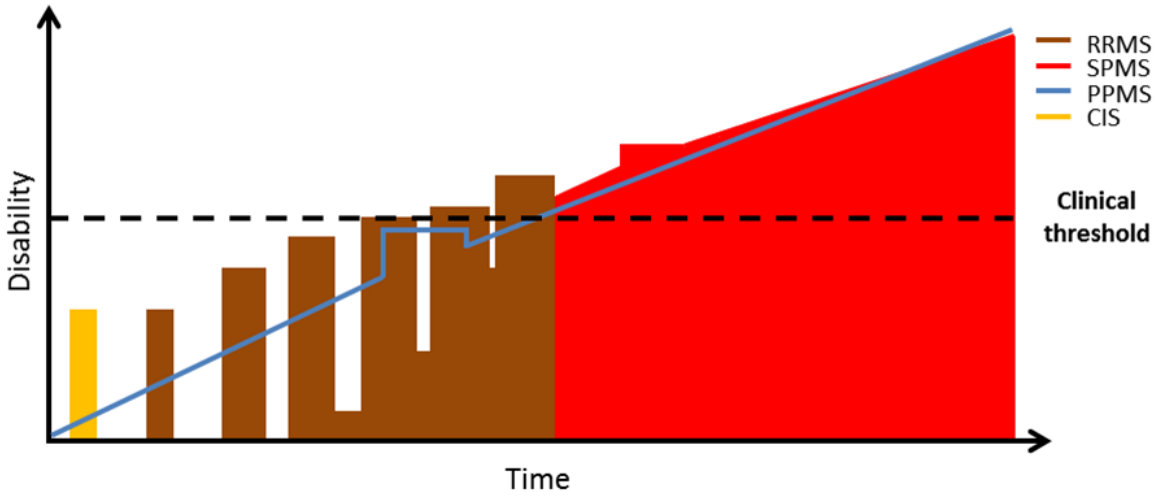

Figure 1.2 MS disease course. Graphical representation of different disease courses in MS. Horizontal dashed line represents the clinical threshold of neurological disability for transition from RRMS to SPMS.

Axonal loss is found to be a major correlate of permanent disability in MS patients (Bjartmar et al., 2000). Reduced axonal densities, as well as axonal swellings and transections indicative of axonal pathology, are found in both actively demyelinating inflammatory lesions and in chronic lesions (Ferguson et al., 1997; Trapp et al., 1998). The former type of lesion is more prominent in RRMS while the latter is found to be a pathological hallmark of progressive forms of MS. Despite the extensive axonal loss observed in active lesions (Trapp et al., 1998), neurological symptoms are still reversible in RRMS patients. This is owed to the great capacity for neuronal compensation in the human CNS suggesting that permanent disability only occurs once a certain threshold of axonal loss is crossed. This phenomenon can also be observed in other neurodegenerative diseases, such as

Parkinson's disease, where clinical manifestation of the disease is observed only when patients lose over 70% of dopaminergic axons (Trapp et al., 1999; Dutta and Trapp, 2011). Functional activation of other non-affected regions of the cortex can compensate for the loss of function due to the axonal loss within lesions. This concept was observed with functional MRI imaging in MS patients (Buckle, 2005; Pantano et al., 2006).

The transient nature of neurological deficits in RRMS suggests that disability in these patients have a different origin compared to progressive forms of MS. MRI in these patients shows gadolinium-enriched lesions indicative of blood-brain barrier (BBB) disruption which leads to infiltration of immune cells and lesion formation. The oedematous nature of these lesions is thought to be a major cause of neurological deficits by blocking the conduction of action potentials (APs) in axons as a result of demyelination and production of reactive species by inflammatory cells. In addition, ongoing demyelination causes the disruption of axonal domains involved in the propagation of APs (discussed in chapter 1.7.2). With time, the ability of the neuron to conduct impulses is partly regained through a re-organization of voltage-gated Na^+ channels along the demyelinated axons. As the inflammation resolves, remyelination can sometimes occur, restoring neuronal conduction of action potentials. The concept that inflammation is the driving force of disability in RRMS is confirmed by the success of anti-inflammatory therapies to prevent relapses and to decrease MRI lesion load (Paty and Li, 1993; Trapp and Nave, 2008). As the disease progresses, patients usually develop SPMS. At this stage the burden of axonal loss presumably oversteps the mechanisms of compensation and patients are presented with increasing and permanent disability. New forming MRI lesions are rarely observed and patients do not respond anymore to anti-inflammatory therapies (Dutta and Trapp, 2011).

Although the average clinical onset of the disease in PPMS is observed at a later age, the disability threshold is reached at the same time as in RRMS (Confavreux and Vukusic, 2006). This might suggest that similar disease processes begin at the same average age in both patients with PPMS and RRMS. However, in PPMS these processes are not clinically visible until they cross the clinical threshold beyond which compensatory mechanisms are no longer sufficient, whereas in RRMS they are also not clinically visible (with only the effects of transient inflammatory attacks on clinical manifestations being observed) until the conversion to SPMS. The use of anti-inflammatory therapy is ineffective in patients with PPMS (Miller and Leary, 2007) pointing to more chronic degenerative events, similar to ones in SPMS. When the accumulated neurodegeneration oversteps the capacity for compensation both groups transit into the state of permanent disability.

1.4 Pathology of MS

The original concept of MS pathology was viewed as the presence of focal white matter lesions with a demyelinated core, partially preserved axons and signs of reactive gliosis (Lassmann, 2005; Lassmann and van Horssen, 2011). Since the second half of the 20th century, and due to major advances in both immuno/histopathology and in vivo imaging, this concept has been significantly altered. The discovery of lesions in the grey matter (both cortical and deep grey matter), diffuse lesions and altered morphology of the so called "normal appearing white matter" (NAWM) point to the complexity of pathological mechanisms involved in MS. Also, the lesions themselves are very dynamic structures where different morphologies and cellular compositions have been observed in respect to the stage of their development. The utilisation of in vitro studies and animal models, mainly Experimental Autoimmune Encephalomyelitis (EAE), has helped in the discovery of many of the immunological and pathological mechanisms that are involved in MS.

1.4.1 Inflammation

Inflammation is a major component of MS pathology. The degree of inflammation varies throughout the disease course and between different subtypes of the disease. Generally, the progressive forms of the disease tend to have lower numbers of gadolinium-positive MRI lesions (indicative of BBB breakdown) compared to the relapsing-remitting stage. Also, in the late stages of progressive forms of the disease, the level of inflammation declines to one observed in age-matched controls (Frischer et al., 2009). The main driving force of inflammation in MS is the infiltration of lymphocytes and monocytes through the BBB. Activated lymphocytes cross the BBB via a series of steps involving interaction between different molecules expressed on endothelial cells and on lymphocytes themselves. The most important of these are cellular adhesion molecules (CAMs) expressed on endothelial cells (mainly ICAM-1 and VCAM-1) and their ligands expressed on activated leukocytes – αLβ2 (LFA-1) and α4β1 (VLA-4; Engelhardt, 2006; Owens et al., 2008; Larochelle et al., 2011). Increased expression of both CAMs (Sobel et al., 1990; Washington et al., 1994) and their ligands (Bö et al., 1996) have been observed in MS lesions. This mechanism has lent itself to the development of a promising drug strategy, namely the targeting of extravasation of immune cells into the CNS. Natalizumab, a monoclonal antibody against VLA-4, is one such drug that has been shown to be effective for the treatment of RRMS. It lowers the numbers of circulating lymphocytes, the $CD4^+$ to $CD8^+$ ratio in the CNS and the total number of $CD4^+$ cells in the brain (Stüve et al., 2006; del Pilar Martin et al., 2008; Ellwardt and Zipp, 2014).

1.4.1.1 T cells

The most dominant type of lymphocytes associated with MS inflammation are T cells. Of these, major histocompatibility complex (MHC) class I-restricted $CD8^+$ T cells are the dominant subtype within lesions where they undergo clonal expansion (Babbe et al., 2000; Neumann et al., 2002). All nucleated cells express MHC class I on their membranes as a part of an important mechanism for the response against intracellular pathogens such as viruses and bacteria. Once antigens are presented via the MHC class I receptor to cytotoxic $CD8^+$ T cells, these T cells produce proinflammatory cytokines (TNFα and INFγ) as well as perforins and granzymes that can induce a cascade which leads to the death of target cells. Upregulation of MHC class I can be observed in all cell types within MS lesions including neurons, oligodendrocytes, astrocytes and microglia (Gobin et al., 2001; Höftberger et al., 2004). Since oligodendrocytes and neurons are known not to express the co-stimulatory molecules needed for the priming of $CD8^+$ T cells (Odeberg et al., 2005), the mechanisms of their activation and potential disruptive roles are speculative and still remain unknown (Friese and Fugger, 2005). Nevertheless, there is a strong correlation between the presence of $CD8^+$ T cells and axonal damage in MS lesions (Bitsch et al., 2000; Kuhlmann et al., 2002; Neumann et al., 2002; Gilmore et al., 2009).

MHC class II-restricted $CD4^+$ T cells are mainly found in the meninges and perivascular spaces of the MS-affected CNS (Lassmann and van Horssen, 2011). The importance of $CD4^+$ T cells for pathogenesis in autoinflammatory conditions comes primarily from the EAE model. It has been shown that mice lacking functional $CD4^+$ T cells (but not $CD8^+$ T cells) were unable to develop EAE upon immunization with myelin oligodendrocyte glycoprotein (MOG; Leuenberger et al., 2013). Some of the proposed mechanisms of $CD4^+$ T cell-mediated pathology include antigen-independent interactions with neurons (Nitsch et al., 2004) and activation of tumour necrosis factor-related apoptosis-inducing ligand (TRAIL) pathway (Vogt et al., 2009). Also, indirect evidence for the role of $CD4^+$ T cells in MS pathology comes from treatment with anti-inflammatory drugs, such as Natalizumab, that reduce the $CD4^+$ T cell population in the CNS and have a positive modulatory effect on the disease course.

Another subset of $CD4^+$ cells which secrete interleukin-17A/E (Th17 cells) has been implicated in the pathology of autoimmune disorders including MS and its animal models (Steinman, 2007; Siffrin et al., 2010). Mechanisms of their actions include the secretion of proinflammatory cytokines, recruitment of neutrophils into the CNS and direct neuronal damage (Jadidi-Niaragh and Mirshafiey, 2011). A further subset of $CD4^+$ regulatory T cells, $CD4^+CD25^+Foxp3^+$ cells (Tregs), which have immunosuppressive properties are also found to have a role in the inflammatory process in MS (Zozulya and Wiendl, 2008). A decrease in Foxp3 levels were found in T cells isolated from the blood of MS patients (Huan et al., 2005). Also, a decreased in vitro proliferation of Tregs isolated from

RRMS patients upon T cell receptor stimulation was observed. Furthermore, the impaired proliferative capacity of these cells correlated with disease severity (Carbone et al., 2014).

1.4.1.2 B cells

B cells are thought to play an important role in the pathogenesis of MS. Post-mortem tissue analysis revealed the presence of B cells throughout the MS-affected CNS – in active demyelinating white matter (Lucchinetti et al., 2000; Henderson et al., 2009), perivascular spaces (Henderson et al., 2009) and the meninges (Serafini et al., 2004; Magliozzi et al., 2007; Howell et al., 2011; Lovato et al., 2011). Also, the presence of oligoclonal bands (indicating the presence of antibodies) in the cerebrospinal fluid (CSF) is the most consistent immunological finding as it is found in more than 95% of patients with MS (Freedman et al., 2005; Disanto et al., 2012). Although these antibodies are a striking feature and are also found to be associated with a risk for conversion from CIS to CDMS (Masjuan et al., 2006; Ignacio et al., 2010), they have been shown not to be reactive against myelin components (Owens et al., 2009) which raises a question regarding their involvement in the disease pathogenesis. In contrast, antibodies isolated directly from MS lesion tissue showed reactivity against myelin basic protein (MBP; Warren et al., 1993) and MOG (O'Connor et al., 2005). Deposition of IgG and complement is found to be one of the characteristics of an active demyelinating MS lesion (Lucchinetti et al., 2000), where there is a strong link between antibody deposition in CNS tissue and their reactivity towards myelin components.

Although the role of auto-antibodies is inconclusive, there is a strong evidence for antibody-independent B cell roles in MS pathogenesis. B cells are able to process and present antigens to T cells and to provide the co-stimulatory signals necessary for their activation. In addition, they are able to produce a variety of cytokines which can modulate the T cell response (Lund and Randall, 2010). The importance of this (antibody-independent) role of B cell in the process of inflammation is highlighted by the positive effects of Rituximab in RRMS. This is a monoclonal antibody against CD20, a transmembrane protein presented exclusively on B cells in all stages of their development apart from the initial stage (pro B cells) and plasma cells (antibody-secreting B cells; Stashenko et al., 1980). Clinical trials with Rituximab in RRMS resulted in a decrease in new gadolinium-enhanced MRI lesions and the proportion of patients with relapses. The depletion of circulating $CD20^+$ cells was near to complete without an effect on the oligoclonal band status (Cross et al., 2006; Hauser et al., 2008; Petereit et al., 2008; Naismith et al., 2010).

1.4.1.3 Microglia/macrophages

The most abundant inflammatory cells in MS lesions are monocyte-derived macrophages and residential microglial cells (Brück et al., 1995; Lucchinetti et al., 2000; Haider et al., 2014). These cell types share great similarities in their physiological and pathophysiological functions (Prinz et al., 2014) and were originally thought be of the same lineage. It is now recognized that the microglial population is derived from a yolk-sac progenitor and populate the early developing CNS (Ginhoux et al., 2013; Kierdorf et al., 2013), whereas CNS-specific monocyte/macrophages originate from bone marrow-derived hematopoietic stem cells and reside within perivascular spaces (Abbott et al., 2010), meninges and the choroid plexus (Chinnery et al., 2010; Dragunow 2013). The main physiological function of these cells (particularly residential microglia) is the maintenance of CNS homeostasis. They show remarkable plasticity and are able to respond rapidly to disruptions in tissue homeostasis (Prinz et al., 2014). In the MS-affected CNS, they are responsible for orchestrating the overall inflammatory process within lesions, directing degenerative insults on myelin/axons, and phagocytosis of cellular (myelin) debris. Additionally, they also have roles during the regenerative process where they stimulate the differentiation of oligodendrocyte progenitor cells (OPCs) and promote remyelination. These actions are put into effect through the production of a variety of cytokines, chemokines, free radicals, and trophic factors.

Activated microglia and macrophages are found in all MS lesions irrespective of their type and status. Nodules of MHC class II-positive microglia are also found in areas of the CNS with completely preserved myelin but signs of oligodendrocyte stress (De Groot et al., 2001). These areas, called “early or preactive lesions” are proposed to be an initial step in the formation of new lesions. The presence of activated microglia/macrophages correlates with the extent of axonal injury in MS lesions (Ferguson et al., 1997; Trapp et al., 1998; Kornek et al., 2000; Bjartmar et al., 2001). Also, in active lesions, microglia/macrophages are loaded with phagocytised components of myelin and axons (Brück et al., 1995; Lucchinetti et al., 2000). These cells are found to be positive for classical proinflammatory markers for such as MHC II and iNOS (Boyle and McGeer, 1990; Haider et al., 2014). The expression of MHC class II molecules together with co-stimulatory molecules on microglia/macrophages (Simone et al., 1995) underlines their potential role in the activation of lymphocytes.

1.4.2 Pathology of MS lesions

Researchers have attempted to classify the diverse array of lesions according to their location (white vs grey matter), state of activity (early, active or chronic), and patterns of demyelination and inflammation.

1.4.2.1 White matter lesions

White matter lesions are the most prominent feature of RRMS and are characterised by extensive demyelination, axonal loss and inflammation. Careful immuno-histological analysis of the tissue distal to the lesion can reveal subtle abnormalities. These fully myelinated areas, called *NAWM*, are lacking peripheral inflammatory infiltrates but are characterised by diffuse, activated microglia (Zeis et al., 2008; Howell et al., 2010; Moll et al., 2011), and are associated with signs of axonal (Howell et al., 2010) and oligodendroglial stress (Zeis et al., 2009; Cunnea et al., 2011).

Preactive lesions are similar to NAWM since they are still myelinated and lacking in peripheral inflammatory infiltrates, but are characterised by the presence of MHC II-positive microglia clusters (De Groot et al., 2001). Oligodendrocytes have been reported to show signs of stress identified through an upregulation of the small heat-shock protein, αB-crystallin (cryαB; Bajramovic et al., 1997). Apart from its anti-apoptotic role in oligodendrocytes, this protein, when secreted, can exert immunomodulatory properties on activated microglia in vitro (van Noort et al., 2013). Although the term “preactive lesion” would suggest that these lesions regularly progress into active demyelinating lesions this is usually not the case. Larger numbers of preactive compared to active lesions are observed in the MS CNS suggesting that much of the microglial inflammation is resolved without progressing further (van der Valk and Amor, 2009).

The most prominent feature of an *active MS lesion* is demyelination often accompanied with the destruction of oligodendrocytes (Brück et al., 2005). Axonal count is decreased and the presence of swollen, transected axons positive for amyloid precursor protein (APP) and non-phosphorylated neurofilaments (identified with the antibody SMI32) is indicative of their state of stress (Trapp et al., 1998; Kornek et al., 2000). Phagocytic macrophages and microglia are the most dominant population of inflammatory cells in these lesions and contain ingested components of both myelin (Brück et al., 1995; van der Goes et al., 2005) and axons (Huizinga et al., 2012). In addition, the presence of T cells, B cells and deposition of IgG and complement within the lesion is detected. Upon detailed histopathological examination of the MS tissue, a further classification into four distinct patterns of

active lesions was suggested on the basis of different immuno-pathological mechanisms (Lucchinetti et al., 2000).

Pattern I and *II* lesions share great similarities with one marked distinction. These lesions are centred on small veins and have a well-defined edge. Demyelination is characterised with an even loss of different myelin components with variable loss of oligodendrocytes in the active lesion centre. Inflammation consists of many phagocytic macrophages but also T cells and B cells. With the resolution of the inflammation (in their chronic states) these lesions are characterised by partial remyelination observed by thinner myelin sheets and increased numbers of oligodendrocytes in the inactive lesion centre. The main distinction between these two patterns is the involvement of humoral immunity in the pathology of pattern II lesions. Within this lesion pattern, a marked deposition of IgG and complement can be observed in the areas of active demyelination.

Pattern III lesions are not centred on inflamed vessels and are characterised by a diffuse, ill-defined lesion border spreading into surrounding periplaque white matter. The inflammation profile of this lesion type consists of activated microglia/macrophages and T cells. Demyelination is characterised by preferential loss of a single myelin component, the myelin-associated glycoprotein (MAG), with the preservation of others such as MBP, proteolipid protein (PLP) and cyclic-nucleotide phosphodiesterase (CNP) in partly damaged myelin sheets. The preferential loss of MAG, a protein expressed in the innermost layer of the myelin sheet, is considered to be an early event in different pathological settings which are primarily targeting oligodendrocytes. This concept has been termed as “dying-back oligodendropathy” and it can also be observed in progressive multifocal leukoencephalopathy (Itoyama et al., 1982), experimental models with toxic oligodendrocyte damage (Ludwin et al., 1981) and in virus-induced demyelination (also targeting oligodendrocytes; Rodriguez, 1995). Pattern III lesions are characterised by the marked presence of apoptotic oligodendrocytes and an overall reduction in their numbers.

Pattern IV lesions were exclusively found in patients with PPMS. Most of their lesion characteristics resemble those found in pattern I lesions. Pattern IV lesions have well defined edges and are centred on inflamed vessels. Inflammatory infiltrates consist of T cells and macrophages. Demyelination is characterised with an even loss of different myelin components and extensive loss of oligodendrocytes which can be also detected in the periplaque area. Extensive loss of oligodendrocytes can be observed in both pattern III and IV lesion. This could be the reason for the absence of remyelination in the later stages of these lesions as opposed to pattern I and II where the presence of remyelination coincides with high numbers of oligodendrocytes in the inactive lesion centre.

With time, active lesions progress into a *chronic* state, where the centre is completely demyelinated and macrophages are re-distributed to the rim of the lesion. Finally, chronic active lesions progress into an *inactive* state characterised by a sclerotic morphology. Macrophages and lymphocytes are rarely present at this stage, and the centre of the lesion becomes hypocellular with a strong astrocytic gliosis (Kipp et al. 2012).

1.4.2.2 Grey matter lesions

Despite early reports of cortical demyelination (Brownell and Hughes, 1962; Lumsden, 1970), very little attention was focused on the grey matter pathology in MS, primarily due to the inability of routine MRI and histopathological investigations to recognize such events (Sharma et al., 2001; Trapp and Nave, 2008). The reason for this lies with the fact that the BBB is not largely compromised in such a lesion and the extent of peripheral immune infiltrates is smaller when compared to active lesions in the white matter (Peterson et al., 2001; Bö et al., 2003). Regardless of this, grey matter lesions are omnipresent (in both cortex and deep grey matter) and associated with both RR and progressive disease courses. They are an early event in the RRMS course (Lucchinetti et al., 2011), in certain cases appearing prior to detection of white matter abnormalities (Popescu et al., 2011). With progression of the disease, the lesion load in the grey matter accumulates, being very prominent in late SP- and PPMS, and correlates with the progression of disability (Vercellino et al., 2005; Calabrese et al., 2012; Honce, 2013). In fact, at such late disease stages, the lesion load in the grey matter is shown to exceed that present in the white matter (Kutzelnigg and Lassmann, 2005; Gilmore et al., 2008). The majority of grey matter lesions are associated with the cortex and subcortical area (Peterson et al., 2001), but they are also frequently found in the deep grey matter, including the thalamus, putamen, caudate nucleus and the spinal cord (Gilmore at al., 2008; Vercellino et al., 2009; Haider et al., 2014).

Although the inflammation in the grey matter is not as pronounced as that observed in white matter lesions, the composition of peripheral inflammatory infiltrates is found to be similar. Demyelination in early grey matter lesions in RRMS is associated with the presence of phagocytic macrophages (Gilmore et al., 2009; Haider et al., 2014) whereas they are rarely present in the chronic lesions of SPMS (Howell et al., 2011).

Meningeal inflammation seems to play a major role in the disease progression since patients with extensive inflammation in the meninges, and therefore greater grey matter damage, are found to have a more progressive disease course (Magliozzi et al., 2010; Howell et al., 2011; Calabrese et al., 2013). Both macrophages and lymphocytes are detected in the inflamed meninges. The most striking

inflammatory feature is the presence of $CD20^+$ B cell follicle-like structures that were associated with increased cortical demyelination and atrophy. Interestingly, a gradient of neurodegeneration was observed with more pronounced neuronal loss in the layers close to the meninges (Magliozzi et al., 2010). This finding points to the possible role for soluble cytotoxic factors in neurodegeneration in MS.

The activation of residential microglial cells is widespread and is the most dominant phenomenon in grey matter pathology (Peterson et al., 2001; Vercellino et al., 2009; Haider et al., 2014; Calabrese et al., 2015). The numbers of activated microglia correlate with both the degree of meningeal inflammation (Howell et al., 2011) and the extent of axonal and dendritic pathology (Peterson et al., 2001). Although there are evidences for the role of microglia in both demyelination (Gray et al., 2008) and glutamate-mediated damage (Vercellino et al., 2007), it still has to be determined whether the activation of these cells is an initiating event in the grey matter pathology or if their role is more protective and activation is a consequence of lymphocyte/macrophage driven inflammation (Calabrese et al., 2015).

Although the concept of grey matter lesions has emerged only in the last two decades, its importance in the MS disease course is great. The observed neurodegeneration, both in the cortex and in the deep grey matter, correlates highly with both irreversible progression of disability (Huitinga et al., 2004; Neema et al., 2009) and impairment in cognitive functions (Bakshi et al., 2000; Houtchens et al., 2007) in MS patients.

Overall, the pathology of MS is characterised by great heterogeneity, observed both in the lesion topology and pathological mechanisms underlying their development. Lesions are observed both in white and grey matter and are characterised by different extents of inflammation and tissue destruction. Although inflammatory demyelination, driven by infiltration of lymphocytes and monocytes, is the most striking feature of MS pathology there is accumulating evidence of both neuronal and oligodendroglial pathology in the absence of such inflammation. This is particularly observed in the NAWM and the grey matter where the presence of cellular stress correlates with the activation of residential microglia suggesting their impotence in the pathology of MS.

1.5 Optic neuritis

The optic nerves are one of twelve pairs of cranial nerves, but unlike the others, they are considered part of the CNS. They are comprised of the myelinated axons of retinal ganglion cells (RGCs), whose cell bodies reside in the innermost layer of the retina. The initial segments of theses axons, which are

residing in the retina, are unmyelinated and comprise the retinal nerve fibre layer (RNFL). Upon exiting the eye, axons become myelinated by oligodendrocytes (Figure 1.3). Optic nerves meet at the optic chiasm where the majority of the axons decussate and proceed towards the lateral geniculate nucleus (LGN). Throughout their lengths, nerves are covered with meninges that are continuous with that encasing the CNS. Projections from the LGN form the optic radiations which terminate in the primary visual cortex of the brain (Kolappan et al., 2009).

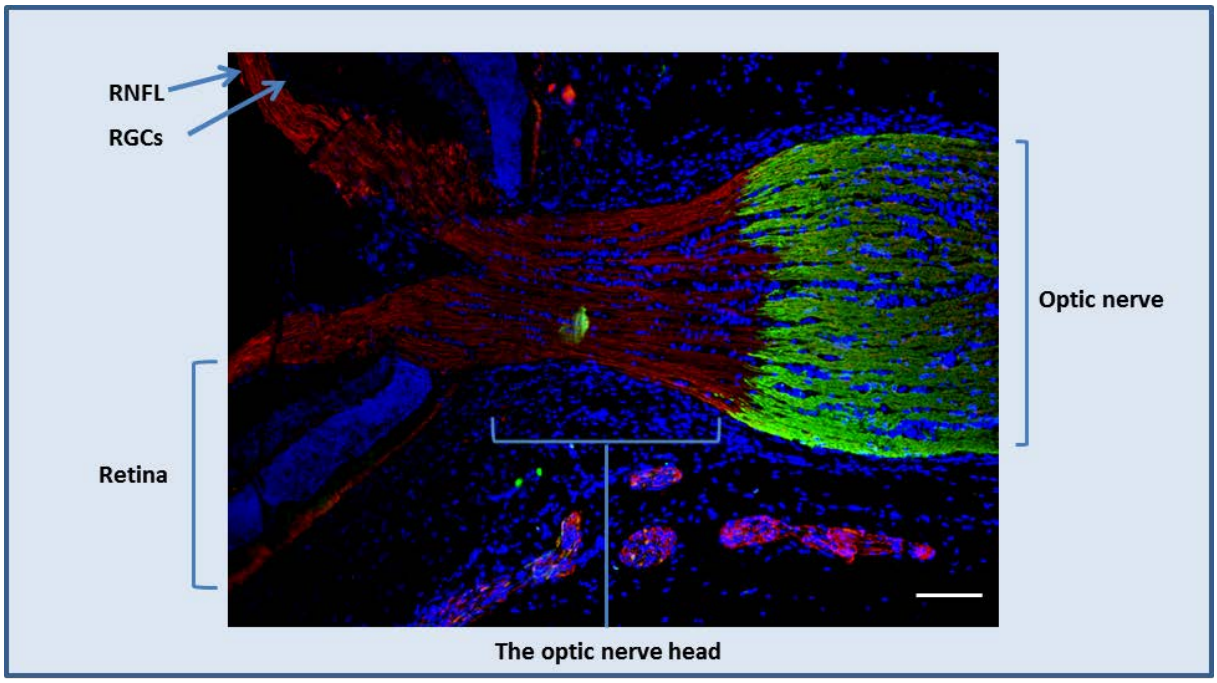

Figure 1.3 The optic nerve. Example image of the initial segment of the rat optic nerve stained with antibodies against neurofilaments for axons (SMI32, red) and MBP for the myelin sheath (green). Cell nuclei were stained with DAPI (blue). Upon exiting the eye, RGCs axons are still unmyelinated in the region of the optic nerve head. Scale bar 100 µm.

Optic neuritis is an inflammatory demyelination of the optic nerve. It is characterised by a loss of vision, ipsilateral eye pain and dyschromatopsia (an inability to perceive colours). It is usually presented unilaterally (only one eye affected) which makes it tougher for the patient to recognize disturbance in vision. Visual loss usually develops within several hours to days, but it usually takes several weeks for the inflammation to resolve and for visual functions to be restored (Toosy et al., 2014). With time, a recurrence of symptoms it is not uncommon (Optic Neuritis Study Group, 2008; Kolappan et al., 2009).

There are different forms of optic neuritis, which vary in manifestation, severity of pathology and aetiology. Typically, optic neuritis is associated with MS or CIS with a risk of conversion to CDMS (Beck et al., 2003; Toosy et al., 2014) and as such will be further discussed.

Acute, unilateral optic neuritis is the first presenting syndrome in 15-20% of patients with MS and it occurs in 50% at some point during the disease course (Wikstorm et al., 1980; Foroozan et al., 2002; Beck et al., 2003; Arnold, 2005). An increased risk for developing CDMS was found in patients presenting with optic neuritis and one or more MRI lesions when compared to patients with optic neuritis alone (72 % vs. 25% probability for MS; Optic Neuritis Study Group, 2008). An increased risk for developing optic neuritis is common in populations with an overall increased risk for MS, with a higher incidence in females (Optic Neuritis Study Group, 1991; MacDonald et al., 2000) and in people living at higher latitudes or of northern European ancestry (Jin et al., 2000). An increased risk for optic neuritis was also observed within individuals carrying a certain HLA haplotype (Frederiksen et al., 1997).

The pathological mechanisms of acute optic neuritis are thought to be similar to ones observed in MS. Considering the rarity of histopathological reports of the visual tract from patients (Green et al., 2010), much of the evidence comes from employing different animal models. Optic neuritis can be modelled with certain variants of EAE (Fairless et al., 2012; Lidster et al., 2013) or by chemically induced demyelination of the optic nerve (You et al., 2011). In patients, the pathology can be monitored with the use of different non-invasive imaging methods (Martinez-Lapiscina et al., 2014). By employing different MRI techniques it was shown that with the onset of acute optic neuritis, affected nerves are swollen (indicative of inflammatory oedema). In the acute phase, a decrease of visual acuity comes from the conduction block caused by oedematous demyelinating lesions. Commonly, visual acuity is restored following an episode of acute optic neuritis, as is confirmed by measurement of visual evoked potentials (VEPs). However, upon follow-up MRI, the affected nerves can still show signs of atrophy (indicative of the axonal loss). Thus, compensatory mechanisms are presumably helping to restore visual acuity. The breakdown of the BBB can also be observed in acute optic neuritis by gadolinium enhancement visualised by MRI. This finding also correlated with the loss of visual acuity (Youl et al., 1991), further strengthening the argument for inflammation-induced conduction block in the optic nerves.

Optical Coherence Tomography (OCT) is an ultrasound-like imaging technique that relies on low coherence interferometry to generate cross-sectional images of the retina with high resolution (1-15 µm; Fujimoto et al., 2000). Using OCT it is possible to discern different retinal layers and to study their morphology in vivo following an insult. Both the RNFL thickness (giving a readout of RGC axonal density) and the macular volume (giving an estimate of RGC survival) can be measured. In several

studies, following an episode of acute optic neuritis both parameters were found to be decreased and to correlate with impairment in the visual function (Trip et al., 2005; Costello et al., 2006) pointing to both axonal and neuronal loss in the retina. Interestingly there are reports of RNFL thinning in the eyes of MS patients that were asymptomatic for optic neuritis (Fisher et al., 2006; Pulicken et al., 2007; Henderson et al., 2008). In addition, a large-scale histopathological study of retinae obtained at autopsy from MS patients irrespective of prior optic neuritis showed loss of RGCs and other neurons in the inner nuclear layer accompanied by activation of microglial cells (Green et al., 2010). These observations of axonal and neuronal loss in the myelin-deficient retina (lacking both myelin and myelin producing cells) provide evidence for the potential of a myelin-independent neuronal pathology in MS.

1.6 Experimental autoimmune encephalomyelitis

With advances in imaging techniques, lesion dynamics in patients can be regularly monitored throughout the course of the disease. Although this provides valuable information regarding the status of the BBB integrity, degree of demyelination and overall tissue atrophy, it fails to provide information regarding the pathogenesis on a cellular and molecular level. Studies of pathological mechanisms in MS are mainly restricted to post-mortem autopsy tissue and relatively rare biopsy samples. Information obtained in such a manner provides only a pathological image, frozen in time, providing merely clues for mechanisms of its development. This hurdle can be overstepped by the use of appropriate animal models that can reproduce different aspects of the complex pathology of MS.

Experimental autoimmune encephalomyelitis (EAE) is an animal model of CNS inflammation. It is characterized by the presence of inflammatory demyelinating lesions which closely resemble those found in MS, both in their localization and pathology (Storch et al., 1998; Kornek et al., 2000). Disease symptoms include sensory loss, optic neuritis, difficulties with coordination and balance (ataxia), muscle weakness and spasms. This model dates back to the early 20th century when it was discovered that rabbits injected with human spinal cord homogenate develop paralysis (Koritschoner and Schweinburg, 1925). Since then, this model has been further investigated and developed, becoming the major animal model in MS research.

EAE can be induced in a variety of species including rodents and primates. The use of different species comes with different benefits. Use of primates (rhesus monkeys or macaques) brings the results closer to human studies, whereas rodent models are more practical and give more

experimental possibilities. Rodents have larger litters, shorter generations and are easier to house. Also, most of the available tools in molecular biology are designed to be used in rodents, particularly the manipulation of genetic material used to dissect molecular pathways involved in the disease course.

EAE is induced by sensitization of the animal with a CNS-derived antigen. There are three different methods of induction:

- *Actively induced EAE* is performed by immunization with an antigen emulsified in an adjuvant. The range of antigens used varies from CNS homogenates, purified myelin, and single myelin proteins/peptides (MBP, PLP, MOG, etc.) to neuronal antigens (neurofilaments, neurofascin 186, contactin-2, etc.). The use of different antigens in different species will produce distinct disease phenotypes (Krishnamoorthy and Wekerle, 2009). The most common adjuvant used is Freund's adjuvant supplemented with heat-inactivated mycobacteria. In some strains of mice, additional injection of *Bordetella pertussis*-derived toxin is necessary for induction of EAE as it facilitates the break-down of the BBB (Linthicum et al., 1982) and is involved in expansion of autoreactive T cells (Hofstetter et al., 2002). Choosing the right antigen for EAE induction has proved to be a crucial step in EAE induction. For example, Brown Norway (BN) rats were thought to be an EAE-resistant strain after the failure to develop pathology upon immunization with guinea pig CNS homogenate and isolated myelin components excluding MOG. This was contributed to their specific genetic background since both Lewis rats and a cross-breed of Lewis and BN rats developed EAE upon immunization (Gasser et al., 1973). Later experiments showed that the, formerly labelled EAE-resistant, BN strain is highly susceptible to immunization with MOG (Stefferl et al., 1999), which produces an extensive antibody-mediated demyelinating pathology. While MOG induces a strong humoral response in rats, the specific H-2b MHC haplotype in C57BL/6 mice restricts this ability (Bourquin et al., 2003). These mice, boosted with a pertussis-toxin injection, develop a chronic EAE course with T cell mediated pathology (Mendel et al., 1995).

- *Adoptive transfer EAE (AT-EAE)* is induced by the transfer of auto-reactive T cells. These cells are isolated from the lymph nodes of an EAE-primed animal, activated *in vitro*, and injected into a naïve donor. The origin of this model dates back to 1960 when Paterson managed to induce *"allergic encephalomyelitis"* with the injection of lymph node cells from previously sensitized rats into naïve rats (Paterson, 1960). Twenty years later, Ben-Nun and colleagues established a protocol for expansion of antigen specific T cells and successfully induced AT-EAE with MBP-specific T cells (Ben-Nun et al., 1981). This model is useful for studying the

role of T cells in the context of autoimmune diseases. *In vitro* manipulation of T cells provides many opportunities for studying cytokine production or tracking of pre-labelled T cells during the disease course in donor mice.

- *Spontaneous EAE* in animals does not occur naturally, but has been reported in some transgenic mice strains (Goverman et al., 1993; Madsen et al., 1999; Krishnamoorthy et al., 2006). For example, T cell receptor (TCR) transgenic mice (called relapsing-remitting mice) carry a TCR specific for MOG peptide 92–106. These mice are backcrossed to the SJL/J background, and most spontaneously develop RR EAE (Pöllinger et al., 2009).

1.6.1 Translational potential of the EAE model

The many similarities observed between the pathological mechanisms in MS and EAE have led to the development of several immunomodulatory therapies currently being used in the treatment of RRMS. As previously mentioned, Natalizumab, a monoclonal antibody against VLA-4, was selected as a potential candidate due to its ability to prevent the adhesion of lymphocytes and monocytes to inflamed vessels of isolated tissue slices. When applied in vivo, it blocked migration of activated leukocytes into the CNS, therefore preventing the development of EAE (Yednock et al., 1992). FTY720 is the first oral immunomodulatory therapy available for the treatment of RRMS. The target of this drug is sphingosine-1-phosphate (S1P) receptor present on activated lymphocytes found in the secondary lymphoid organs. FTY720 is thought to downregulate the expression of this protein thus preventing the extrusion of lymphocytes from these organs into the bloodstream (Matloubian et al., 2004). In vivo, FTY720 was effective in preventing the onset of MBP-induced EAE in Lewis rats (Fujino et al., 2003) and PLP-induced EAE in SJL mice (Webb et al., 2004). In 2010 it was approved by the Food and Drug Association (FDA) in the U.S. for the treatment of RRMS since it was shown to reduce the rate of relapses and delay the onset of the progressive phase (Kappos et al., 2010).

Despite the success of these and other immunomodulatory therapies (such as glatiramer acetate and Laquinimod) there have been some trials that have failed the translation from EAE clinical application. TNF-α is a major proinflammatory cytokine implicated in the pathology of both MS (Hofman et al., 1989; Sharief et al., 1991) and EAE (Merrill et al., 1992). Although the modulation of TNF-α, both by antibody-mediated therapy (Selmaj et al., 1991) and genetic knock-down (Körner et al., 1997), positively affected the EAE course in mice, it failed to have such an effect in MS patients and in some cases it exacerbated the disease (Lenercept MS study group., 1999). It was later discovered that the mode of action of this cytokine depends upon the receptor it is bound to. While

TNFR1 exerts proinflammatory actions upon activation (Eugster et al., 1999), TNFR2 is found to have a role in neuroprotection and remyelination (Arnett et al., 2001). Although the trial proved to be a failure in its original concept, targeting of the TNF-α should not be discarded as potential strategy in MS treatment. It was recently shown that strategic targeting of TNFR1 can achieve neuroprotective effects in the mouse model of EAE (Williams et al., 2014).

The failure of translation calls for greater caution when interpreting result from animal models. Although they share great similarities in terms of pathological mechanisms, and EAE has been proven to be a good model for developing human therapies, one has to keep in mind that EAE is not MS per se. While in the animal studies, EAE is induced by sensitization to a certain antigen in genetically identical animals kept under pathogen-free conditions, the aetiology of MS still remains unknown and involves a complex interplay between different genetic and environmental factors.

1.6.2 Autoimmune optic neuritis in MOG-immunized BN rats

As previously mentioned, optic neuritis is a syndrome commonly associated with MS. In experimental settings it can be modelled by induction of EAE with MOG. Immunization with this myelin protein, particularly enriched in the spinal cords and optic nerves of rodents, leads to “classical EAE pathology” characterized with inflammatory demyelination of the spinal cord but also to development of autoimmune optic neuritis (AON) in both mice (Williams et al., 2011) and rats (Storch et al., 1998).

BN rats, immunized with MOG, develop AON with great incidence (Meyer et al., 2001; Fairless et al., 2012). The onset of optic neuritis correlates with the onset of clinical disability which reflects the inflammatory demyelination of the spinal cord. The pathology of AON is characterized by inflammatory demyelination of the optic nerves (Meyer et al., 2001), accompanied by retinal atrophy (Hein et al., 2012) and a loss of RGCs (Meyer et al., 2001). A decrease in visual function, assessed by measurement of both visual evoked potentials and electroretinography, correlates with the disease pathology (Meyer et al., 2001).

While studying the mechanisms of RGC degeneration, Hobom and colleagues discovered that the reduction of RGCs precedes the clinical phase of AON (Hobom et al., 2004). At this time point there was no evidence of inflammatory demyelination or axonal loss in the optic nerves. The decrease of RGC numbers is accompanied by an up-regulation of the signaling molecules Bax and Caspase-9, pointing to the process of apoptosis. This finding suggested that the processes involved in RGC apoptosis appear to be independent of the optic nerve pathology since it precedes BBB breakdown

(Boretius et al., 2008) and subsequent inflammatory demyelination. This phenomenon reflects the observation in MS patients where the primary retinal pathology could be observed independent from optic neuritis (Fisher et al., 2006; Saidha et al., 2011).

Subsequent work on this model was focused on the induction phase of the disease in order to discover the molecular mechanisms underlying the early loss of RGCs (Fairless et al., 2012). The disruption of the blood-retinal barrier and activation of residential retinal microglia were found to be early events in the induction phase, correlating with the timing of neuronal loss. In accordance with previous reports, no evidence of major optic nerve pathology, such as demyelination and axonal loss, could be detected at this time point. Interestingly, careful examination of the ultrastructure of axons revealed the presence of shrunken axons and vacuolization of the periaxonal space within completely preserved myelin sheets. Though it was noted that there was no infiltration of inflammatory cells in the optic nerve parenchyma at this time point, increased numbers of activated residential microglia were observed. These cells had a specific spatial distribution – the majority of $ED1^+$ cells were present in the most proximal part, the optic nerve head (ONH), and were decreasing with distance along the optic nerve. It was also noticed that the BBB was permeable in the region of the ONH even in naïve animals, suggesting that soluble factors from the periphery could be responsible for the activation of microglial cells in this vicinity and for induction of the subtle axonal changes observed.

In light of these discoveries further work is needed in order to discover the origins of both RGC degeneration and subtle axonal changes during the induction phase of AON as well as the role of residential microglial cells and the blood-brain/retinal barrier in this early pathology. This model of AON is highly relevant in the research of MS-related optic nerve and retina degeneration as it recapitulates many pathological aspects observed in patients. The potential of the AON model for developing treatments in the human disease was already shown. A phase III clinical trial for the use of erythropoietin in the treatment of acute optic neuritis (TONE; NCT01962571) was based on a study where erythropoietin was shown to improve the survival and the function of RGCs in the AON (Sättler et al., 2004; Diem et al., 2005).

1.7 Mechanisms of axonal degeneration in MS

Neurodegeneration is recognized as the pathological correlate of neurological disability in MS patients (Bjatmar et al., 2000). Extensive loss of both axons and neurons is observed in all sub-types of MS and is showed to correlate with the degree of inflammation. The extent of axonal loss in the

disease course of MS varies and is found to be as high as 70% in white matter lesions at autopsy (Mews et al. 1998; Ganter et al., 1999; Lovas et al., 2000). Historically, neurodegeneration in MS was thought to be a secondary event associated with the progressive disease course. This concept has been changed as it is now recognized that widespread axonal loss and brain atrophy is present from the beginning of the disease. Atrophy of the cortex and the spinal cord, as well as the presence of neurofilaments in the CSF, are indicative of neurodegeneration and can be detected already in patients with CIS (Chard et al., 2002; Kuhle et al., 2011). Also, signs of acute axonal damage are associated with active demyelinating lesions occurring early in the disease course (Kuhlmann et al., 2002). It should be noted that the presence of diffuse axonal injury is also evident in areas of NAWM distant to inflammatory lesions (Bjartmar et al., 2001; Kutzeinigg et al., 2005; Howell et al., 2010; Singh et al., 2013). These areas, though lacking peripheral inflammatory infiltrates, contain increased numbers of diffusely distributed activated microglia.

Within active demyelination lesions, in addition to a loss of myelin, many axons appear dysmorphic and swollen. In addition, many axons appear transected with up to 11,000 transected axons per mm^3 being observed (Trapp et al., 1998). Accumulation of APP in areas of axonal swellings is indicative of disrupted axonal transport (Ferguson et al., 1997; Kornek et al., 2000). Another sign of axonal stress is a change in the organization of its cytoskeleton. In healthy, myelinated axons, neurofilament side arms are heavily phosphorylated resulting in an increase in the axonal diameter (Sanchez et al., 1996). Within demyelinating lesions, a dramatic increase in the presence of non-phosphorylated neurofilaments is detected. This phenomenon is particularly observed in the ovoids at the transected ends of axons (Trapp et al., 1998).

1.7.1 Inflammatory mediators of axonal damage

Both activated microglia and macrophages are considered to be the main effector cells in the pathology of MS. As previously mentioned, their presence is detected in all lesion types and it correlates with tissue damage, both in the setting of inflammatory demyelination and in the absence of peripheral immune infiltrates (as observed with microglial activation in preactive lesions and NAWM).

The proposed role of activated microglia/macrophages in axonal injury could be drawn from the observation from active MS lesions, where these cells could be found in contact with the ovoids of transected axons within the lesion (Trapp et al., 1998). Also, in addition to myelin, axonal components could be found within phagocytic microglia/macrophages (Huizinga et al., 2011). Although this can implicate the direct destruction of axons by these cells it also could reflect the

phagocytosis of axonal debris produced by other destructive means. Inflammatory cells, including activated microglia/macrophages, are able to secret a plethora of potentially disruptive substances that could be detrimental to axons. These include various cytokines, free radicals and proteolytic enzymes (Hohlfeld, 1997; Dutta and Trapp 2011).

One enzyme with an ability to produce disruptive agents is the inducible nitric oxide synthase (iNOS) which is expressed by activated microglia/macrophages within MS lesions (Bö et al., 1994; Liu et al., 2001). iNOS catalyzes the production of nitric oxide (NO) by conversion of L-arginine to citrulline. NO, a gas which has many biological roles, and to a larger extent, its derivate peroxynitrite, are known to produce a variety of disruptive effects including the oxidation and nitration of proteins, peroxidation of lipids, inactivation of enzymes, DNA damage and activation of matrix metalloproteases. One of the most deleterious effects of these radicals is their ability to interfere with mitochondrial respiration leading to a decreased production of adenosine triphosphate (ATP) and a resulting energy deficit (Pacher et al., 2007). This decrease in ATP levels can lead to an impairment in the function of Na^+/K^+ ATPase, a key molecule in keeping the ionic homeostasis of axons. It has also been described that NO can cause a reversible conduction block in axons from the isolated spinal cord of rats. This phenomenon was even more pronounced on axons with chemically induced demyelination (Redford et al., 1997) mimicking the axonal status within the inflammatory lesion. Although the effect of the blockade was transient, a subsequent study showed that the application of NO to electrically active healthy axons of the rat spinal cord in vivo, can cause an axonal/myelin pathology (Smith et al., 2001).

A more detailed study of the role of reactive oxygen and nitrogen species (ROS/RNS) in axonal injury was performed using in vivo two-photon imaging of the mouse spinal cord (Nikić et al., 2011). It was shown that the application of reactive species can induce dysmorphic changes in axons, comparable to ones observed in the lesions of EAE mice and in acute MS lesions. This could be rescued by the application of ROS/RNS scavengers. The role of ROS/RNS in the pathology of MS has been extensively studied in autopsy tissue of active lesions (Haider et al., 2011). Within these lesions, many oligodendrocytes were observed with oxidized DNA in their nuclei and traces of lipid peroxidation in their cytoplasm. In addition, oxidized phospholipids were found in both swollen axons with disturbed transport and in neurons with fragmented dendritic processes.

Another substance with proposed damaging effects in MS pathology is glutamate. Inflammatory cells, and also neurons and astrocytes under pathological conditions, could be the source of the excessive levels of glutamate detected in acute MS lesions (Matute et al., 2001; Ye et al., 2003; Srinivasan et al., 2005). Excessive release of glutamate can over-activate metabotropic and ionotropic glutamatergic receptors leading to an increase in intracellular Ca^{2+} levels and subsequent

cell death (Dong et al., 2009). This can affect both neurons and oligodendrocytes within the lesion through the activation of different glutamate receptors. This concept has been investigated in the EAE model by application of compounds which block different glutamate receptors. Selective blockade of AMPA receptors led to increased survival of oligodendrocytes both in the setting of inflammatory demyelination (Pitt et al., 2000) and under hypoxic condition (Tekkök and Goldberg, 2001). In both models, the observed preservation of axonal structure and function could be attributed to the primary oligodendroglial protection. The role of NMDA receptors in oligodendrocyte pathology remains unclear. The expression of NMDA receptors is observed in myelinating processes of oligodendrocytes and they are suggested to be activated under ischemic conditions in the white matter (Karadottir et al., 2005; Micu et al., 2006). On the other hand, a recent study showed that the targeted genetic deletion of NMDA receptors in oligodendrocytes allowed the normal formation of myelin sheets in mice and did not interfere with the pathology of the MOG-induced EAE in these animals (Guo et al., 2012). Systemic blockade of NMDA receptors has shown to have protective effects in different EAE models. In these studies, protective effects of the blockers were attributed to different mechanisms. In one study, the protection is attributed to the preservation of the integrity of the BBB, resulting in reduced inflammation and tissue damage (Paul and Bolton, 2002). The other study reported the protection in a manner independent of the inflammation process, suggesting that NMDA blockade had a direct neuroprotective effect (Wallström et al., 1996). Similar observations have been reported in the model of AON (Sühs et al., 2014). The systemic application of NMDA blockers led to an improvement of the EAE disease course through the reduction of inflammation and, presumably as a result of this, demyelination and axonal damage. Interestingly, the blockade also decreased RGC death during the pre-inflammatory, induction phase of the disease, further suggesting a direct neuroprotective effect of the NMDA blockade. These studies underline an important role for glutamate in the pathology of the CNS (including MS) and suggest that careful, strategic targeting of over-activation of its receptors could have beneficial outcomes.

1.7.2 Pathological mechanisms in demyelinated axons

Although acute lesions are characterized by marked signs of axonal injury and transections, the majority of axons appear to survive the initial inflammatory attack. Instead, axonal loss and brain atrophy becomes more pronounced in the later, chronic progressive stages of the disease. Within chronic lesions lacking on-going inflammation, up to 70% reduction in axonal counts could be observed. The mechanism of degeneration of these chronically demyelinated axons still remains speculative. This is in part owed to an inability to produce an animal model that reflects the chronic

nature of demyelinating MS lesions (Trapp and Nave, 2008). Nevertheless there are compelling arguments that a loss of trophic support from the oligodendrocytes and a chronic state of hypoxia and energy deprivation in chronically demyelinated axons are the driving forces of neurodegeneration. The evidence for the former hypothesis comes from animal studies with genetically modified mice lacking minor myelin components such as MAG and CNP. Although the myelination status of axons in these mice is not compromised, they still develop a late-onset, slow-progressing axonal pathology (Li et al., 1994; Yin et al., 1998; Lappe-Siefke et al., 2003). These findings suggest that the trophic support of oligodendrocytes is necessary for long-term axonal viability. This phenomenon might play a role in the pathology of pattern III and IV lesions which contain extensive oligodendrocyte apoptosis (Lucchinetti et al., 2000).

The latter hypothesis is based on the assumption that chronically demyelinated axons that survive an initial inflammatory attack are left in a persistent hypoxia-like state which eventually leads to their degeneration (Stys, 2004; Trapp and Stys, 2009). The underlying mechanisms behind this phenomenon include disruptions in ionic homeostasis and their energy status, and subsequent activation of proteolytic enzymes (Figure 1.4).

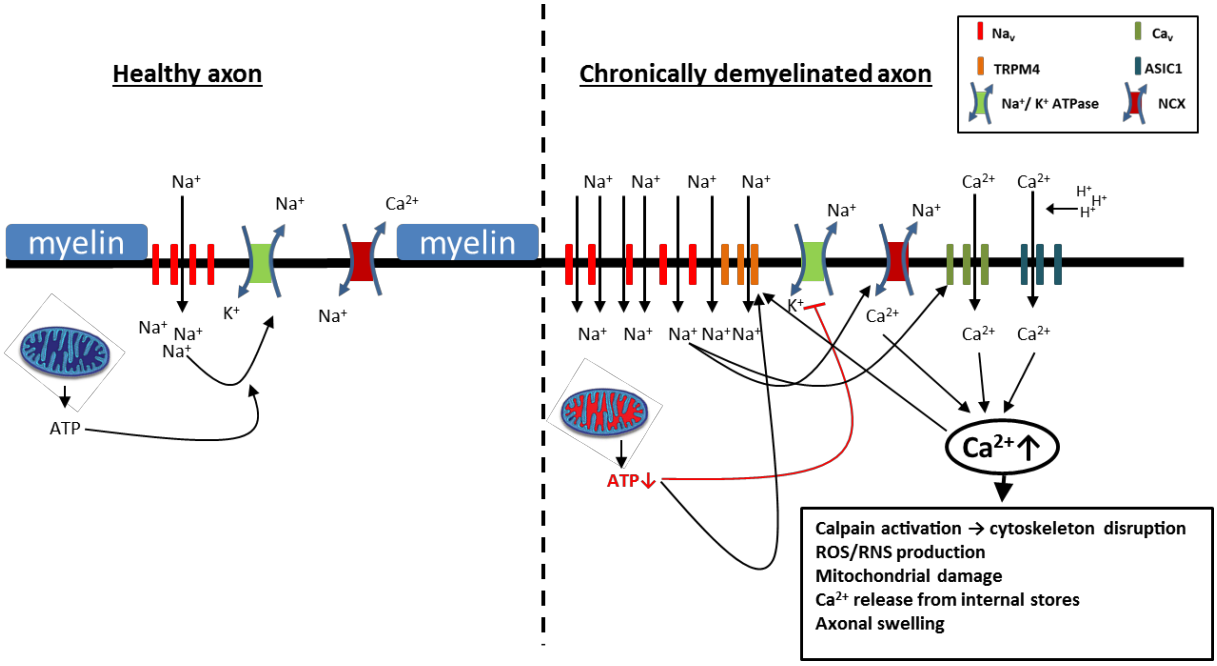

Figure 1.4 Proposed molecular mechanisms leading to axonal degeneration in MS. Contribution of different ion channels and pumps to Ca^{2+} overload and subsequent initiation of events that could lead to degeneration of chronically demyelinated axons.

In healthy axons, voltage-gated sodium channels (Na_V) are clustered at unmyelinated axonal segments (the nodes of Ranvier) and are responsible for the inward current of the AP. Following the

successful propagation of an AP, the membrane resting potential is restored through the action of different channels and pumps in the axon. One of the most important pumps in this process is the enzyme Na^+/ K^+ ATPase which mediates the exchange of intra-axonal Na^+ for extra-axonal K^+. Considering that this process goes against the concentration gradients for both ions, the pump heavily relies on the energy provided by ATP.

Following demyelination, Na_V become dispersed along the denuded axons (Craner et al., 2004; Black et al., 2007a). As a consequence, the attempt to restore proper saltatory conduction is characterized by a greater influx of Na^+ into the axolema, which would, in turn, increase the energy demand for the proper clearance of Na^+ by Na^+/ K^+ ATPase. It is considered that this increased demand in ATP would be hard to meet even in healthy axons where the function of the mitochondria is not compromised. In injured axons within the MS lesion, this process is further compromised by the impaired ability of the mitochondria to produce ATP. A gene expression study of MS tissue revealed a decreased expression of genes involved in oxidative phosphorylation and a reduction in the activity of the respiratory chain complexes I and III (Dutta et al., 2006).

As a result of this inability to effectively pump Na^+ back out across the plasma membrane, axons are found in a prolonged state of depolarization which, though the activation voltage-gated calcium channels (Ca_V), leads to an influx of Ca^{2+}. Ca_Vs are synthesized in the neuronal cell body and transported along the axons to their terminals where they exert their physiological role in synaptic transmission (Alberts et al., 1989). Upon axonal injury in MS lesions, axonal transport is compromised and these channels are shown to accumulate in axonal swellings and to be incorporated into the plasma membrane (Kornek et al., 2001). Increased Na^+ levels in the axoplasm can also contribute to accumulation of Ca^{2+} through the reverse action of Na^+/Ca^{2+} exchanger (NCX). The physiological role of this pump, located in the axonal membrane of the nodal region, is to maintain low levels of intracellular Ca^{2+} through utilizing the high Na^+ gradient across the axonal membrane. However, if Na^+ levels in the axoplasm reach a concentration of approximately 20 mM, the pump will operate in a reverse, Ca^{2+} import mode (Stys et al., 1997) which would further lead to the accumulation of Ca^{2+} within the axoplasm. Upon demyelination, the expression of NCX shows a diffuse pattern, similar to that observed for Na_V (Craner et al., 2004).

It was recently suggested that non-selective cation channels contribute to ionic disturbances in injured axons within MS lesions. One member of the transient receptor potential (TRP) ion channel family, the melastatin-like TRP 4 (TRPM4) channel, is a non-selective channel which gates exclusively monovalent cations and is activated by increases in intracellular Ca^{2+} and low levels of ATP (Guinamard et al., 2010). Following demyelination in MS, a redistribution of TRPM4 from the neuronal cell body to its axons was observed. The importance of this channel in axonal pathology

was confirmed by both its physiological and genetic inactivation, leading to reduced neuronal and axonal loss and an overall improvement of the EAE disease course (Schattling et al., 2012). Another non-selective cation channel implicated in axonal pathology belongs to the family of the acid-sensing ion channels (ASICs). ASIC1 is a Na^+-permeable channel which under acidic conditions, such as ones found within MS lesions, becomes permeable to Ca^{2+} (Yermolaieva et al., 2004). The expression of ASIC1 is observed predominately in injured axons in MS and its pharmacological inhibition leads to a reduction in neuronal and axonal degeneration in EAE (Vergo et al., 2011).

Collectively, these events can result in the abnormal accumulation of Ca^{2+} in the axoplasm of a denuded axon which will in turn activate a series of events leading to axonal degeneration. Increased Ca^{2+} levels can result in the production of reactive species by activation of the neuronal nitric oxide synthase (nNOS) which can lead to further release of Ca^{2+} from internal stores and also mitochondrial damage further contributing to energy failure (Kapoor et al., 2003; Stys, 2004). In addition, the activation of the calcium-activated protease (Calpain) can mediate the disruption of the cytoskeleton by targeting microtubules, spectrin and neurofilaments (O'Brien et al., 1997; Liu et al., 2008). Calpain activity was observed in both lesions and NAWM of MS brains (Shields et al., 1999). In the model of AON in BN rats, the activity of this protease correlated with increased Ca^{2+} levels in the retina and the optic nerve (Hoffmann et al., 2013). In the retina, increased Ca^{2+} levels and calpain activity correlated in particular with the onset of RGC death, implying their importance in the process of neurodegeneration. This was further supported by the pharmacological inhibition of this protease, which led to a decrease in the extent of the pathology in both compartments.

Given the unmet need for neuroprotective therapies for the treatment of neurodegeneration in MS, the above described mechanisms provide interesting opportunities for intervention. The blockade of Na_V could, at least in part, decrease the amount of Ca^{2+} accumulation and have a favourable outcome on axonal viability. This concept was considered as an interesting strategy for axonal protection taking into consideration the availability of different Na_V blockers in the treatment of cardiac arrhythmia and epilepsy. Systemic treatment with different blockers initially reduced axonal loss and neurological disability in EAE (Lo et al., 2003; Bechtold et al., 2004; Bechtold et al., 2006). However, follow-up studies with phenytoin and carbamazepine, demonstrated that upon withdrawal of therapy, mice developed an exacerbated disease course and increased inflammation (Black et al., 2007b). The reason for this is probably due to the role of Na_V in the activation of inflammatory cells, mainly microglia/macrophages (Craner et al., 2005). Lamotrigine, one of the Na_V blockers that showed promising results in animal studies (Bechtold et al., 2006), was tested in clinical trials for the treatment of SPMS. Unfortunately the therapy did not manage to decrease the extent of brain atrophy in patients, which was the primary outcome measurement of the trail (Kapoor et al., 2010).

Studies targeting different components of this degenerative cycle have led to important discoveries of mechanisms that lead to axonal loss in the inflammatory demyelinating setting of both animal models and MS. The chronic nature of the human disease and the overall systemic roles that potential targets have imply that great caution is required when attempting to translate results from the animal model to the clinic. Potential therapies have to be designed to be highly specific in preventing the deleterious effects while preserving the normal physiological functions of these molecules.

1.7.3 Disruption of axonal domains

To ensure proper rapid, saltatory conduction, myelinated axons are divided into distinct domains. Each domain has a specialized molecular architecture to support their functional properties (Figure 1.5). Sodium channels are clustered in the nodal domain (nodes of Ranvier) and are responsible for the inward current flow necessary for AP generation while potassium channels, mainly clustered in the juxtaparanodal domain, are responsible for the ending of the AP of axons. These two domains are separated by a paranodal domain which serves as an anchoring point for the myelin loops of the oligodendrocyte. Besides its role in the anchoring of the myelinating sheet, the paranodal domain is responsible for limiting the lateral diffusion of membrane components, such as sodium and potassium channels. The fourth, internodal domain is not believed to have specialized protein components.

Nodal domains, as well as the axon initial segment (AIS), lack myelin sheets. They are sites for generation (AIS) and regeneration (nodes of Raniver) of APs which are propagated along the axon via saltatory conduction. These domains are enriched in Na_V, which are heteromeric complexes consisting of one pore-forming α subunit and two transmembrane ß subunits (Catterall, 2000). There are ten types of Na_V based on the different α subunits that they express (Na_V 1.x; Goldin, 2001), which have similar functions but differ in their activation kinetics (Yu and Cattarall, 2003). The α subunit undergoes a developmental transition, with Na_V 1.2 being present in newly forming nodes but later replaced by Na_V 1.6 in mature nodes (Boiko et al., 2001). Another major component of the nodal region is the cytoskeletal protein Ankyrin G, which is essential for the assembly of the node. It binds directly to the α subunit of Na_V (Bouzidi et al., 2002) and also with high affinity to ßIV-spectrin, a cytoskeletal protein found at both nodes and the initial segment of axons (Berghs et al., 2000; Komada and Soriano, 2002). ßIV-spectrin provides a link between the channel complex and the actin cytoskeleton (Bennett and Gilligan, 1993).

Neurofascin 186 kD (Nfasc 186) is a member of the L1 subfamily of IgCAMs along with NrCAM. They are both expressed on nodes and the initial segment of axons where they associate with Ankyrin G (Lambert et al., 1997; Figure 1.5Ciii). Interplay between these three molecules is highly important for correct clustering of Na_V at the nodal region. The critical role that Nfasc186 plays in correct formation of the node has been demonstrated by Nfasc186 knock-out animals which were lacking in the proper nodal composition of their axons (Sherman et al., 2005).

AIS has a similar molecular composition as the nodal region. The main difference is the presence of both Na_V 1.2 and Na_V 1.6 subtypes in mature initial segments, whereas on adult nodes Na_V is the dominant subtype (Boiko et al., 2003).

The main feature of the paranodal domain is a cis complex of two adhesion molecules Contactin-1 and Caspr (Figure 1.5Fiii). Caspr is a transmembrane, glycoprotein member of the neurexin superfamily (Bellen et al., 1998). Its cytoplasmic domain binds to a cytoskeletal 4.1B protein. It also has an SH3 binding domain which implies the possible role for Caspr in neuronal signalling pathways (Menegoz et al., 1997; Peles et al., 1997). Mice deficient in Caspr exhibit tremor, ataxia and significant motor paresis, with a failure to form normal paranodes and a disrupted organization of paranodal loops. In these animals Contactin is undetectable in paranodal regions and potassium channels are displaced from juxtaparanode to paranode (Bhat et al., 2001). The Contactin-1/Caspr complex plays a major role in anchoring oligodendrocyte myelin loops to the axon. This is achieved through its interaction with Neurofascin 155kD, a phosphorylated, glial isoform of Neurofascin (Charles et al., 2002; Tait et al., 2000; Figure 1.5Eiii).

The juxtaparanodal domain lies underneath compact myelin sheets located between the internodal and paranodal regions. The main feature of this domain is the presence of two delayed rectifier potassium channels (K_V) K_V 1.1 and KV 1.2, their associated ß subunits and a complex of the cell adhesion molecules Caspr2 and TAG-1 (Rhodes et al., 1997). Caspr2 is associated with K_V through unidentified PDZ domain proteins. These PDZ binding domains are the major structural difference between Caspr and Caspr2 (Poliak et al., 1999). Caspr2 also contains a domain for binding 4.1B protein (Poliak et al., 2001). Caspr2 also binds to TAG-1, a GPI-anchored protein that is expressed both on neurons and myelinated glia (Poliak et al., 2003; Traka et al., 2003). Although this protein has a similar sequence to contactin-1 (Furley et al., 1990), this cis Caspr2/TAG-1 interaction is not as tight as Caspr/Contactin-1 at the paranode (Poliak et al., 2003).

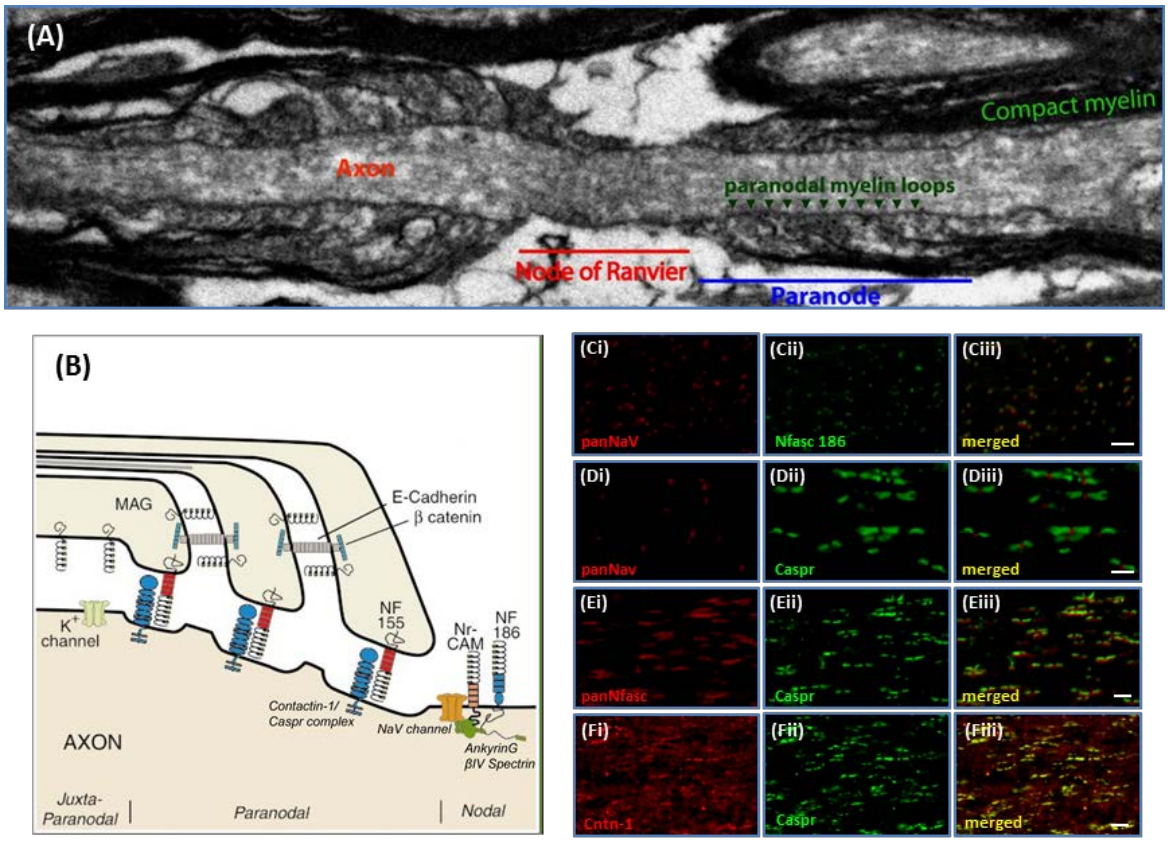

Figure 1.5 Polarized domains of myelinated axons in the CNS. (A) Ultrastructure of a healthy optic nerve axon from the BN rat. (B) Schematic representation of different molecules involved in the organization of axonal domains. Image adapted from Trapp and Kidd, 2000. (Ci-Fiii) Immunofluorescent staining with antibodies against different components of axonal domains in the healthy optic nerve of the BN rat. Scale bars 5 µm.

It has been suggested that early clinical symptoms of MS patients could be attributed to a reduction in the conduction velocity caused by inflammation and a disruption in the organisation of axonal domains (Compston and Coles, 2002). Several studies have examined the expression patterns of different components of axonal domains in chronic progressive MS. Within lesions, nodal domains were mainly observed with elongated profiles of Na_V along denuded axons (Coman et al., 2006). Co-localization was observed with their membrane clustering partner, Nfasc 186. The disruption of the nodal domain was found to correlate with axonal injury since elongated Nfasc 186 profiles were present on axons positive for SMI32, a marker for non-phosphorylated neurofilaments (Howell et al., 2006). Paranodal domains were mainly absent within the chronic lesion as reflected by the lack of immunoreactivity for both axonal Caspr (Wolswijk and Balesar, 2003) and oligodendroglial Nfasc 155 (Howell et al., 2006). In the absence of parnodal domains, K_V, normally present in the juxtaparanodes, were found adjacent to Nfasc 186 (Howell et al., 2006). The observed absence of the paranodal region in the centre of chronic lesions reflects the demyelinated status of these axons. While the loss of Nfasc 155 is a direct effect of myelin loss, the downregulation of the axonal Caspr

could be a secondary event due to the loss of its oligodendroglial interaction partner. In contrast, paranodal regions were still present in both active lesions and at the border of chronic lesions. In these areas, paranodes had a disrupted profile characterised by wider and elongated patterns of Nfasc 155 (Howell et al., 2006) and Caspr (Wolswijk and Balesar, 2003; Coman et al., 2006) staining associated with SMI32 positive axons. K_V also had an elongated profile which often diffused into the paranodal domain as observed by its overlap with Nfasc 155. The observed disruption of paranodal and juxtaparanodal domains did not, however, appear to result in a widening of the nodal gap or the distribution of NaV (Howell et al., 2006).

These studies highlight that paranodal disruption could be an early event in the disorganization of axonal domains under inflammatory conditions. In active lesions and at the borders of chronic lesions where inflammation still persists, disruption of paranodal domains can be detected on injured axons that still appeared myelinated. Following demyelination, paranodal regions are lost and nodal and juxtaparanodal components diffuse along denuded axons. This concept was further strengthened by a later study of NAWM MS tissue (Howell et al., 2010). Upon careful examination it was shown that SMI32 positive axons in these areas contained elongated Nfasc 155/Caspr positive paranodes in the absence of inflammatory demyelination. These areas lacked peripheral inflammatory infiltrates and were characterised by the diffuse presence of residential HLA-DR/iNOS positive microglia. The extent of paranodal disruption and axonal injury correlated with the density of activated microglia.

The response of humoral immunity has been considered to play a significant role in the pathogenesis of MS as indicated by the presence of IgG/complement deposition in a subset of active lesions (Lucchinetti et al., 2000). The major pathological role of these autoantibodies is attributed to their ability to induce demyelination, reflecting their specific reactivity against myelin proteins such as MOG (O'Connor et al., 2005) and MBP (Warren et al., 1993). It was recently suggested that the action of humoral immunity could be also aimed against axonal components. Two proteomic-based studies identified adaptive immune responses against components of axonal domains in a subset of patients with progressive MS. In one study, pan-specific anti-Neurofascin antibodies were detected in the serum of 20% of the patients examined (Mathey et al., 2007). These antibodies showed an ability to bind the extracellular domains of both Nfasc 155 and 186 in vitro. Their pathological capacity was tested through the adoptive transfer EAE model with co-injection of the isolated antibodies. Animals that received pan-Neurofascin antibody had an exacerbated disease accompanied by a greater degree of axonal injury when compared to EAE animals that received only control IgG. Interestingly, although in vitro these antibodies bound to both isoforms, upon their transfer into the animal model, they bound exclusively to the nodal region, showing an overlapping pattern with Na_V.

In the second study, the juxtaparanodal Contactin-2/TAG-1 complex was identified as an autoantigen for both antibody and T cell responses in MS patients (Derfuss et al., 2009). They showed both an increased proliferation of Contactin-2 specific T cells in patients compared to controls and elevated Contactin-2-specific antibodies in the MS CSF. Adoptive transfer of Contactin-2 specific T cells was sufficient to induce the EAE-like pathology in rats, although the severity of the disease course and the extent of the spinal cord pathology was less when compared to MOG-specific T cell adoptive transfer. Interestingly, the extent of cortical pathology was much greater in the Contactin-2-specific T cell transfer suggesting a possible role in the grey matter pathology observed in MS patients.

Both studies provide evidence of an adaptive immune response towards axonal antigens. However, although the transfer of such autoreactive T cells/antibodies into the animal model can affect the pathology of EAE, their involvement in MS pathology is still to be determined. These findings also suggest that the disruption of axonal domains can be a directed process in addition to being a result of proinflammatory attack by both residential and peripheral immune cells.

1.8 Summary

MS is a complex disease which involves interplay between different genetic and environmental factors. The pathology of the disease is characterised by atrophy of the CNS as a result of an aberrant immune response towards the self-antigen. The inflammatory response involves the breakdown of the BBB and infiltration of autoreactive immune cells and antibodies from the periphery, but also the activation of residential immune cells. This leads to the generation of demyelinating lesions accompanied by destruction of neurons and glial cells. However, neurodegeneration is recognized as an early component of the disease pathology, where it might even precede classical inflammatory demyelination (as has been described for grey matter lesions and retinal degeneration which are unmyelinated regions). The importance of neurodegeneration has been emphasised by its strong correlation with the extent of neurological disability in patients.

The success of current MS therapies in the reduction of inflammation-driven relapses is marred by their inability to produce beneficial outcomes in the progressive stages of the disease which are characterised by extensive neurodegeneration. So far there is an unmet need for neuroprotective strategies in the treatment of MS which would improve the currently irreversible neurological decline in patients. There is a great effort in the scientific community in understanding the cause and mechanisms of neurodegeneration in MS. This is achieved by examination of sparse biopsy and

autopsy material but also through utilizing different animal models which are able to reproduce many pathological aspects of the disease.

2 Aim of the study

The visual system provides great advantages for studying neurodegenerative processes in general. Compartmentalization of the retinal ganglion cell bodies in the retina and their axons in the optic nerves allows for dissecting the contribution of the individual compartments in neurodegeneration. A variety of functional tests and imaging techniques can be used to monitor the effect of potential therapies on the outcome of the disease. The model of AON in BN rats has been shown to be an interesting approach for studying neurodegenerative processes in MS. The activation of the adaptive, innate and humoral immune system in this model is representative of the pathological heterogeneity observed in the MS lesions (Fairless et al., 2012). The dynamics of the pathological events in both the optic nerve and the retina is similar to those observed in acute optic neuritis in patients, a common early manifestation of MS. Previous work on this model mainly focused on the retinal compartment and the mechanisms of early degeneration of the RGCs observed during the course of AON (Hobom et al., 2004; Fairless et al., 2012). At this time point, although the optic nerve compartment appears macroscopically normal, subtle changes could be detected. This is observed both functionally, through a decrease in visual acuity (Hobom et al., 2004), and morphologically by ultrastructural axonal changes and activation of residential microglial cells (Fairless et al., 2012).

The aim of this study is to closer investigate the changes in the axonal and myelin compartments of the optic nerve during the course of AON, focusing on the induction phase of disease. Combining functional testing (by measurement of VEPs) and immunohistochemical analysis would allow us to gain more insight into pathological correlates of visual impairments in optic neuritis which could lead to determining possible targets for therapeutic intervention. Structural correlates of impaired visual functions in this and other animal models of optic neuritis have not been addressed so far in detail, but they are likely to involve disruptions in axonal domains involved in AP propagation. Taking this into consideration, particular focus of this thesis will be placed on the axonal domains during the course of the disease. Disruption of axonal domains is considered to be an early event in MS lesion development (Coman et al., 2006; Howell et al., 2006; Howell et al., 2010) and further understanding of the origin of these disruptions could help to unravel the mechanisms of axonal pathology in MS.

3 Methods

3.1 Animals

Female Brown Norway rats 8–10 weeks of age and a weight of 140-160 g were used in all EAE experiments. Sprague Dawley (SD) rat pups at postnatal day two (P2) were used for the purpose of extracting and culturing primary glial cells. Both strains were obtained from Charles River (Sulzfeld, Germany) and kept under environmentally-controlled conditions in the absence of pathogens with free access to food and water. All experiments that involved animal use were performed in compliance with the relevant laws and institutional guidelines of Baden Württemburg.

3.2 Induction of MOG-EAE and animal scoring

BN rats were immunised with whole recombinant rat MOG (a kind gift of Prof Christine Stadelmann, Dept of Neuropathology, University of Göttingen; Fairless et al., 2012). The emulsion was mixed in a 1:1 ratio containing 100 µg of MOG in phosphate-buffered saline (PBS, Sigma-Aldrich, St. Louis, Missouri, USA) and complete Freund's adjuvant (Sigma-Aldrich) containing 200 µg of heat-inactivated *Mycobacterium tuberculosis* H37RA (Difco Microbiology, Kansas, USA). Rats were anesthetized with 5% isoflurane inhalation and injected intradermally at the tail with 200 µl of emulsion. Additional sham-immunised rats were injected as a control with emulsion containing only PBS in complete Freund's adjuvant (containing *Mycobacterium tuberculosis*). Rats were observed daily for clinical signs of EAE. The grading system used to score neurological symptoms is presented in Table 3.1.

Animals were kept until the desired time point in the pre-clinical or clinical stage of the disease course. Animals that developed signs of severe ataxia or reached a score of 3.5 or greater were sacrificed.

score	clinical symptoms
0.5	*distal tail paresis*
1	*complete tail paralysis*
1.5	*complete tail paresis and mild hind leg paresis*
2	*unilateral severe hind leg paresis*
2.5	*bilateral severe hind limb paresis*
3	*complete bilateral hind limb paralysis*
3.5	*complete bilateral hind limb paralysis and paresis of one front limb*
4	*complete paralysis (tetraplegia), moribund state, or death*

Table 3.1. Grading of neurological symptoms in BN MOG-EAE.

3.3 Isolation and culturing of primary oligodendrocytes

P2 SD pups were decapitated and optic nerves were quickly dissected under a microscope. Each nerve was cut into small pieces (≈1 mm in length) and kept in RMPI 1640 medium (Invitrogen, Carlsbad, California, USA) on ice until the process of dissection was finished. Following dissection, nerves were incubated in 2 ml of RPMI medium containing 5 % trypsin (25 mg/ml from bovine pancreas; Sigma-Aldrich) and 500 U of DNase I (Roche, Mannheim, Germany) for 10 minutes at 37° C. Trypsin activity was stopped by addition of 10% foetal calf serum (FCS; Gibco, Carlsbad, California, USA) and the suspension was centrifuged for 5 minutes at 1.1 rcf. Supernatant was discarded and the pellet containing cells was re-suspended in 500 µl of the *proliferation medium*. Cells were seeded in flasks pre-coated with poly-L-lysine (PLL; Sigma,USA). Half of the medium was exchanged twice a week. After two weeks in culture many cells with a morphology resembling oligodendrocyte precursor cells (OPCs) could be observed. At that point, medium was taken out and cells were detached by incubation in 1% trypsin in PBS for 10 mins at 37° C. The suspension was collected and trypsin activity was stopped by addition of 10% FCS in RMPI 1640 medium. Cell number was

determined by counting cells in a haemocytometer. Following centrifugation for 5 minutes at 1.1 rcf, supernatant was discarded and the pellet containing cells was re-suspended in the proliferation medium. Cells were seeded on PLL-coated glass coverslips (ø 13 mm; VWR, Radnor, Pennsylvania, USA) in a 24 well plate with a density of 15-20,000 cells/coverslip. Cells were stimulated to differentiate into mature oligodendrocytes by switching to the *differentiation medium*.

Basic medium consisted of RPMI 1640 medium supplemented with 1% Sato's medium, 1% insulin (form bovine pancreas, 0.5 mg/ml; Sigma), 1% Na-pyruvate (100 mM; Sigma), 2% L-glutamine (2 mM; Sigma) and 1% Pen-Strep (10,000 U/mL; Gibco).

Proliferation medium consisted of basic medium supplemented with 0.1% platelet-derived growth factor (PDGF, rat recombinant, 10 ng/ml; R&D systems, Minneapolis, Minnesota, USA) and 0.15% basic fibroblast growth factor (bFGF, human recombinant, 10 ng/ml; PeproTech Inc., New Jersey, USA).

Differentiation medium consisted of basic medium supplemented with 0.1% ciliary neurotrophic factor (CNTF, rat recombinant, 10 ng/ml; PeproTech Inc., USA), 0.1% N-acetyl-L-cysteine (3 mg/ml; Sigma, USA) and 1% triiodothyronine (T3, 15nM; Sigma,USA).

The differentiation stage of the oligodendrocytes was assessed by immuno-staining with different markers of their developmental stages. All oligodendrocytes were $Olig2^+$ irrespective of their stage of development. OPCs were characterised by bipolar morphology and staining with an antibody against neural/glial antigen 2 (NG2). Mature oligodendrocytes were characterised by their numerous branch-like processes which were positively stained for MBP and CNPase. Purity of the oligodendroglial cell culture was determined by staining cells with the Olig2 antibody. The average percentage of Olig2+ cells was 70.64 ± 7.78% (n = 4 separate experiments).

3.4 Measurement of visual evoked potentials (VEP)

Five days prior to immunisation, animals were anaesthetised with an intraperitoneal injection (i.p.) containing a mixture of 10% ketamine (0.6 ml/kg; Atarost GmbH and Co., Twistringen, Germany) and 2% xylazine (0.3 ml/kg Albrecht, Aulendorf, Germany) and the head was secured in a stereotaxic frame. The skin was excised and the skull was exposed. Holes were drilled in the skull above the primary visual cortex (1 mm frontal and 3.5 mm lateral to lambda on each side) for the placement of the recording electrode. An additional hole was drilled in the area of the cortex that is not involved in the visual stimulation response (motor cortex, 1 mm frontal and lateral from bregma).

Measurements of VEPs were performed using the UTAS Visual Diagnostic System (LKC Technologies, Gaithersburg, USA). Animals were placed on a heated pad and temperature was kept at 37° C. Prior to recording, pupils were dilated with 0.5% atropine (Ursapharm, Saarbrücken, Germany) and the animal was dark adapted for 10 minutes. For recording of VEPs, a needle electrode was placed in the visual cortex, 0.5 mm deep. The reference electrode was placed 0.5 mm deep in the motor cortex and the ground electrode was placed subcutaneously in the tail. During the recording process desiccation was prevented by Liquifilm® O.K. eye drops (Allergan, Westport, Ireland). Since optic neuritis in MOG-EAE brown Norway rats is usually presented bilaterally, the recording procedure was performed on one eye only (the recording electrode was placed in the side of the visual cortex contra-lateral to the eye that was presented with a stimulus) to minimize the animal's exposure time to anaesthesia.

3.4.1 Measurement of VEP in response to flash stimulus (fVEP)

Animals were placed in a dome equipped with an LED ganzfeld stimulator. Flash stimuli were presented at an approximate distance of 20 cm with 0 dB intensity and a frequency of 1 Hz. A total of 100 sweeps were averaged per recording. The recording procedure was repeated twice during the induction phase of the disease (at day 5 and day 10 p.i.) and in the beginning of the clinical phase (when animals reached a clinical score of 1.0). The signal amplitude (µV) and latency (ms) were calculated from the first negative (N1) to the second positive (P2) peak of the response using software provided by the UTAS Visual Diagnostic System. Three consecutive fVEP recordings were averaged for every time point in the disease course.

3.4.2 Measurement of VEP in response to different pattern stimuli (pVEP)

Immediately following the fVEP recordings, animals were again dark adapted for 10 mins and placed 20 cm in front of a 15" CRT monitor with the display centred with the pupil axis. A series of pattern stimuli consisting of vertical bars (2, 4, 8, 16 and 32 bars) alternating with a 2 Hz frequency at 66 % contrast (constant mean luminance 15 cd/m^2) was presented to the animal in an ascending order of complexity. Animals were given a 5 minute relaxation period between the stimuli. To determine the noise level, recordings were made in the absence of pattern stimulus (monitor switched off). Amplitudes of pVEP were calculated from the amplitude spectrum of the fast Fourier transformation as the amplitude of the second harmonic (Porciatti et al., 1999; Meyer et al., 2001) using the software provided by the UTAS Visual Diagnostic System. At defined time points during the course of

disease, visual acuity was presented as the maximal spatial frequency (cycle per degree of the visual angle) at which animals were able to produce the response with the amplitude greater than one determined as the noise level.

Following the last recording (at the beginning of the clinical phase of EAE), animals were perfused and the optic nerves processed for histological staining (LFB) to confirm the presence of AON.

3.5 Tissue collection and processing

3.5.1 Preparation of frozen tissue sections

At desired time points during the disease course, rats were sacrificed by overdose i.p. injection containing a mixture of 20% ketamine (1.2 ml/kg) 4% xylazine (0.6 ml/kg) and perfused via the aorta with 4% paraformaldehyde (PFA). Tissue was dissected and placed in 4% PFA overnight for post fixation. Prior to dissection of optic nerves, tissue was placed in PBS for 12 hours. Optic nerves with eyes attached were dissected and cryoprotected in 30% sucrose (Applichem GmbH, Darmstadt, Germany) in PBS overnight. On the next day, nerves were put into plastic base moulds containing Cryoblock embedding medium (Medite, Burgdorf, Germany) and frozen usingcold isopentane (Acros Organics BVBA, Geel, Belgium), cooled with liquid nitrogen. Frozen blocks were kept at -80°C prior to cutting. Eight µm thick longitudinal sections and 1.5 µm thick cross sections were cut using a cryostat (Leica, Wetzlar, Germany) at -20°C. Sections were transferred to SuperFrost® Plus microscope slides (Thermo Scientific, Waltham, Massachusetts, USA) and kept at -20°C prior to staining.

3.5.2 Preparation of tissue lysates

At desired time points during the disease course rats were sacrificed by inhalation of CO_2. Optic nerves were dissected and mechanically homogenized in a glass homogenizer (Kontes, Vineland, New Jersey, USA) with ice cold lysis buffer containing cOmplete Protease Inhibitor Cocktail® (Roche, Mannheim, Germany). Lysates were sonicated for 5 seconds to further disrupt the integrity of the tissue. Cell debris was pelleted at 13,000 rpm at 4°C for 15 mins. Supernatants were collected and kept at -80°C prior to use.

The total protein concentration in the sample was determined using a bicinchoninic acid (BCA) assay (Pierce, Rockford, Illinois, USA) following the instructions provided by the manufacturer.

3.5.3 Serum collection

Blood was taken from animals after they were sacrificed for either tissue sections or lysates. Blood was collected with a 2 ml syringe directly from the heart and stored in plastic tubes overnight at 4˚C to coagulate. Up to 6 ml could be collected from one animal. On the next day, samples were centrifuged at 4°C for 15 min at 13,000 rpm to separate the serum and cellular component. Serum (supernatant) was aliquoted and stored at -80˚C prior to use.

3.6 Electron microscopy

At appropriate time points during the disease course animals were perfused with a mixture combination of 1% PFA and 2.5% glutaraldehyde in PBS. Optic nerves were dissected and fixed in buffered isotonic 2% osmium tetroxide solution for 1 h, followed by dehydration in ethanol and subsequent embedding in epoxy resin. Fifty nm thick longitudinal sections were cut on an ultramicrotome and contrasting was performed with uranyl acetate/lead citrate. Sections were observed and images were taken with an EM910 electron microscope (Zeiss, Jena, Germany) at 10,000x magnification.

3.7 Luxol Fast Blue/Periodic acid Schiff stain (LFB/PAS)

This histological stain is commonly used to observe myelin (Kluver and Barrera, 1953). It is based on an acid-base reaction with the base of the lipoprotein in myelin replacing the base of the dye and causing a colour change. The myelin is stained blue whilst the areas that lack myelin are counterstained purple with PAS.

Frozen longitudinal optic nerve sections were stained to determine the presence of demyelination. Slides were first put in 96% ethanol for 5 mins and then in 0.1% LFB solution (Solvent blue 38, Sigma-Aldrich) and incubated at 60˚C overnight. The next day, after cooling down to room temperature, slides were transferred to 90% ethanol for one min. Each slide was then placed in 0.5% lithium carbonate solution (Fluka/Sigma-Aldrich) and kept until the colour changed from blue to turquoise. After that slides were briefly washed in 70% ethanol and then in water. From water, they were transferred to 1% periodic acid (Sigma-Aldrich) for 10 mins and washed under running tap water for 5 minutes. In next step, slides were incubated for 30 mins in Schiff's reagent (Sigma-Aldrich) followed by washing under running tap water for 5 for a blue colour to develop. Following counterstaining

with haematoxylin (to visualize cell nuclei) slides were dehydrated in ascending ethanol concentrations and mounted with Roti® - Histokitt II (Carl Roth, Karlsruhe, Germany).

3.8 Immunofluorescent staining

3.8.1 Immunofluorescent staining – general protocol

Slides containing tissue sections were taken from -20˚C and left at RT to thaw and dry. Sections were then rehydrated by washing in Tris-buffered saline (TBS). Since tissue fixation can lead to masking of the desired epitope, an antigen retrieval step was introduced where necessary (see Table 1.2). Heat-induced antigen retrieval was performed with 0.2% citrate buffer at pH 6.0. Slides were immersed in boiling buffer and temperature was kept between 70˚ and 90˚C. After 15 mins, slides were left in the buffer and allowed to cool down to RT. Following additional washing in TBS, blocking of unspecific antibody binding was prevented by incubation with blocking buffer (containing 10% normal goat/rabbit serum in 0.1% TBS Triton X-100, TBS-Tr) for 1 hour at RT. Sections where then incubated overnight at 4˚C with the appropriate primary antibody dilution in blocking buffer. On the next day, slides were washed in PBS and incubated with appropriate secondary antibody conjugated with fluorescent dye for 1 hour at RT. After the final wash in TBS, slides were mounted with anti-fade Vectashield Mounting Medium (Vector laboratories, Burlingame, California, USA) covered with glass cover slips. If needed, visualisation of cell nuclei was accomplished by mounting sections with Vectashield Mounting Medium containing 4',6-diamidino-2-phenylindole (DAPI). A detailed list of the blocking buffers, primary and secondary antibodies used are given in Tables 1.2 and 1.3.

Fluorescent microscopy and image acquisition was performed using either a conventional Eclipse 80i microscope (Nikon; Shinagawa, Tokyo, Japan) or a LSM 700 confocal microscope (Zeiss).

Antibody	Company	Sub-type	Dilution	Blocking buffer	Antigen retrieval
Neurofilament light (Nf-L)	Millipore, Billerica, Massachusetts, USA	Rabbit polyclonal	1:500	10% NGS/ 0.1% TBS-Tr	none
Non-phosphorylated neurofilaments (SMI32)	Covance, Princeton, New Jersey, USA	Mouse IgG1	1:2000	10% NGS/ 0.1% TBS-Tr	none
Anti-Neurofilament Marker (SMI312)	Covance	Mouse IgG1 cocktail	1:1000	10% NGS/ 0.1% TBS-Tr	none
Caspr	Abcam, Cambridge, UK	Rabbit polyclonal	1:1000	10% NGS/ 0.1% TBS-Tr	none
Contactin-1	R&D systems	Goat IgG	1:100	10% NRS/ 0.1% TBS-Tr	Citrate buffer pH 6.0
Pan-Neurofascin	NeuroMab/ UC Davis, California, USA	Mouse IgG1, clone L11A741	1:1000	10% NGS/ 0.1% TBS-Tr	Citrate buffer pH 6.0
Neurofascin 186	Abcam	Rabbit polyclonal	1:500	10% NGS/ 0.1% TBS-Tr	Citrate buffer pH 6.0
Pan-Na_v	Sigma-Aldrich	Mouse IgG1	1:200	10% NGS/ 0.1% TBS-Tr	Citrate buffer pH 6.0
Olig2	Millipore	Rabbit polyclonal	1:500	10% NGS/ 0.1% TBS-Tr	Citrate buffer pH 6.0
Myelin basic protein (MBP)	Sigma-Aldrich	Rabbit polyclonal	1:300	10% NGS/ 0.1% TBS-Tr	Citrate buffer pH 6.0
Neural/glial antigen 2 (NG2)	Millipore	Rabbit polyclonal	1:300	10% NGS/ 0.1% TBS-Tr	Citrate buffer pH 6.0
αB-crystallin (CRYαB)	Abcam	Mouse IgG1, clone 1B6.1-3G4	1:1000	10% NGS/ 0.1% TBS-Tr	Citrate buffer pH 6.0
Glial fibrillary acidic protein (GFAP)	Sigma-Aldrich	Rabbit polyclonal, IgG serum fraction	1:500	10% NGS/ 0.1% TBS-Tr	none
CD68 (ED1)	Serotec, Kidlington, UK	Mouse IgG1	1:500	10% NGS/ 0.1% TBS-Tr	none

Table 1.2 List of primary antibodies used for immunoflorescent staining.

Antibody	Company	Sub-type	Conjugate	Dilution
Goat anti-mouse	Jackson labs/Dianova, West Grove, Pennsylvania, USA	IgG	**Cy3**	1:400
Goat anti-mouse	Invitrogen	IgG	**Alexa 488**	1:400
Goat anti-rabbit	Jackson labs/Dianova	IgG	**Cy3**	1:400
Goat anti-rabbit	Invitrogen	IgG	**Alexa 488**	1:400
Rabbit anti-goat	Invitrogen	IgG	**Alexa 488**	1:400
Goat anti-rat	Vector laboratories	IgG	**Biotin**	1:200

Table 1.3 List of secondary antibodies used for immunofluorescent staining.

3.8.2 Immunofluorescent staining – double immunofluorescent staining

Two different protocols were used for double immunofluorescence staining depending on the nature of the primary antibodies used. If the antibodies were raised in a different species (eg. mouse and rabbit) a parallel approach was undertaken. In this instance, sections (and/or cultured cells) were incubated with a mixture of two different primary antibodies and, subsequently, the mixture of appropriate secondary antibodies conjugated with different fluorophores.

A sequential approach was used if the desired antibodies were raised in the same species or in different species but when the serum and origin of primary antibody would interfere (eg. using goat serum when one of the primary antibodies was raised in goat). In this approach, sections would be stained using the general protocol for the first antibody (as described in section 3.8.1). After the final wash (following incubation with first secondary antibody) the whole protocol would be repeated again for the second primary antibody.

For all immunostaining procedures, appropriate controls were performed. For a negative control, the primary antibody was omitted – sections/cells were incubated instead with the blocking buffer. For a positive control a double staining was performed with different antibodies recognizing identical or neighbouring structures (eg. double staining with different paranodal markers, nodal and paranodal markers, different axonal/myelin markers, etc. as shown in Figure 1.5Ciii, Diii, Eiii, Fiii).

3.8.3 Immunocytochemistry

The staining procedure for cultured cells was similar to that used for tissue sections but with minor modifications:

- Medium was removed from 24 well plates and coverslips were carefully washed with ice cold PBS. Cells were then fixed with 4% PFA for 10 mins and washed with 0.02% PBS-Tween 20 (PBS-T; Sigma-Aldrich). For the purpose of improving penetration of the antibodies, cells were permeabilized with different detergents. For staining of cytoplasmic antigens, cells were treated with 0.1% PBS-Tween 20 for 10 mins at RT whereas for the detection of nuclear antigens (such as the transcription factor Olig2) 0.1% PBS-Tr was used. Following permeabilization, cells were washed and non-specific binding was blocked by incubation with 10% NGS in 0.1% PBS-T for 30 mins at RT. Following blocking, cells were incubated overnight at 4˚C with the appropriate primary antibody diluted in blocking buffer. The next day, cells were washed and incubated with a fluorescent conjugated secondary antibody for 1 hour at RT. After washing, coverslips were mounted on glass slides with mounting medium containing DAPI.

3.8.4 Immunofluorescent staining for antibody deposition

IgG deposition in the optic nerves was examined with the use of a biotinylated secondary antibody. Frozen longitudinal sections were thawed, rehydrated in PBS and blocked with 10% NGS in 0.1 % PBS-Tr for 30 mins. After washing in PBS, sections were incubated with a biotinylated goat anti-rat secondary antibody. Deposition was visualised by incubating sections with streptavidin–Alexafluor 555 in 1% bovine serum albumin (BSA; Sigma-Aldrich)-PBS for 30 mins at 37°C. After washing, sections were mounted with mounting medium containing DAPI.

To investigate the expression of different proteins with respect to IgG deposition, sections were processed for immunoflorescent staining with the desired antibody, followed by the protocol for antibody deposition staining.

3.9 Terminal deoxynucleotidyl transferase dUTP nick end labelling (TUNEL) assay

The TUNEL assay is a commonly used method to investigate the presence of apoptotic cells (Gavrieli et al., 1992). The assay is based on the addition of labelled deoxyuridine triphosphate (dUTP) to the ends of fragmented DNA in cells that are undergoing the process of apoptosis. This reaction is catalysed by an enzyme deoxynucleotidyl transferase (TdT).

The assay was performed on frozen longitudinal optic nerve sections. After rehydration in PBS, sections were treated with proteinase K (20 µg/ml; Roche) for 5 mins at RT. Endogenous peroxidases were inactivated with 3% H_2O_2 followed by rinsing in Tris buffer (10 mM Tris-HCl, pH 8.0; Carl Roth). Sections were equilibrated in TUNEL dilution buffer (TDB; Roche) for 10 mins at RT. The TUNEL reaction was performed in TDB containing TdT (0.15 U/µl; Promega, Madison, Wisconsin, USA) and biotin-16-dUTP (10 µM; Roche) for 60 min at 37 °C. A positive control was performed by pre-treating sections with DNase I (3 u/ml; Roche) and a negative control was performed by omitting biotin-16-dUTP from the TUNEL reaction. The reaction was terminated by washing the sections in saline sodium citrate solution (30 mM $Na_3C_6H_5O_7$ containing 300 mM NaCl; both from Sigma-Aldrich) for 15 mins. After rinsing in PBS, non-specific binding sites were blocked with 2% BSA-PBS for 20 mins at RT. Sections were then rinsed in PBS and incubated with the same blocking solution containing streptavidin–Alexafluor 488 or 555 conjugate (1:700; Molecular Probes/Thermo Fisher) for 30 mins at 37 °C. After rinsing with PBS, sections were mounted using anti-fade mounting medium containing DAPI for visualisation of cell nuclei and quantified under the Nikon Eclipse 80i microscope with 20 x magnifications.

A combination of immunofluorescent staining and TUNEL assay was performed in order to detect the presence of apoptotic oligodendrocytes. Briefly, following the immunofluorescent staining with the anti-Olig2 antibody, sections were washed in PBS and the TUNEL assay was performed.

3.10 Western blotting

The expression of different proteins during the course of the disease was examined by Western blotting. Briefly, samples containing 50 µg of total protein were diluted in 2x sample buffer (Anamed Elektrophorese, Groß-Bieberau, Germany) and incubated at 95°C for 10 mins. Samples were loaded onto a 4–20 % gradient Mini-PROTEAN® TGX Stain-Free™ Precast gels (BioRad, Hercules, California, USA). Proteins were separated by sodium dodecyl sulfate polyacrylamide gel electrophoresis (SDS-PAGE) for 1hr and 20 mins at 120 V in a running buffer containing 25 mM Tris Base (Carl Roth), 190 mM glycine (Sigma) and 0.1% SDS (Carl Roth). Following electrophoresis, proteins were transferred to a polyvinylidene difluoride (PVDF) membrane (BioRad) with the semi-dry blotting technique using Trans-Blot® Turbo™ Transfer System (BioRad). Different blotting settings (provided by the transfer system) were utilized depending on the molecular weight of the protein investigated. A successful transfer was confirmed by staining the membrane with Ponceau (Sigma-Aldrich).

The membrane was blocked with the appropriate agent in 0.1% TBS-T for 1 hr at RT and incubated with appropriate antibody in the same buffer overnight at 4°C. On the following day, the membrane was washed in TBS-T and incubated with the corresponding HRP-conjugated secondary antibody for 1 hr at RT. A list of different blocking agents and primary/secondary antibodies is given in Table 3.4. Following the washing step, the membrane was incubated with the ECL Prime reagent (Amersham, USA) for one minute and imaged using the ChemiDoc™ XRS+ Imaging System (BioRad).

Protein expression was measured by ImageJ software using the images generated with the imaging system. The expression of the protein in the sample was normalised to the expression of the house-keeping protein Glyceraldehyde 3-phosphate dehydrogenase (GAPDH, mouse antibody, clone 6C5, Millipore). A minimum of 3 samples per time point were used in the final quantification for each protein.

Protein	Blocking buffer	Primary antibody dilution	Secondary antibody
Caspr	5% milk 0.1% TBS-T	1:1000	Donkey anti-rabbit HRP-conjugated, 1:5000
Contactin-1	5% milk 0.1% TBS-T	1:100	Donkey anti-goat HRP-conjugated, 1:5000
Non-phosphorylated neurofilaments (SMI32)	5% BSA 0.1% TBS-T	1:2000	Sheep anti-mouse HRP-conjugated, 1:5000
αB-crystallin	5% BSA 0.1% TBS-T	1:500	Sheep anti-mouse HRP-conjugated, 1:5000
GAPDH	5% milk 0.1% TBS-T	1:250	Sheep anti-mouse HRP-conjugated, 1:5000

Table 3.4 Combination of different blocking agents and primary/secondary antibodies for Western blotting. All secondary antibodies were purchased from Amersham (Buckinghamshire, GB).

3.11 Enzyme-linked immunosorbent assay (ELISA) for detection of MOG antibodies in the serum

The titres of MOG antibody in the sera of animals were measured with the ELISA protocol adapted from Lindner et al. 2013. Transparent 96 well plates were coated with 5 µg/ml of whole recombinant MOG protein in PBS and kept overnight at 4°C. On the following day, wells were washed 3 times with

0.05% PBS-T and blocked with 1% BSA/PBS for 1 hr at 37°C. Following a further washing step, sera from different time points during the disease was applied and incubated for 1 hr at 37° C. Three different dilutions of the sera in the blocking buffer were used (1:1000, 1:10,000 and 1:100,000) with each dilution used in duplicate. After incubation with serum, wells were washed and incubated with an HRP-conjugated goat anti-rat secondary antibody (polyclonal IgG; Imgenex, Littleton, Colorado, USA) 1:5000 in the blocking buffer for 1 hr at 37° C. Following the final washing step, a colorimetric reaction was performed by the addition of tetramethylbenzidine (TMB) substrate (eBioscience, San Diego, California, USA). After 15 minutes at RT, the reaction was stopped by the addition of 0.16 M H_2SO_4 and the absorbance was measured at 450 nm.

3.12 Treatment with ROS/RNS scavengers

In order to the investigate a possible role of ROS/RNS in the optic nerve pathology during the induction phase of AON, a treatment study was performed with a cocktail of 3 different scavengers of these reactive species. Eight BN rats, immunised with MOG, were divided into 2 experimental groups – one receiving the cocktail (n=4) and the control group receiving the equivalent dimethyl sulfoxide (DMSO; 3%; Carl Roth) solvent (n=4). The volume of both control and treatment i.p. injections was 500 µl.

The cocktail consisted of:

- 20 mg/kg FeTPPS (5,10,15,20-Tetrakis(4-sulfonatophenyl)porphyrinato Iron (III), Chloride; Calbiochem/Millipore)
- 50 mg/kg PBN (N-tert-Butyl-α-phenylnitrone; Sigma-Aldrich)
- 15 mg/kg EUK134 (chloro((2,2‘-(1,2ethanediyl*bis*((nitrilo-kN)methylidyne))*bis*(6-methoxyphenolato-kO))) -manganese; Cayman chemical, Ann Arbor, Michigan, USA) dissolved in 3% DMSO.

Daily treatment with i.p. injections commenced at day 5 p.i. On the day of the final injection (at day 10 p.i.), animals were sacrificed with ketamine/xylazine overdose, perfused and optic nerves processed for longitudinal sections (Figure 3.1).

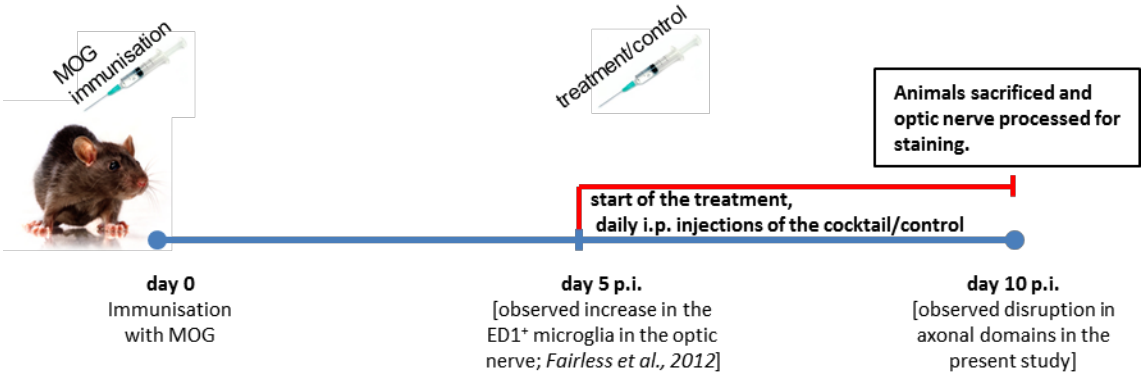

Figure 3.1. ROS/RNS scavenger treatment study plan.

3.13 Intravitreal injection of glutamate

In order to induce a primary retinal insult, eight to ten-week-old BN rats were injected intravitreally with glutamate. Animals were kept under anaesthesia by inhalation of 5% isoflurane. In total, 100 nM of glutamate (4 µl of 25 mM glutamate in saline) was injected intravitreally using a 10 µl Hamilton syringe over the course of 5 minutes. Seven days following the injection, animals were sacrificed with ketamine/xylazine overdose, perfused and optic nerves were dissected and processed for longitudinal sections.

3.14 Serum transfer

Blood was collected by heart puncture from MOG immunised BN rats at both day 10 p.i. and at the onset of EAE. Serum was extracted from the blood and concentrated by centrifugation in Amicon® Ultra 15 mL centrifugal filters (Millipore) for 30 mins at 3000g at 4° C. Serum from 2 day 10 p.i. animals was pooled and concentrated 2 times and serum from individual EAE animals was concentrated 4 times. A volume of 1000 µl of concentrated sera was injected intravenously via the tail vein of naïve BN rats under isoflurane anaesthesia. Blood samples were collected from recipient animals prior to and at days 1 and 3 post serum-transfer (pst). At day 5 pst, animals were overdosed with ketamine/xylasine. Blood was collected by heart puncture, animals were perfused and optic nerves processed for longitudinal sections. The process of sera isolation from blood samples is described in section 3.5.3. The titre of MOG antibodies in the serum at different time points throughout the experiment was determined by ELISA (as described in section 3.11).

3.15 Statistical analyses

Measurements of axonal disruptions and microglia distribution were quantified in a blinded manner using images acquired by either standard fluorescence or confocal microscopy. All data are presented as their mean values ± standard error of the mean (SEM). Statistical significance was assessed by using the appropriate tests provided by the SigmaPlot 12.5 software. For comparing two experimental groups, statistical significance was assessed first for normalcy by Shapiro-Wilk test followed by either two-tailed student's t-test (for normally distributed data) or by Mann-Whitney rank sum test (for not normally distributed data). One way analysis of variance (ANOVA) combined with Dunnett's method was used for comparing multiple experimental groups versus controls. Two levels of significance were defined: p value ≤ 0.05 was considered significant and p value ≤ 0.01 was considered highly significant.

4 Results

4.1 Characterisation of the visual function and optic nerve pathology during the course of AON in the MOG-EAE model in BN rats

4.1.1 Disease course

Following immunisation with MOG, female BN rats develop the progressive form of EAE characterised by extensive demyelinating lesions in the spinal cord. The disease symptoms are presented with ascending paralysis of the tail and limbs, with typical onset around 2 weeks following immunisation. In addition to the classical, paralytic EAE disease course representing lesions in the spinal cord, BN rats develop AON with high incidence. The onset of AON is timed with the onset of EAE neurological deficits (Fairless et al., 2012).

Following immunisation with MOG, rats were scored daily for the appearance of signs of neurological deficits. The average day of onset of the disease was between day 13 and 14 p.i. with the symptoms starting as early as day 11 post immunisation (13.64 ± 0.68 days p.i.; n = 15; Figure 4.1). In addition to healthy, unimmunised animals, sham immunised animals were also used as controls. These animals failed to develop any signs of neurological deficits or AON.

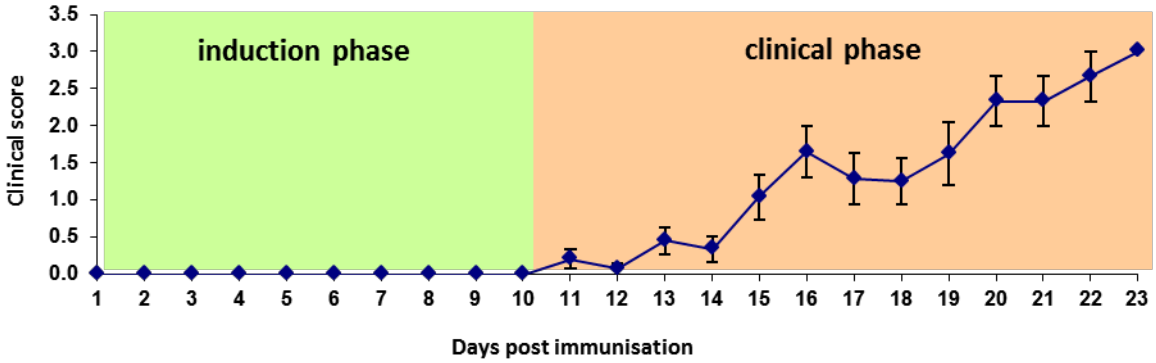

Figure 4.1. MOG-EAE disease course. In its initial stage MOG-EAE is characterised by a clinically silent phase (induction phase). This is followed by the clinical phase, characterised with progressive neurological deficits. The grading system for scoring neurological deficits is explained in Table 3.1. (n = 15 animals).

4.1.2 Impairment in visual functions precedes the onset of the clinical phase of disease

Recordings of VEPs in response to both pattern and flash stimuli were used to investigate visual function of the optic system during the course of the disease. Animals were subjected to visual testing prior to immunisation, during the induction phase (on days 5 and 10 p.i.) and at the onset of the clinical phase of the disease when they reached a clinical score of 1.0 (day 1 or 2 of EAE).

The response to flash stimuli in healthy animals was observed as a waveform with a small positive peak (P1) followed by a large negative peak (N1) and a second positive peak (P2; Figure 4.2A). The amplitude and the latency of the signal were measured between N1 and P2 peak (Figure 4.2A). The average signal latency measured in healthy animals was 32.18 ± 1.62 ms and the average signal amplitude was 129.25 ± 13.27 µV. Response to flash stimuli did not change during the induction phase – no decrease in amplitude (day 5 p.i. 147.36 ± 13.39 µV; day 10 p.i. 150.15 ± 16.36 µV) or increase in latency could be detected (day 5 p.i. 32.53 ± 2.67 ms; day 10 p.i. 37.42 ± 2.61 ms). Upon developing AON, the response to flash stimulus was altered with a significant decrease in amplitude (EAE 64.48 ± 15.86 µV; $p < 0.01$; Figure 4.2C) and an increase in signal latency (EAE 63.56 ± 4.79 ms; $p < 0.001$; Figure 4.2D). Sham immunised animals, used as controls, did not have altered responses to flash stimuli up to two weeks post-immunisation (Figure 4.2E, F).

Following the final recording animals were sacrifices and optic nerves were examined for the presence of AON-related pathology. Histological staining with LFB showed the presence of demyelinated areas with an increased cellular count indicative of inflammation (observed by counter-staining of cell nuclei with haematoxylin) in the optic nerves of MOG immunised animals (Figure 4.2G, Gi). This was not observed in sham immunised animals at the equivalent time points (day 15 following sham immunisation; Figure 4.4H, Hi).

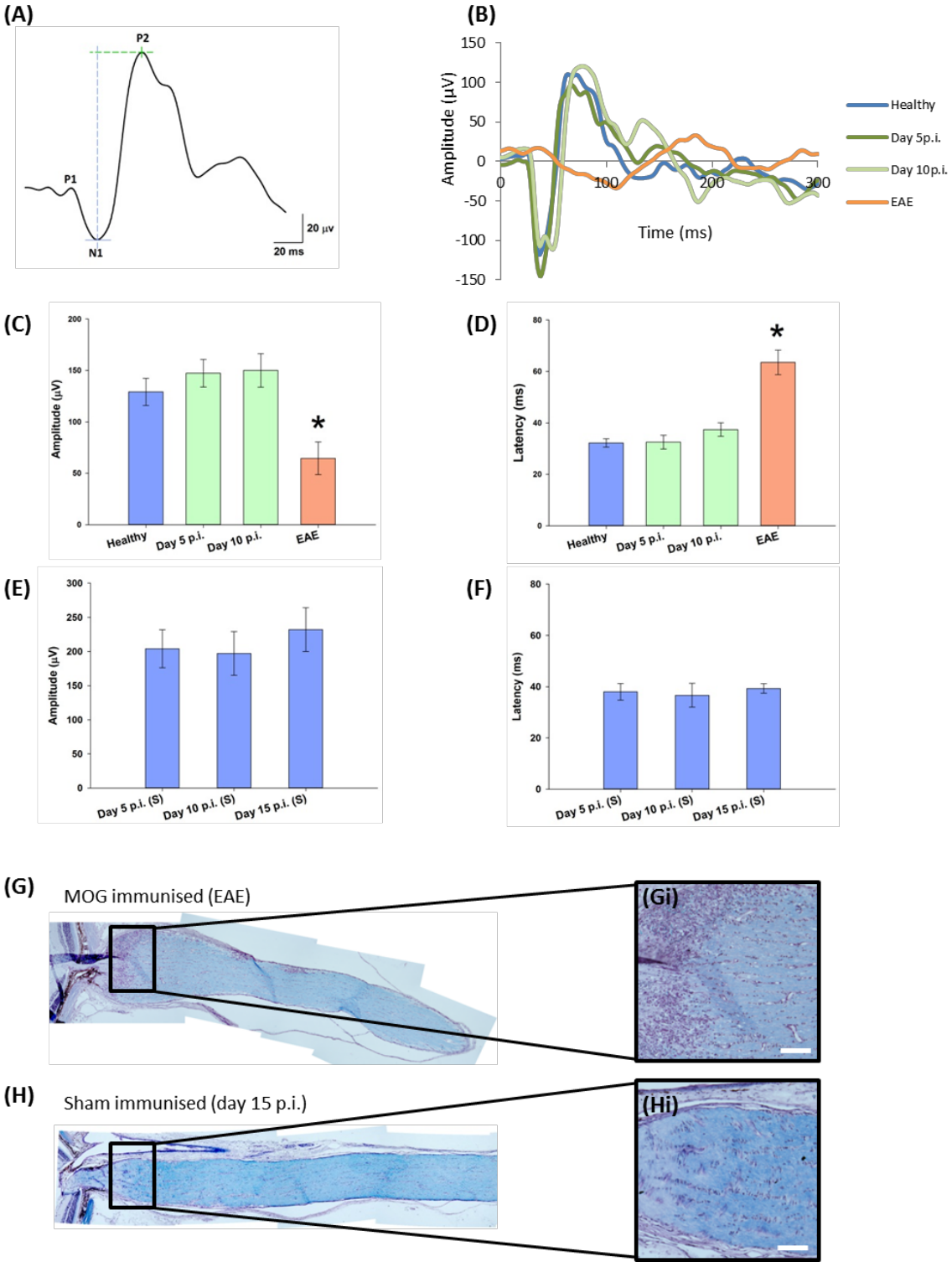

Figure 4.2. Visual evoked response to flash stimuli during AON. (A) Typical waveform of flash VEP (blue and green lines represent the measurements of the amplitude and the latency of the signal). (B) Representative responses to flash stimuli at different time points during the disease course. Quantification of signal amplitudes and latencies to flash stimuli in MOG (C and D respectively; n = 8) and sham immunised animals (E and F respectively; n = 4). Statistical significant decrease in signal amplitude (* $p < 0.01$ compared to healthy, ANOVA) and increase in latency (* $p < 0.01$ compared to healthy, ANOVA) was observed in following the onset of the clinical phase of disease but not in sham-immunised animals at equivalent time points. Histological staining with LFB showed the presence of AON in MOG-immunised animals following the onset of the clinical phase of the disease (G, Gi) but not in sham-immunised animals at equivalent time point (H, Hi).

Pattern VEP recordings were performed in order to asses the visual acuity of animals during the course of the disease. VEP responses to pattern stimuli are considered to be more sensitive to pathological alterations within the optic system than those in response to flash stimuli. Prior to immunisation, all animals were able to respond to the full range of low-contrast stimuli (66% contrast of alternating bars) from the simplest to the most complex pattern (vusial acuity 0.89 ± 0 c/deg). In the early in the induction phase (day 5 p.i.) animals did not show significant reduction in visual acuity (0.67 ± 0.11 vs. 0.89 ± 0 c/deg in healthy, $p = 0.16$). Only 3 out of 7 animals failed to respond to the most complex stimulus (32 bars). However, in the late induction phase (day 10 p.i.) animals did show significant reduction in visual acuity (0.44 ± 0.12 c/deg vs. 0.89 ± 0 c/deg in healthy, $p = 0.002$) with four out of 7 animals not responding to patterns with a complexity of 8 or more bars. With the onset of AON visual acuity was almost completely lost (0.09 ± 0.04 c/deg vs. 0.89 ± 0 c/deg in healthy, $p < 0.001$). Three out of 7 animals failed to respond even to the simplest pattern presented (2 bars). In animals that responded to pattern stimulation (4 out of 7) the maximal stimulus that evoked a response was either 2 (n = 2) or 8 bars (n = 2). Sham immunised animals retained full visual acuity throughout the course of the experiment (Figure 4.3C).

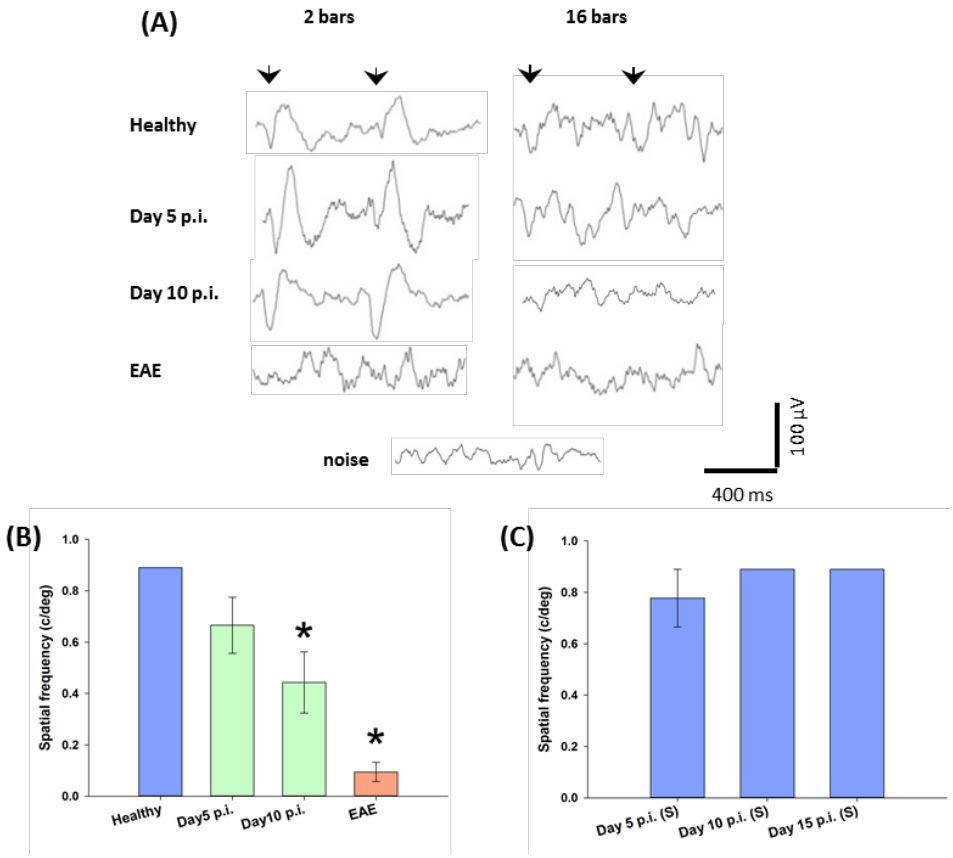

Figure 4.3. Visual response to pattern stimuli during AON. (A) Representative traces in response to 2 and 16 bar stimuli throughout EAE time course. Arrows indicate the timing of pattern reversal. (B) Significant decrease in visual acuity was detected starting from the late induction phase of the disease (***** $p < 0.01$, ANOVA; n = 7). (C) Sham immunisation did not affect visual acuity of animals at equivalent time-points (n = 4).

4.1.3 Inflammatory demyelination of the optic nerve is timed with the onset of the clinical phase of disease

In order to determine structural correlates of the imapaired visual functions observed during the course of disease optic nerves were processesd for histological and immunhistochemical staining. Longitudinal sections of nerves from different time points during the disease course were stained with LFB to investigate myelianation status durin the disease course. In parallel, sections were stained with antibodies against both the axonal and the myelin components: SMI 312, a pan axonal marker; and an antibody against MBP (Figure 4.4).

Apart from the initial segment of the optic nerve (ONH) and the retinal nerve fibre layer, axons in healthy animals are fully myelinated as assessed by both LFB staining and double immunofluorescent staining with markers for both axons and myelin (Figure 4.4Bi - Ciii). In the late induction phase, at the same time that a decrease in visual acuity was observed, there was no change in the myelination

status of the optic nerve axons (Figure 4.4Di - Eiii). Following the onset of the clinical phase, a pathology characteristic of AON could be detected. That is, demyelinating lesions containing increased hypercellularity could be detected along the optic nerve as early as day 1 of EAE (Figure 4.4Fi - Giii).

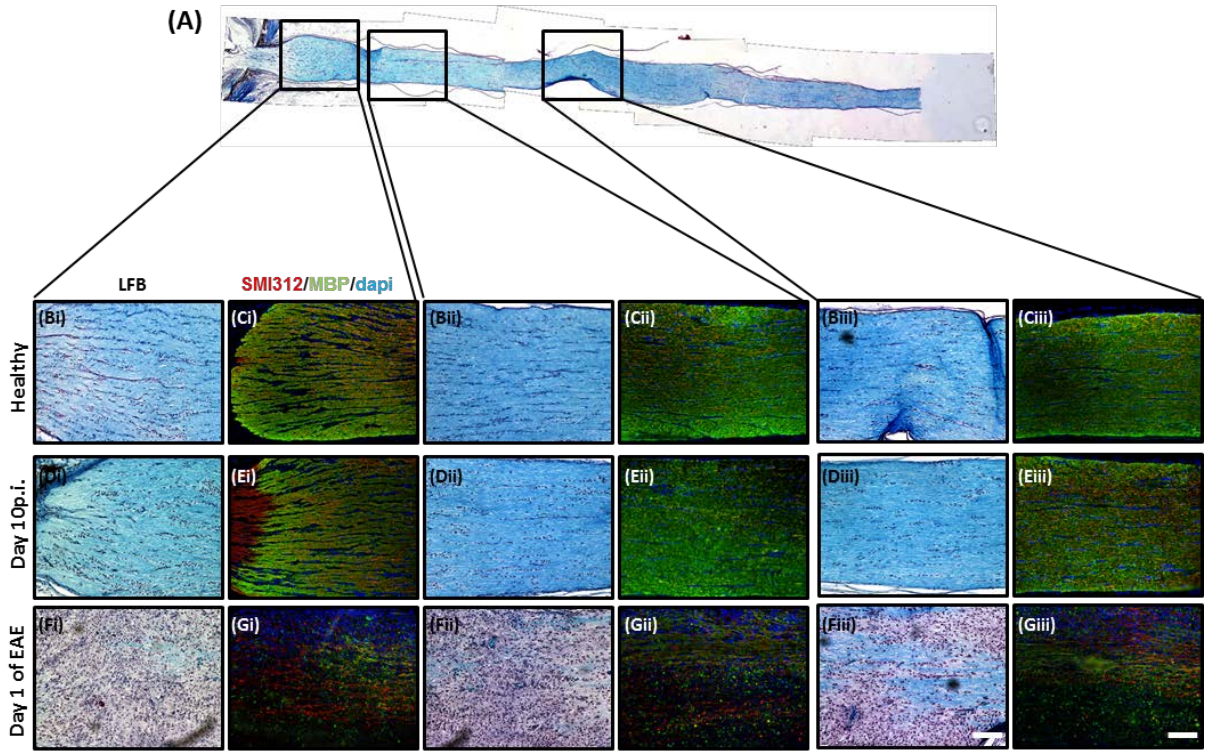

Figure 4.4. Inflammatory demyelination starts with the onset of the clinical phase of AON. (A) Example image of a healthy optic nerve stained with LFB. Black squares indicate optic nerve segments displayed in the panel below at different time points along the course of AON. Representative longitudinal sections of the optic nerve throughout the AON time course stained with LFB and antibodies against MBP (green) and SMI 312 (red) – healthy (Bi – Ciii), day 10 p.i. (Di – Eiii) and onset of the clinical phase of AON (Fi - Giii). Large areas of demyelination are observed with the onset of the clinical phase of AON (Fi - Giii). Scale bars 100 µm.

Inflammatory lesion were characterised with numerous cells positive for CD68 (ED1) – a glycoprotein expressed on tissue macrophages and blood derived monocytes. These cells were characterised by a foamy morphology characteristic of reactive macrophages (Figure 4.5A - Bi). The majority of $ED1^+$ macrophages were found in areas of demyelination (Figure 4.5A, Ai) and axonal stress, assessed by staining with SMI32 (Figure 4.5B, Bi). Within these areas macrophages are often found with the presence of MBP^+ structures in their cytoplasm, indicative of their role in phagocytosis of myelin components under inflammatory conditions (figure 4.5Ai). A marked presence of axonal pathology is evident within these areas of inflammation. Many swollen axons could be found within areas of macrophage infiltration (figure 4.5Bi). Within the lesion centre many of the $SMI32^+$ axons were

completely demyelinated (figure 4.5Ci) whereas, towards the lesion border swollen axons still associated with myelin sheets could be detected (figure 4.5Ci).

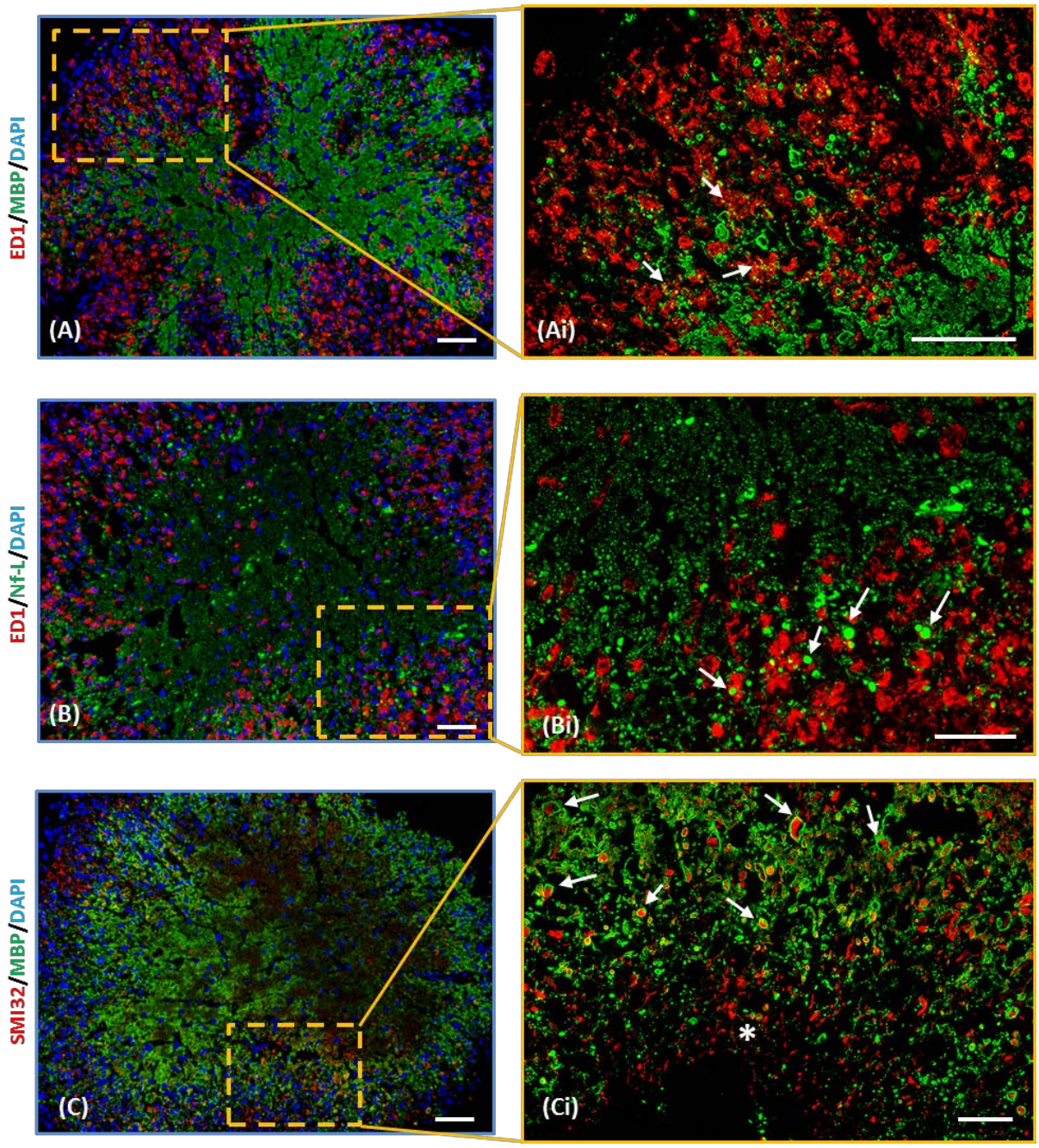

Figure 4.5. Optic nerve pathology following the onset of the clinical phase of AON. Optic nerve cross sections from the onset of AON (day 1 EAE) stained with markers for myelin (myelin basic protein – MBP; A, Ai, C, Ci - green), axons (neurofilament light – Nf-L; B, Bi – green; Non-phosphorylated neurofilaments – SMI32; C, Ci - red) and activated microglia/macrophage (ED1; A, Ai, B, Bi - red). $ED1^+$ microglia/macrophages are observed in areas of demyelination (A, Ai) and axonal stress, indicated by swollen Nf-L positive axons (Bi, arrows). Furthermore, MBP^+ particles are found in $ED1^+$ cells within demyelinated areas implying their role in phagocytosis of myelin (Ai, arrows). Many swollen, $SMI32^+$ axons with preserved myelin sheaths (Ci, arrows) are detected at the edges of demyelinating lesions (Ci, asterisk) following the onset of the clinical phase of AON. Scale bars 50 µm.

In addition to signs of axonal pathology (observed by demyelination and swellings) a reduction in axonal densities could be observed from the onset of the clinical phase of the disease (Figure 4.6C). As the disease progresses there are only few axons still remaining in the optic nerve (Figure 4.6D).

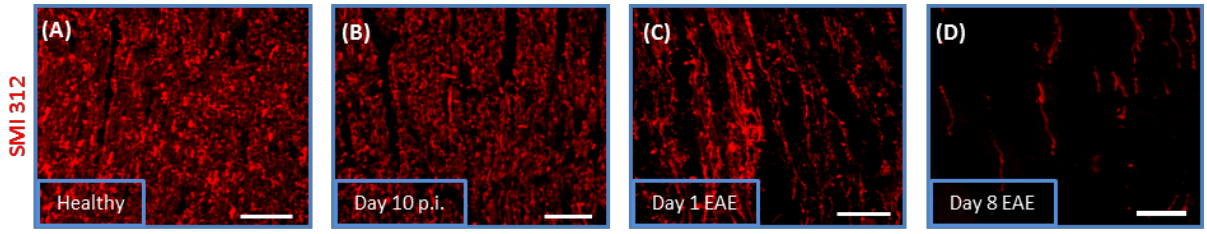

Figure 4.6. Reduction in axonal densities starts with the onset of the clinical phase of AON. Staining with pan-axonal marker (SMI312) revealed the presence of axonal loss in optic nerves during the clinical phase of disease (C, D). Scale bars 100 µm.

4.2 Evidence of cellular stress in different compartments precedes the onset of AON

4.2.1 Loss of axonal domains observed with the onset of AON

A proper organization of highly specialised axonal domains is necessary for efficient signal conduction along myelinated axons. Considering that a decrease in visual acuity was observed during the induction phase in the absence of axonal loss and demyelination, a detailed examination of axonal structures with particular focus on nodal and paranodal domains was performed. Investigation of axonal domains was performed with the use of different antibodies recognizing different molecular components of axonal domains (Figure 1.5Ci - Fiii). Antibodies against Na_v and Neurofascin 186 were used as markers of nodal domains while antibodies against Caspr and Contactin-1 were used to label paranodal domains (see Figure 1.5 in Introduction for details).

Longitudinal optic nerve sections were stained with antibodies against Caspr and Na_v for the purpose of quantifying the numbers of axonal domains at different time points along the course of AON (Figure 4.7A - E). Only complete axonal domains consisting of Na_v^+ nodes flanked by $Caspr^+$ paranodes on both sides were counted. There was no significant difference in the numbers of axonal domains between healthy (7317.33 ± 356.88 paranodes per mm^2) and optic nerves from animals during the induction phase (6344.89 ± 268.97 at day 10 p.i.). Upon development of AON a substantial reduction in the numbers of the axonal domains could be observed. Already at the onset of the

clinical phase of the disease a 50 % reduction was observed (day 1 EAE, 3667.56 ± 334.95; 50.12 % of the healthy value; $p < 0.001$). As the disease progresses this effect becomes more pronounced where only one third of the healthy value could be detected (day 4 EAE, 2433.78 ± 303.53; 33.26% of the healthy value; $p < 0.001$). Following the onset of AON the reduction in density of axonal domains could be observed within inflammatory lesions (as observed with the increased cellular count with nuclear labelling with dapi). The extent of axonal domain loss following the onset of the clinical phase of disease correlates with the previously reported extent of demyelination (Fairless et al., 2012).

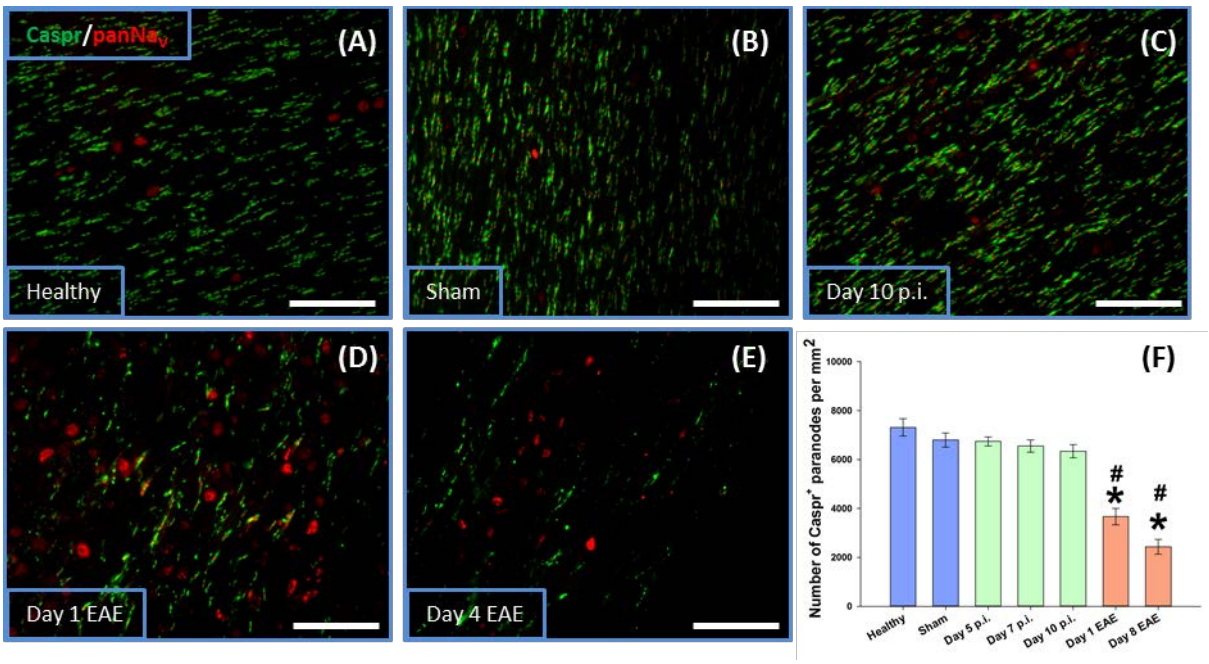

Figure 4.7. Loss of axonal domains starts with the clinical phase of AON. Representative images of optic nerves stained with antibodies against Caspr (green) and Na_V (red) in healthy (A), sham (B), day 10 p.i. (C) and in animals during the clinical phase of disease (day 1 EAE, D and day 4 EAE, E). (F) A significant reduction in axonal domains was observed with the onset of the clinical phase of AON (* $p < 0.01$ compared to healthy; $^{\#}$ $p < 0.01$ compared to sham, ANOVA; n = 6 animals per time point, except in sham where n = 3). Scale bars 50 µm.

In order to confirm the reduction of axonal domains with onset of the clinical phase of AON observed by immunofluorescent staining, quantification of axonal paranodal proteins (caspr and contactin-1) in optic nerve was performed by Western blotting. Significant reduction of Caspr and Contactin-1 protein levels in optic nerve lysates was detected from the onset of the clinical phase of the disease by Western blotting (figure 4.8).

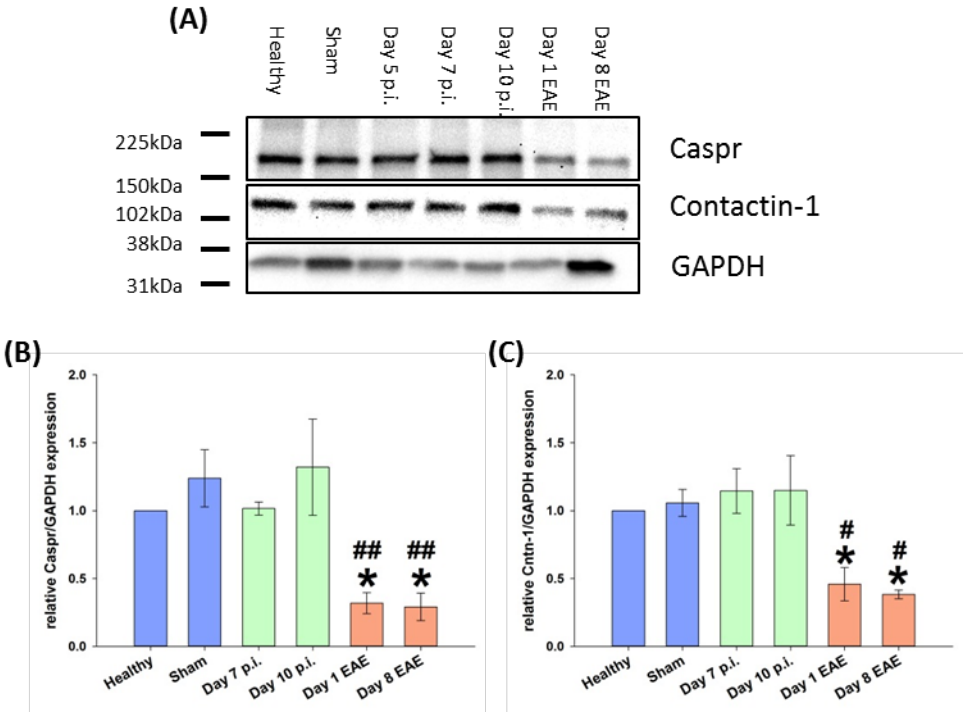

Figure 4.8. Reduction in expression of paranodal proteins starts with the onset of the clinical phase of AON. (A) Representative Western blots incubated with antibodies against Caspr (180 kDa), Contactin-1 (118 kDa) and GAPDH (38 kDa). Statistically significant decreases in both Caspr and Contactin - 1 were seen with the onset of the clinical phase of disease (B and C respectively; * $p < 0.05$ to compared healthy, $^{\#}$ $p < 0.05$ and $^{\#\#}$ $p < 0.01$ compared to sham, ANOVA; n = 5 samples per time point).

4.2.2 Disruption in axonal domain architecture precedes the onset of the clinical phase of AON

Upon quantification of the axonal domains throughout time course of AON subtle changes in their morphology were observed already during the induction phase of AON, preceding their loss. In healthy animals axonal domains occurred as dense clusters of Na_V reactivity flanked by compact $Caspr^+$ paranodes (figure 4.9A). At the late stage of the induction phase (at day 10 p.i.) a substantial portion of axonal domains appeared with altered architecture. Both the nodal gap (stained with pan-Na^V antibody) and the $Caspr^+$ paranodal domains appeared with diffuse and elongated profiles (Figure 4.9B). Measurements of the length of both nodal and paranodal domains throughout the course of AON revealed statistically significant elongation in both compartments starting from the late induction phase (day 10 p.i.). The criteria for inclusion was identical to one used for quantification of axonal domains – the length of axonal domains was measured only in axons with a pan-Na_V^+ nodal gap flanked by two $Caspr^+$ paranodes.

In healthy animals, the average length of the pan-Na_V^+ nodal domain was 1.27 ± 0.02 µm (n = 1450 nodes measured from 6 different animals, lengths ranging from 0.64 to 2.66 µm). At day 10 p.i. a significant elongation in the nodal domain could be observed. The average length of Na_V^+ nodes was 1.66 ± 0.03 µm (n = 1500 nodes / 6 animals, lengths 0.75 - 5.56 µm, $p < 0.001$). The average length of $Caspr^+$ paranodal domains in healthy animals was 3.23 ± 0.08 µm (n = 1450 paranodes / 6 animals, lengths 1.71 - 6.64 µm). Significant elongation was also observed in the paranodal domain at day 10 p.i.. The average length of the $Caspr^+$ paranodes was 3.58 ± 0.07 µm (n = 1500 paranodes / 6 animals, lengths 1.73 - 7.53 µm, $p = 0.003$). With onset of AON, this phenomenon became more pronounced with some axons appearing with swellings in the paranodal domains (figure 4.10C, Ci). The average length of a nodal domain at day 1 of EAE was 2.11 ± 0.05 µm (n = 1450 nodes / 6 animals, lengths 0.93 - 10.53 µm, $p < 0.001$) and at day 4 of EAE it was 2.02 ± 0.08 µm (n = 1709 nodes / 6 animals, lengths 0.84 - 12.14 µm, $p < 0.001$). The average length of the paranodal domains at day 1 of EAE was 3.59 ± 0.07 µm (n = 1425 paranodes / 6 animals, lengths 1.9 - 7.38 µm, $p = 0.002$) and at day 4 of EAE it was 3.82 ± 0.05 µm (n = 1615 paranodes / 6 animals, lengths 1.76 - 8.23 µm, $p < 0.001$). Within demyelinated lesions, axonal domains were completely disrupted with only traces of Caspr immunoreactivity detectable on $SMI32^+$ stressed axons (figure 4.9I). Following demyelination, and in the absence of paranodal regions Na_V reactivity was dispersed along naked axons (figure 4.9J). Identical staining patterns were observed with antibodies against other components of nodal (Neurofascin 186) and paranodal domains (pan-Neurofascin, Contactin-1) throughout the course of AON (data not shown).

In order to further investigate these observations, electron microscopy was employed to analyse the ultrastructure of axonal domains. Similar patterns were observed upon examining the ultrastructure of axonal domains by electron microscopy. In healthy animals, myelinating loops of oligodendrocytes were tightly anchored in the paranodal regions of the axon which were separated by an unmyelinated nodal gap (Figure 4.10D). At day 10 p.i., although axons were still ensheathed with compact myelin, subtle changes could also be detected in their domains. Detachment of myelinating loops from the paranodal domains and a widening of the nodal gap could be observed on some axons (Figure 4.10E). Following the onset of AON, paranodal regions were found with clear signs of early pathology characterised by detachment of myelinating loops and an “unravelling” of the myelin sheath (Figure 4.10F).

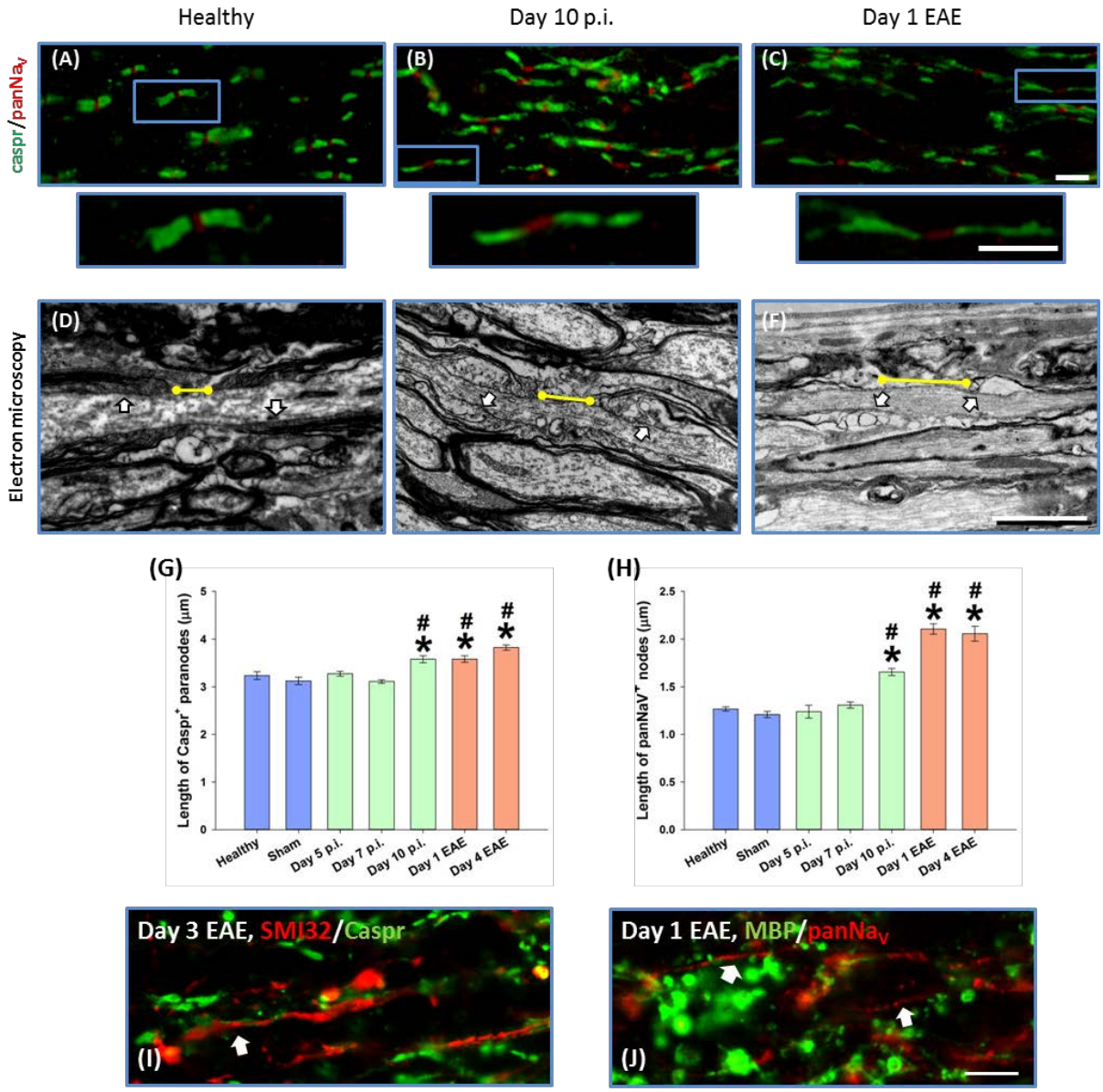

Figure 4.9. Disruption of axonal domains starts during the induction phase of the disease. A double staining with pan-NaV (red) and Caspr (green) was used to investigate the integrity of nodal and paranodal domains (respectively) throughout the disease course (A-C). Ultrastructure of axonal domains by electron microscopy reflects the patterns observed with immunostaining (D-F; yellow lines indicate the length of the nodal domains, arrows indicate paranodal domains). Quantification of axonal domains from immunostaining show statistically significant elongation in both paranodal (G) and nodal (H) domains starting from the end of the induction phase (* $p < 0.01$ compared to healthy, # $p < 0.01$ compared to sham, ANOVA; n = 6 per time point). (I) Representative image of a stressed $SMI32^+$ axon within demyelinating lesion with only traces of Caspr immunoreactivity present on disrupted paranodal domain (arrow). (J) Diffuse Na_V distribution along demyelinated axons (arrows). Scale bars: A – C, J and I 5 µm, F 2.5 µm.

4.2.3 Evidence of axonal stress is detected prior to the onset of the clinical phase of AON

Early signs of axonal disruption were detected in the nodal and paranodal domains prior to the onset of inflammatory demyelination. Paranodal domains form the contact zone between axons and glia where myelination loops of oligodendrocytes anchor to the axon. For the purpose of investigating the presence of axonal stress throughout the course of AON a double staining with SMI32 (an antibody recognising non-phosphorylated neurofilaments, npNF, a stress marker for myelinated axons; Trap et al., 1998) and MBP was performed on longitudinal optic nerve sections. Considering that NF are often hypophosphorylated in the unmyelinated nodal region (Howell et al., 2011 and author's own observation) only $SMI32^+$ structures longer than 20 µm were counted.

In healthy optic nerves, SMI32 immunoreactivity was detected mainly on the unmyelinated nodal regions and only the odd $SMI32^+$ axon could be detected (Figure 4.10A, Ai; 167.53 ± 23.14 $SMI32^+$ axons/mm^2). Similar staining pattern was observed in the induction phase, at day 7 p.i. (figure 4.10B, Bi; 208.82 ± 39.67 $SMI32^+$ axons/mm^2). In the late induction phase, when a decrease in visual acuity and a disruption in axonal domains was observed (day 10 p.i.), a statistically significant increase in $SMI32^+$ axons was detected (figure 4.10C; 394.06 ± 31.54 $SMI32^+$ axons/mm^2, $p = 0.02$). These axons were still myelinated, as demonstrated by double staining with MBP (figure 4.10Ci). Following the onset of AON, a marked presence of $SMI32^+$ axons was detected (figure 4.10D; 816.74 ± 99.42 $SMI32^+$ axons/mm^2, $p < 0.001$), both in the demyelinated lesion centre and on the lesion border where axons were still myelinated (figure 4.10Di).

The observed increase in the npNF was confirmed by Western blotting. A statistically significant increase in npNF could be detected in optic nerve lysates at day 10 p.i. (figure 4.10G, $p = 0.009$) and day 1 of EAE (figure 4.10G, $p < 0.001$).

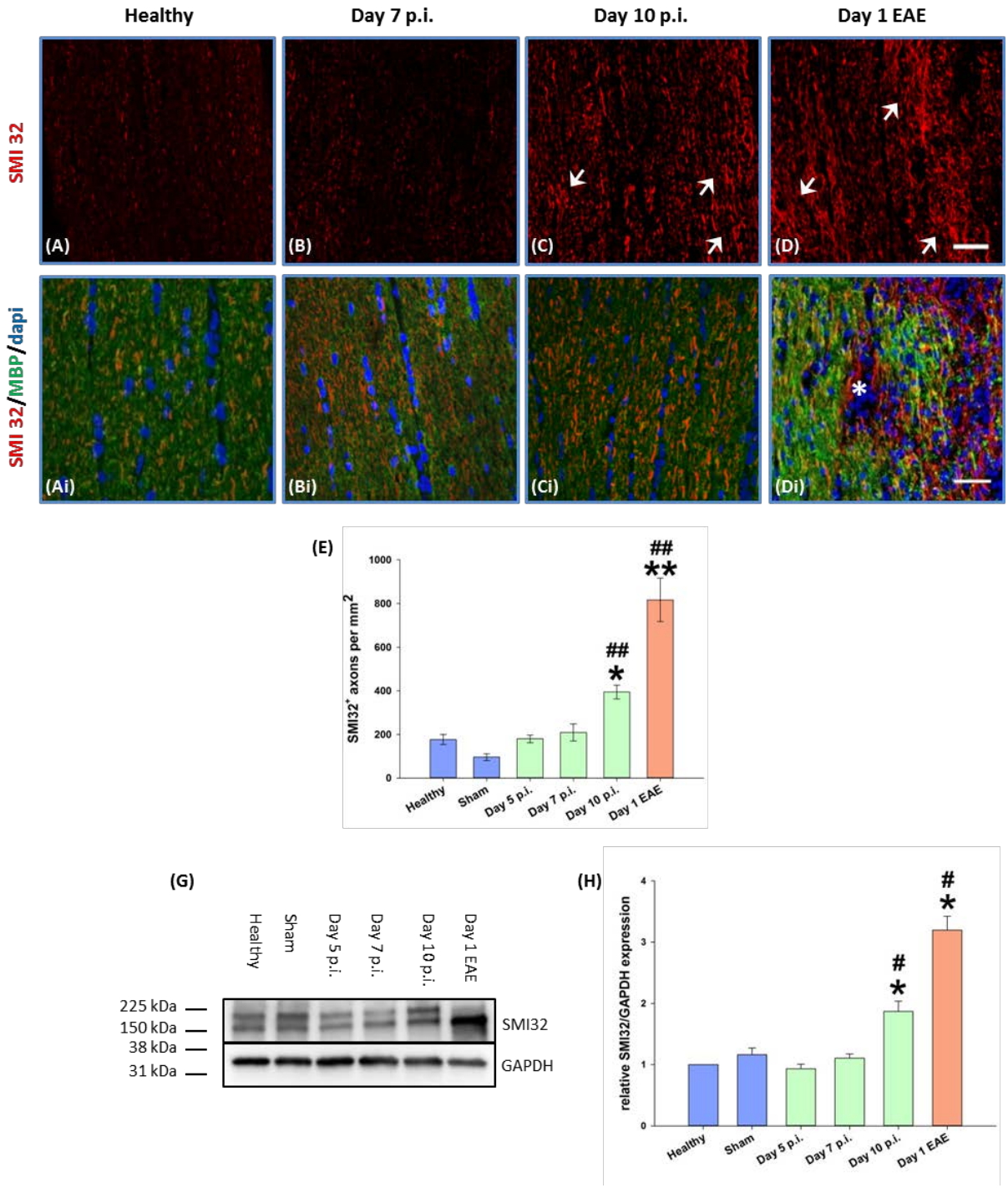

Figure 4.10. Increased presence of npNF observed from the induction phase of AON. Representative images of optic nerves from healthy (A, Ai), day 7 p.i. (B, Bi), day 10 p.i. (C, Ci) and day 1 EAE (D, Di) animals stained with SMI32 and MBP antibodies. Arrows indicate the presence of $SMI32^{+}$ axons at day 10 p.i. (C) and day 1 of EAE (D). Demyelinating lesion is indicated by asterisk (Di). (E) Statistically significant increase in $SMI32^{+}$ was detected at day 10 p.i. and at the onset of AON. (* $p < 0.05$ and ** $p < 0.01$ compared to healthy. $^{\#\#}$ $p < 0.01$ compared to sham, ANOVA; n = 6 animals per time point for MOG immunised and healthy, n = 3 for sham). Scale bars 50 µm. (F) SMI32 antibody recognises two bands at approximately 180 and 200 kDa. (G) Statistically significant increase of npNF protein levels were detected in the optic nerves at day 10 p.i. and at the onset of AON (* $p < 0.01$ compared to healthy; $^{\#}$ p < compared to sham, ANOVA; n = 3 samples per time point).

The first signs of axonal stress were detected in the late induction phase as indicated by increased npNF staining/blotting. In order to investigate a possible relationship between the cytoskeletal alteration and disruption of axonal domains, a double staining against Caspr and npNF was performed on longitudinal sections of optic nerves form day 10 p.i.. The length of Caspr$^+$ paranodes were measured and compared in respect to their presence on SMI32$^+$ axons (Figure 4.11). The average length of paranodes on SMI32$^+$ was 4.94 ± 0.04 µm (ranging from 2.98 to 9.86 µm), greatly exceeding the average length of paranodes not associated with SMI32 immunoreactivity (3.28 ± 0.02 µm; ranging from 2.04 to 5.26 µm, $p < 0.001$). It should be noted that the average length of SMI32 independent paranodes is similar to those found in healthy animals (3.23 ± 0.08 µm). This suggests a possible connection between the disruption of the axonal cytoskeleton and the paranodal domains.

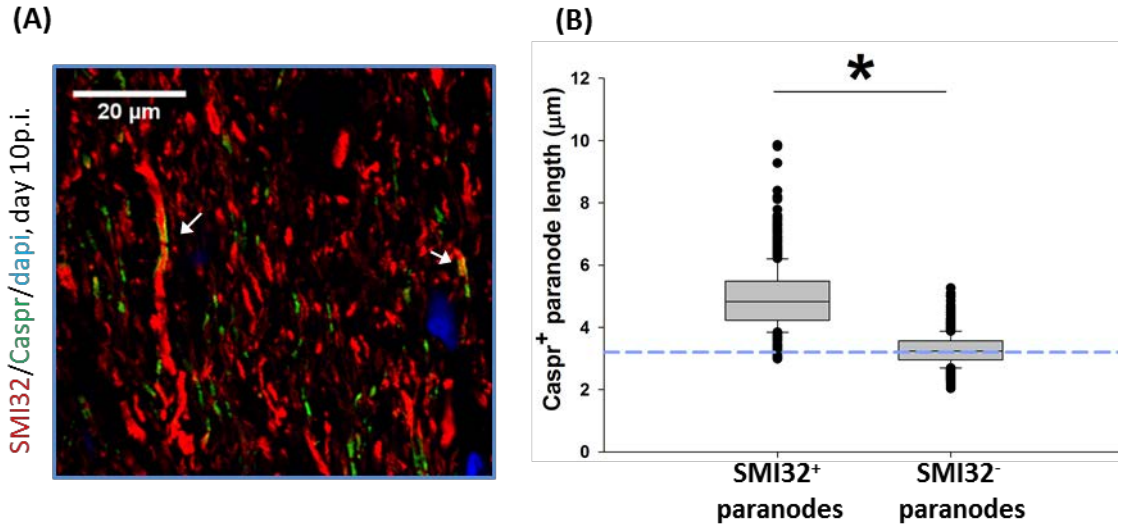

Figure 4.11. Accumulation of npNF correlates with disruption of paranodal domains in the induction phase of AON. (A) Elongated paranodal domains were detected on axons containing npNF (arrows). (B) Statistically significant increase in the length of paranodes associated with SMI32$^+$ axons (* $p < 0.01$, Mann-Whitney Rank Sum Test; n = 716 paranodal domains per group measured from 6 different day 10 p.i. animals). Dashed blue line indicates the average paranodal length in healthy optic nerves.

4.2.4 Apoptosis of oligodendrocytes is not detected before the onset of the clinical phase of AON

In order to investigate whether a disruption in the axo-glial junction in the paranodal domain is triggered by oligodendrocyte apoptosis, a combination of TUNEL labelling and immuno-labelling with Olig2 (a marker for the oligodendrocyte lineage) was performed on optic nerve sections from healthy, day 10 p.i. and animals from the onset of the AON. TUNEL$^+$Olig2$^+$ were absent in both

healthy animals (figure 4.12A) and those from the late induction phase (figure 4.12B). Upon development of AON, double positive cells were detected in the optic nerves. Apoptotic oligodendrocytes were found in associated with inflammatory lesions, indicated by the increased cellular count observed with DAPI (figure 4.12C, D).

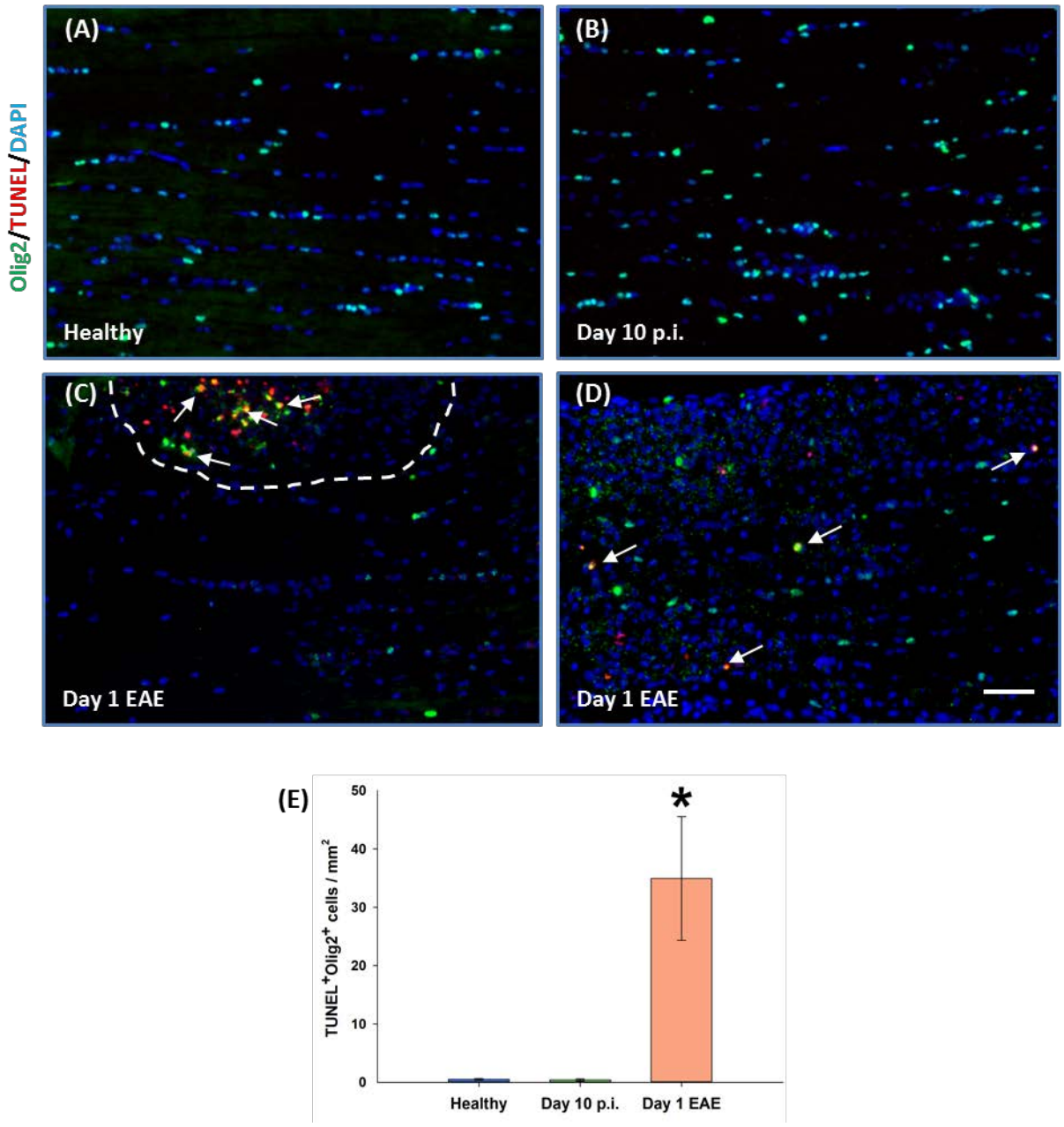

Figure 4.12. Oligodendrocyte apoptosis starts with onset of the clinical phase of AON. Representative images of optic nerves from healthy (A), day 10 p.i. (B) and day 1 EAE (C, D) labelled with TUNEL assay (red) and Olig2 (green). Apoptotic oligodendrocytes could be observed within the inflamed optic nerve (C - lesion indicated with dashed line, D; arrows) from the onset of AON (* $p < 0.01$ compared to healthy, ANOVA). Scale bar 50 µm.

4.2.5 CryαB as a marker of glial stress

Since oligodendrocyte apoptosis was not seen during the induction phase when axonal stress began, the presence of sub-lethal oligodendrocyte stress was also addressed. This was achieved through the detection of alpha B – crystalline (CryαB) - a small heat shock protein expressed by glial cells of the CNS. It is known to be up-regulated in oligodendrocytes in response to oxidative and heat-induced stress (Goldbaum and Richter-Landsberg, 2001). An increase in cryαB in oligodendrocytes has been observed in MS, both during the early stages of lesion development (Bajramovic et al., 1997) and in normal-appearing white matter associated with activation of microglia (van Noort et al., 2010).

The expression of cryαB in different cell types in the optic nerves of BN rats was assessed with double immunostaining using different markers of glial cells. The majority of cryαB$^+$ staining was associated with Olig2$^+$ nuclei (Figure 4.13A) but not with NG2$^+$ (Figure 4.13B, NG2$^+$ indicated with an asterisk) indicating their presence in differentiated oligodendrocytes but not oligodendrocyte precursor cells (OPCs). As expected some of the cryαB staining co-localised with staining for glial fibrillary acidic protein (GFAP), the intermediate filament protein expressed in astrocytes in the CNS (Figure 4.13C). However, staining for cryαB was not detected in ED1$^+$ microglia/macrophages (Figure 4.13D).

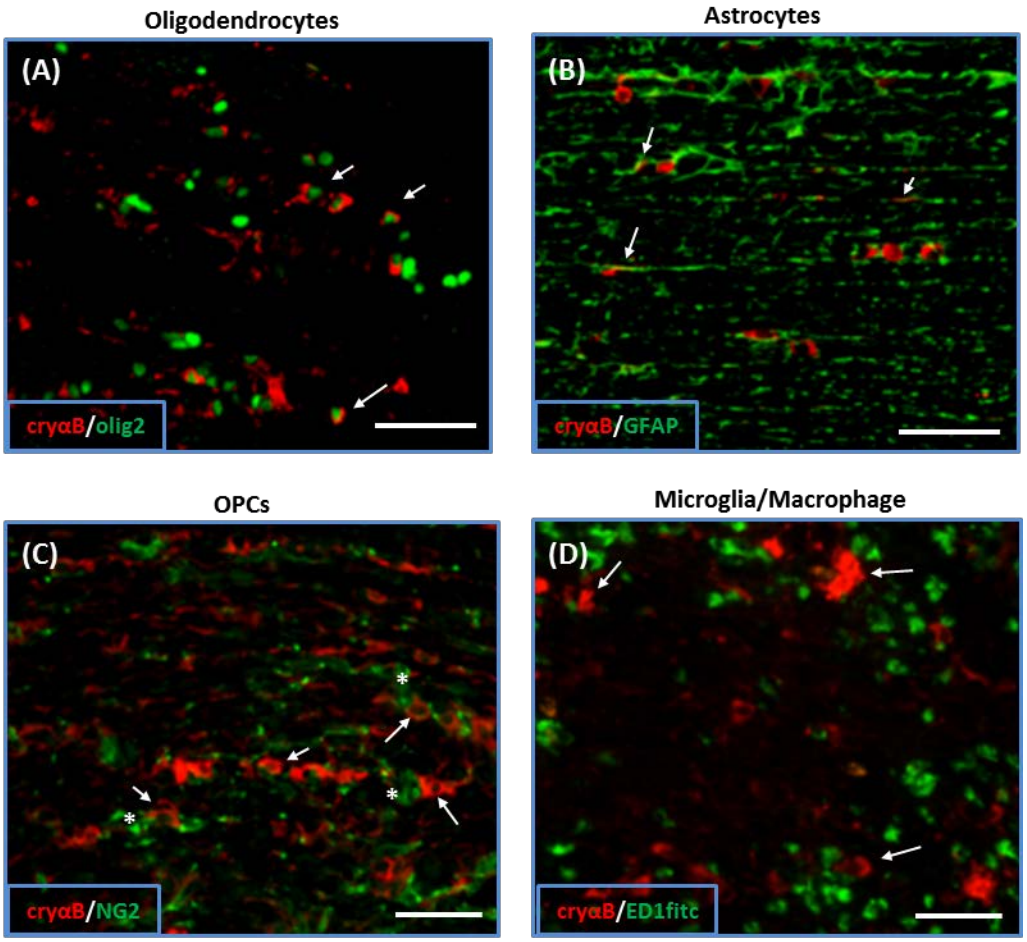

Figure 4.13. Expression of cryαB in different populations of glial cells in the optic nerve. The expression of cryαB (indicated by arrows) was detected in oligodendrocytes (A, arrows; healthy optic nerve) and astrocytes (B, arrows; healthy) but not in OPCs (C, arrows; day 1 EAE) and microglia/macrophages (D, arrows; day 1 EAE). Scale bars 50 µm.

Primary cultures of oligodendrocytes were used in order to investigate the expression of cryαB production under stress conditions. OPCs were isolated from SD rat pups at P2 and differentiated in vitro into mature oligodendrocytes.

In order to induce oxidative stress in mature, MBP^+ oligodendrocytes, cells were incubated for 3 hours at 37°C with different concentrations of hydrogen peroxide (H_2O_2) and linsidomine (Sin-1, a NO donor). Following this, cells were washed with PBS and allowed to recover in their normal (differentiation) medium overnight. On the next day, cells were fixed and stained with antibodies against MBP and cryαB. For the control group, an identical procedure was followed but with omission of the agents of oxidative stress. This group contained oligodendrocytes with well-defined MBP+ processes, but with low or absent staining for cryαB in the perinuclear cell body (Figure 4. 14A). Upon induction of oxidative stress, a change in the morphology of the oligodendrocyte

processes could be observed, with a punctate pattern of MBP staining of lower intensity (Figure 4.14B – I). Increased perinuclear cryαB$^+$ staining was detected in these cells. In cells treated with higher concentrations of ROS/RNS donors, cryαB$^+$ staining could also be detected in the oligodendrocyte processes (Figure 4.14E, I). These results are in agreement with previous report of up-regulation of cryαB in cultured cortical oligodendrocytes under conditions of oxidative and heat-induced stress (Goldbaum and Richter-Landsberg, 2001).

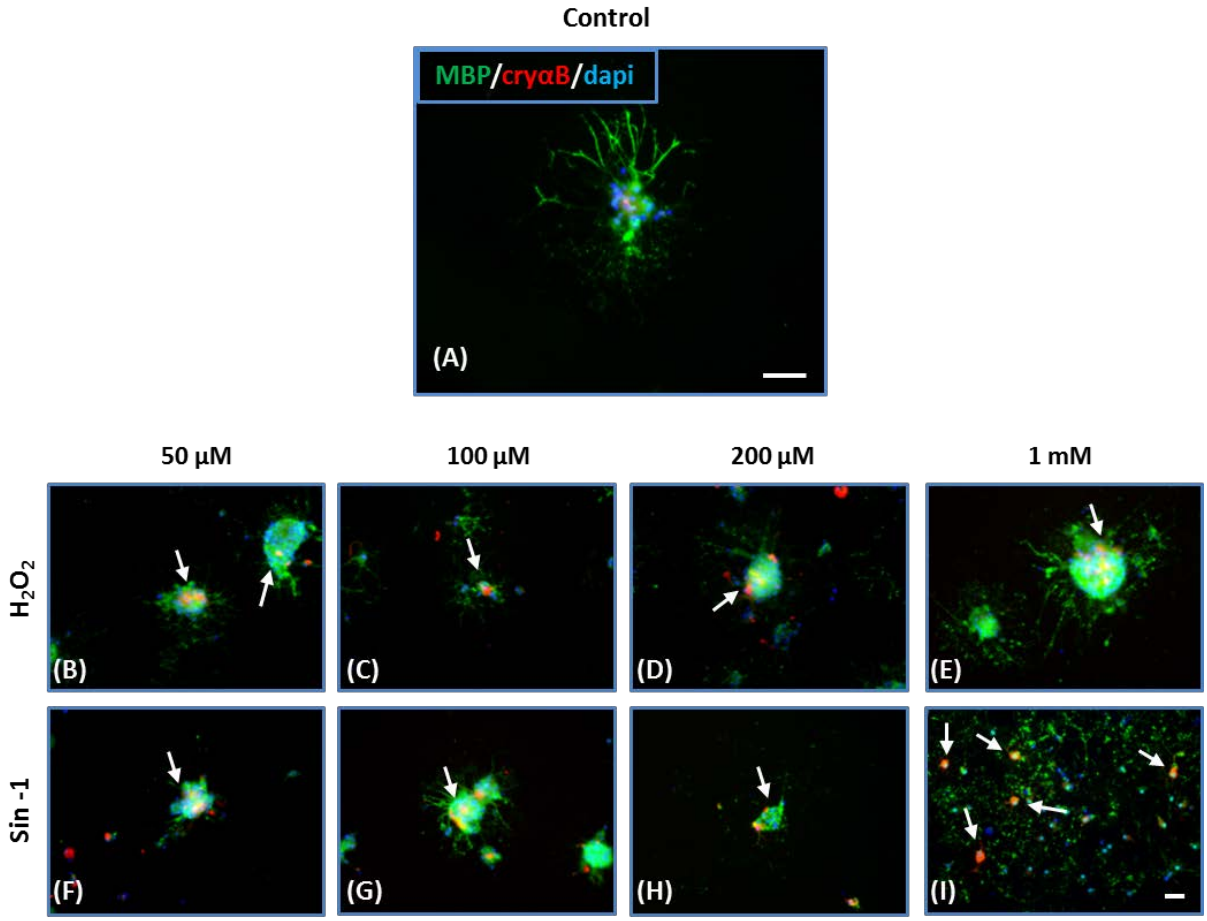

Figure 4.14. Oxidative stress leads to expression of cryαB in primary oligodendrocyte cultures. (A) Mature, MBP$^+$ (green) oligodendrocyte does not show expression of cryαB under control conditions. Incubation of primary optic nerve oligodendrocytes with different concentrations of reactive oxygen (B, C, D, E) and nitrogen species (F, G, H, I) led to an increased expression of the heat shock protein cryαB (red, B – I, arrows). Scale bars 50 µm.

4.2.6 Oligodendrocyte stress precedes the onset of AON

In order to investigate the presence of oligodendrocyte stress during the course of AON, longitudinal optic nerve sections were stained with antibodies against cryαB and Olig2. In both healthy animals and

those from the induction phase of AON, Olig2$^+$ oligodendrocytes were observed throughout the length of the optic nerve as having cryαB expression located as a small rim surrounding the nucleus. Interestingly, differences between the animal groups could be seen in the area of the ONH. While in healthy animals the cryαB staining pattern in the ONH was similar to that observed in the distal areas of the optic nerve (figure 4.15A), at day 10 p.i. a different pattern was detected. Oligodendrocytes in the ONH at day 10 p.i. had an increased intensity of perinuclear cryαB, with additional staining of the proximal segments of their processes (figure 4.15B). Upon development of clinical AON, an increased presence of oligodendrocyte stress was associated with inflammation in the vicinity of the ONH (figure 4.15C). Olig2$^+$ cells with strong cryαB immunoreactivity were also detected along the length of the optic nerve, both within and on the borders of inflammatory lesions (figure 4.16B). In agreement with the observation of increased immunostaining for cryαB, Western blot analysis of optic nerve lysates revealed a two-fold increase of the cryαB protein starting from day 10 p.i. (figure 4.15D, E).

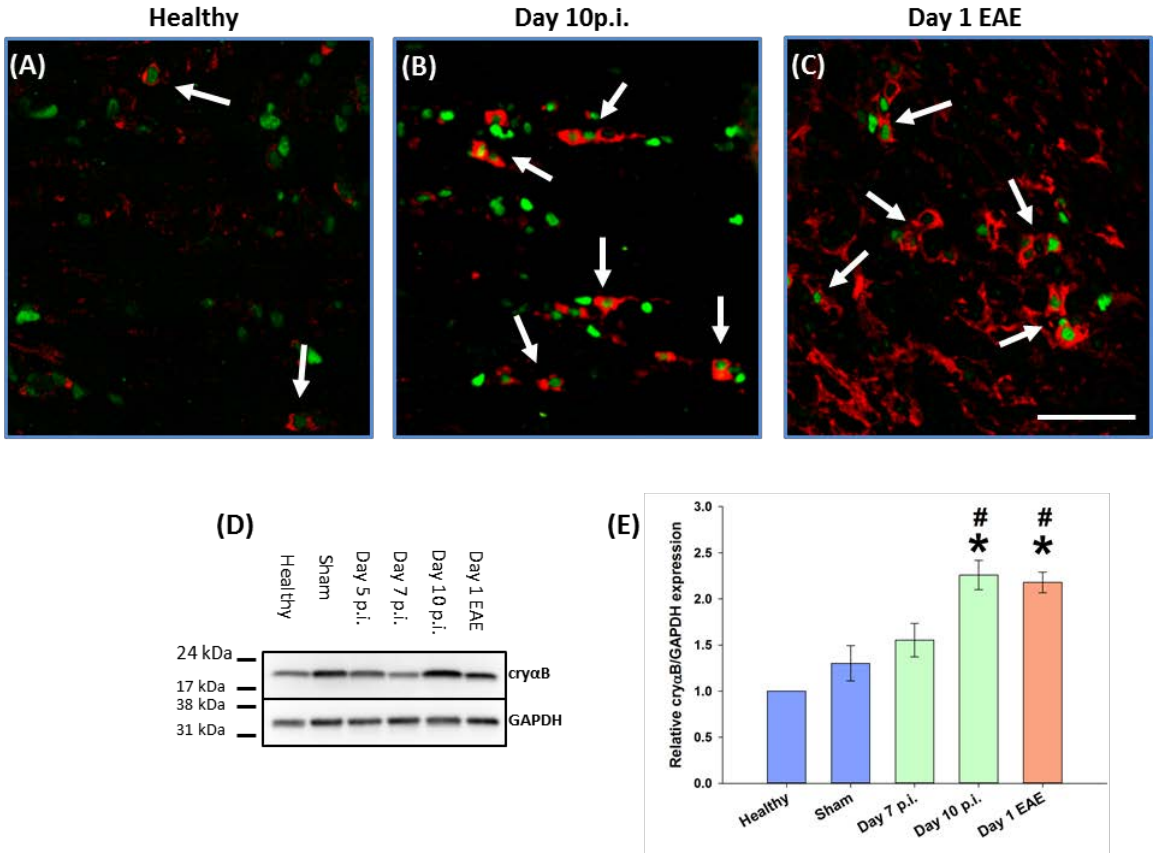

Figure 4.15. Oligodendrocyte stress starts in the induction phase of AON. Representative images of the ONH stained with antibodies against Olig2 (green) and cryαB (red) in healthy (A), day 10 p.i. (B) and day 1 EAE (C) animals. (D) Increased CryαB protein levels are seen as the disease course progresses, as detected by Western blot (a single band was detected with a molecular weight of approximately 21 kDa). (E) Quantification of protein expression (relative to GAPDH) revealed a statistically significant increase of cryαB protein from day 10 p.i. (* $p < 0.01$ compared to healthy and # $p < 0.01$ compared to sham, ANOVA). Scale bar 10 µm.

As previously mentioned, the expression of cryαB could also be detected at low levels in $GFAP^+$ astrocytes in healthy animals. However, during the induction phase of AON the increased expression of cryαB was seen to be associated with $Olig2^+$ cells rather than with GFAP staining. Similarly, at the onset of AON where staining of cryαB was detected within demyelinating lesions, this was seen mainly on oligodendrocytes (4.16A, B, Ci, Di), however it was also observed, although to a lesser extent, to be associated with GFAP staining (Figure 4.16Ci). The later stages of the clinical phase of AON are characterised by the marked presence of reactive gliosis indicated by hypertrophy of $GFAP^+$ astrocytic processes. These reactive astrocytes were characterised by increased expression of cryαB as indicated by the overlapping staining pattern with GFAP (Figure 4.16D, Di).

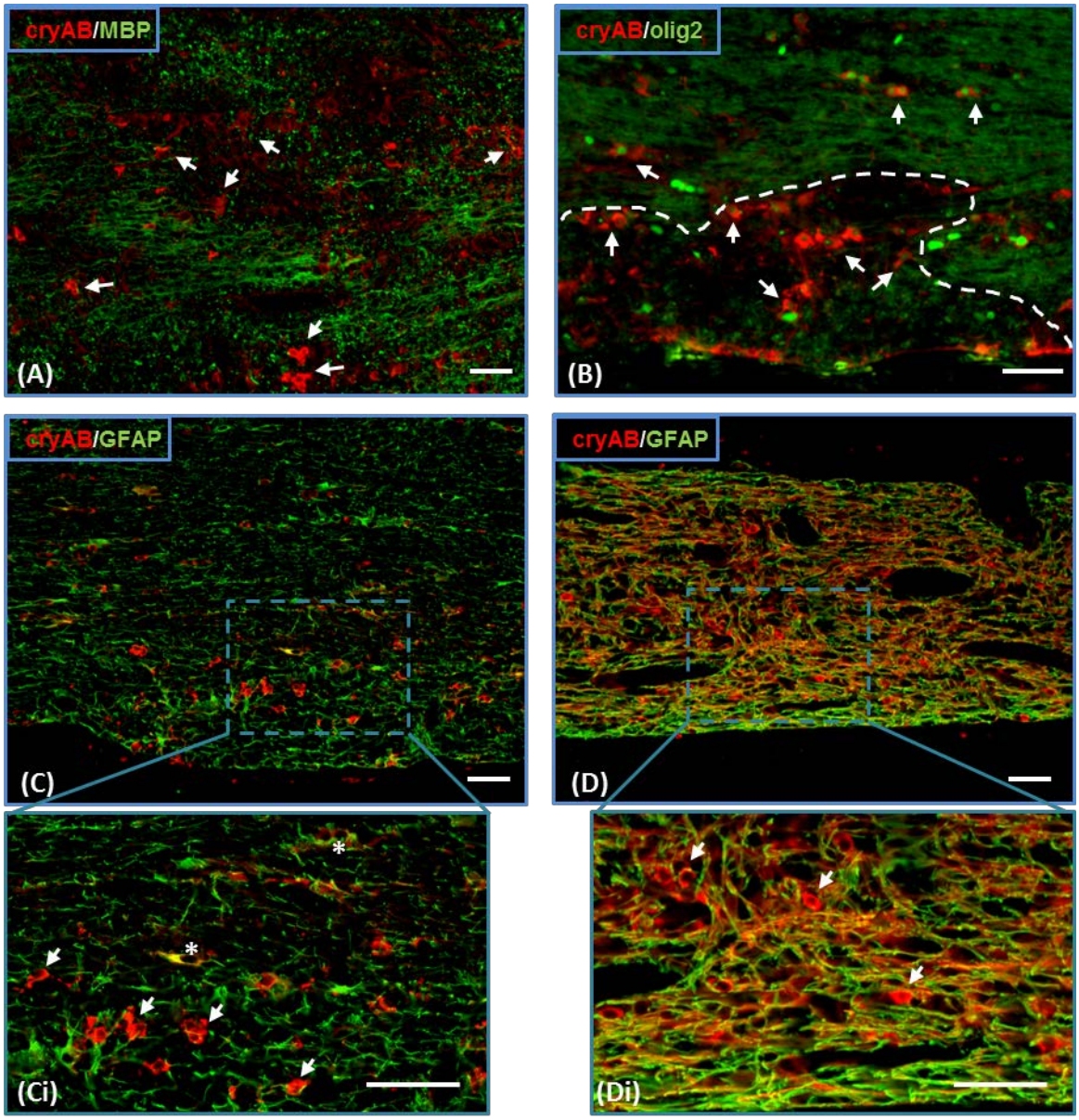

Figure 4.16. Expression of cryαB in glial cells following the onset of the clinical phase of AON. (A) CryαB staining (red, indicated by arrows) can be detected in demyelinating lesions, indicated by the lack of MBP staining (green). (B) CryαB^{+} oligodendrocytes (arrows) are often found at the edges of lesion (lesion border indicated with a dashed line; cryαB – red, Olig2 - green). (C, Ci) Double staining with GFAP (green) at the onset of the clinical phase of AON reveals that a majority of cryαB^{+} staining is not associated with astrocytes (Ci, arrows) although some co-localization of GFAP and cryαB could be detected (Ci, asterisk). (D, Di) With the progression of the disease (day 4 EAE) cryαB positive staining can be detected in both oligodendrocytes (Di, arrows) and in hypertrophic astrocytic processes (Di, indicated by co-localization of GFAP and cryαB staining; GFAP – green, cryαB - red). Scale bars 50 µm.

4.3 Disruption of axonal domain architecture correlates with activated microglia in the late induction phase of AON

The induction phase of AON is characterised by the absence of parenchymal infiltration of immune cells but an increase in the numbers of residential activated microglia. These cells have a specific spatial distribution – increased numbers of $ED1^+$ microglia are present in the area of the ONH and their numbers decrease with increasing distance from this region (Fairless et al., 2012). Double staining with Caspr and ED1 antibodies was performed on optic nerve sections from day 10 p.i. in order to investigate whether the areas of axonal stress correlate with the activation of residential microglia. Images were acquired using the confocal microscope at set positions along the length of the optic nerve (Figure 4.17A) and quantification of $ED1^+$ microglia and paranodal measurements were performed.

The distribution pattern of $ED1^+$ microglia was similar to one previously reported (Fairless et al., 2012) – the larger numbers of microglial cells were observed in the vicinity of the ONH and decreased with increasing distance in the late induction phase of AON (day 10 p.i.). An identical pattern was observed for the distribution of $Caspr^+$ paranodal lengths – paranodal domains in the vicinity of the ONH (1 mm from the ONH) were more elongated compared to ones in the distal part of the optic nerve (Figure 4.17B). There was a positive linear correlation between the distribution of $ED1^+$ microglia and the lengths of $Caspr^+$ paranodes (Figure 4.17C; $R = 0.71$, $p < 0.001$).

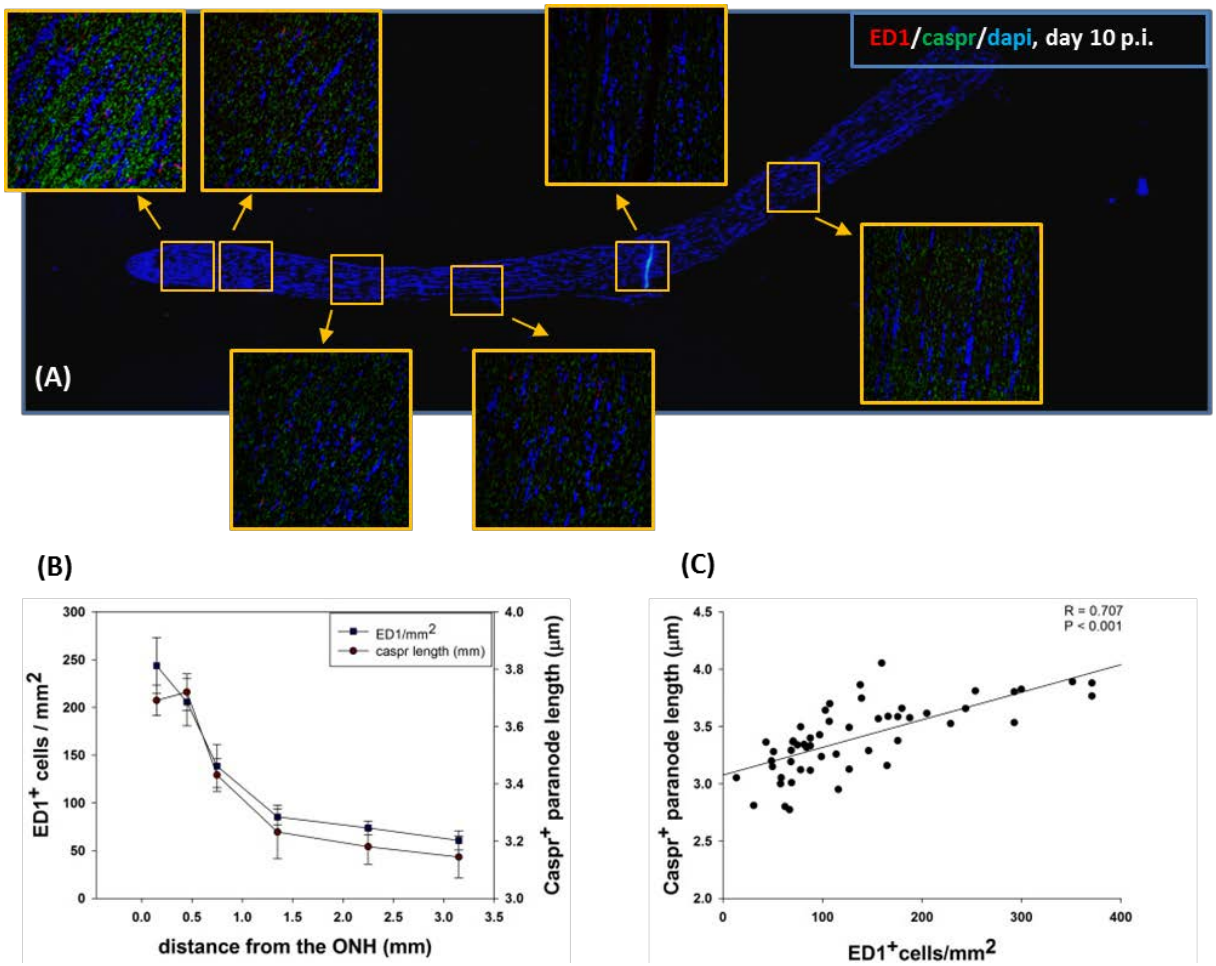

Figure 4.17. Disruption of paranodal domains correlates with activation of microglia in the late induction phase of AON. (A) Quantification of ED1$^+$ microglia and disruption of paranodal domains was performed at set positions along the length of the optic nerve at day 10 p.i.. (B) The distribution of microglia and axonal domain lengths are observed with the same pattern, that is decreasing with increased distance from the ON-H. (C) A positive correlation between microglia activation and axonal domain lengths was observed (R = 0.707; n = 53 images analysed from 9 different day 10 p.i. optic nerves).

Since the correlation of paranodal length and the density of activated microglia might just reflect their common relationship with the distance from the ON-H, it was next investigated whether there was actually a more direct relationship between these two observations by examining paranodal domains in the close vicinity of microglia in the late induction phase of AON (at day 10 p.i.; Figure 4.18). The length of paranodal domains were measured within a 20 µm radius of ED1$^+$ cells and compared to the length of paranodal domains not associated with activated microglia. It could not be excluded that there might be activated microglia within 20 µm distance in the z-axis but the use of confocal microscopy and generation of 8 µm thick z-stack images could, at least, in part cover this possibility. There was a statistically significant difference between the lengths of paranodes associated with (3.5 ± 0.02 µm, lengths ranging from 1.72 to 7.11 µm) and independent from ED1$^+$ microglia (2.87 ± 0.02 µm, 1.6 to 5.56 µm).

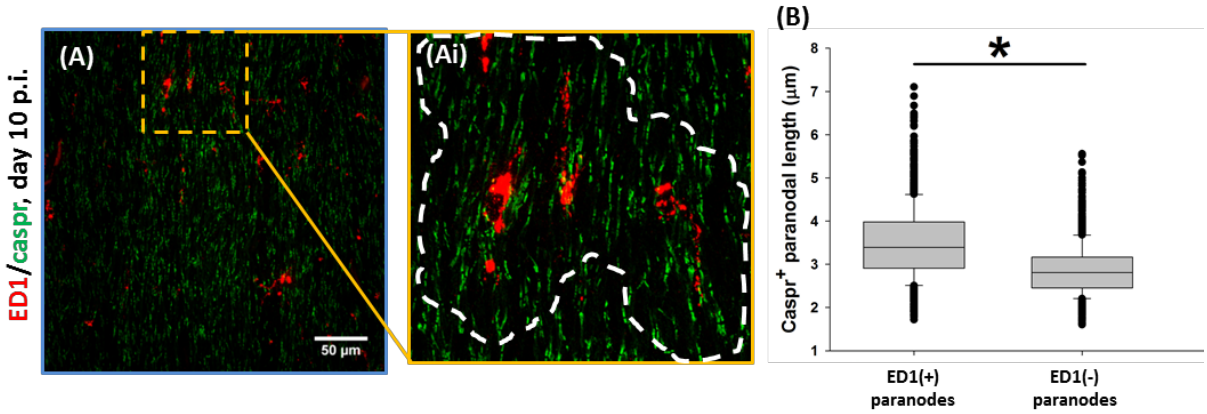

Figure 4.18. Elongated paranodal domains are located in the vicinity of activated microglia in the late induction phase of AON. (A, Ai) The length of paranodal domains was measured within a 20 µm radii of ED1$^+$ cells (Ai, indicated with white dashed line). (B) Paranodal domains in the vicinity of microglia had significantly elongated profiles when compared to ones not associated with ED1$^+$ positive cells (* $p < 0.01$, Mann-Whitney Rank Sum Test, n = 1209 paranodes per group, from 6 different day 10 p.i. animals). Scale bar 50 µm.

The observed correlation of activated microglia and elongated paranodes may reflect a disruptive effect of the activated microglia on the paranodes. For example, activated microglia, along with infiltrating macrophages, are known to be the main source of ROS/RNS within the inflammatory lesions in MS and EAE which may disturb local axonal function.

In order to determine whether the observed axonal stress and paranodal elongation in the induction phase of AON is mediated by the production of ROS/RNS by activated microglial cells, a treatment study with ROS/RNS scavengers was performed. The treatment consisted of a cocktail of 3 different ROS/RNS scavengers (FeTPPS, EUK 134 and PBN) previously shown to be able to prevent axonal injury in the EAE model (Nikic et al., 2011). The treatment was administered by daily injection of the cocktail (or vehicle in the control group) starting from day 5 p.i., the time-point when increased numbers of activated microglia are first detected (Fairless et al., 2012). The treatment was terminated at day 10 p.i. and optic nerves were examined for the presence of axonal stress (number of npNF$^+$ axons and the integrity of paranodal domains). In the control group, the extent of axonal stress was similar to that previously detected at day 10 p.i. with similar npNF levels (423.31 ± 35.69 SMI32$^+$ axons/mm^2 in treatment group vs. 394.06 ± 31.54 SMI32$^+$ axons/mm^2 at day 10 p.i.) and elongation of paranodal domains (average length 3.71 ± 0.17 µm, ranging from 1.99 to 6.39 µm vs. 3.58 ± 0.07 µm at day 10 p.i.). Application of ROS/RNS scavengers failed to prevent axonal stress – both the disruption of paranodal domains (3.69 ± 0.11 µm, ranging from 1.87 to 7.84 µm) and the presence of npNF in the axons (442.68 ± 33.32 SMI32$^+$ axons/mm^2) was observed suggesting that these processes are not mediated by the production of RON/RNS species by activated microglia in the induction phase of AON (Figure 4.19).

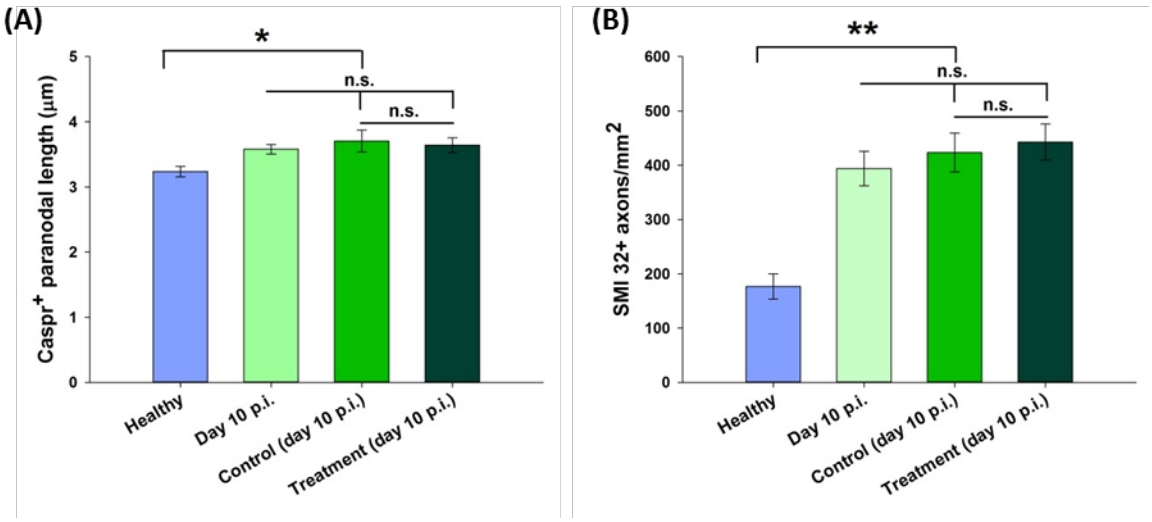

Figure 4.19. Axonal stress in the induction phase of AON is not mediated by ROS/RNS. Scavenging of ROS/RNS failed to prevent disruption of paranodal domains (A) and the presence of npNF in axons (B) in the induction phase of AON (* $p < 0.05$ and B, ** $p < 0.01$ compared to healthy, ANOVA; n = 4 animals per treatment group).

4.4 Low levels of anti-MOG autoantibodies are sufficient to induce oligodendrocyte stress in the ONH

In order to determine the cause of axonal and glial stress in the optic nerve during the induction phase of AON, it was next considered whether circulating antibodies could play a role. Autoantibodies play a role in the pathology of MS as their presence, together with complement deposition, is a hallmark of type II active demyelinating lesions (Lucchinetti et al., 2000). This phenomenon is also reflected in some animal models of EAE, particularly MOG-induced EAE in BN rats. In this model, extensive demyelination in the CNS, particularly in the spinal cords and the optic nerve, is accompanied with increased titre of autoantibodies in the serum and their deposition within demyelinating lesions in a similar manner as described in active MS lesions (Stefferl et al. 1999). The presence of anti-MOG antibodies in the serum is detected already in the late induction phase of the disease (day 10 p.i.) in MOG-immunised BN rats (Fairless et al., 2012). In a similar manner, the deposition of IgG in the optic nerve precedes the onset of the inflammatory demyelination. At this time point, deposition of IgG could be observed in the ONH (Fairless et al., 2012), the area characterised with the presence of early oligodendrocyte stress (Figure 4.15B). With the onset of AON, strong cryαB immunoreactivity could be detected in newly forming lesions characterised by antibody deposition and very little demyelination (Figure 4.20). This suggests that anti-MOG antibodies could have a role in the early oligodendrocyte stress observed in the induction phase of AON.

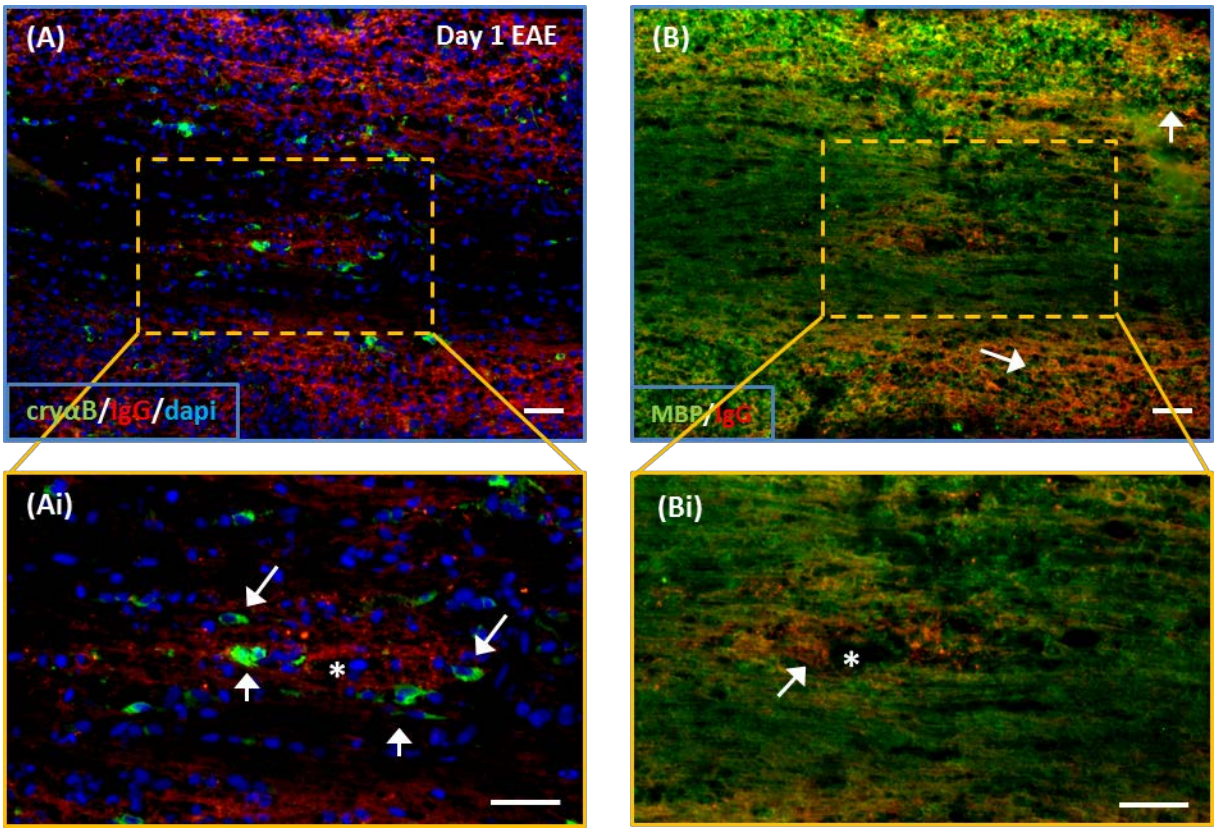

Figure 4.20. Deposition of autoantibodies is observed in areas of demyelination and glial stress following the onset of AON. Sections stained for the deposition of antibody and cryαB (A, Ai) show the presence of glial stress (Ai arrows, indicated by cryαB^{+} staining, green). Staining of a serial section with MBP (B, Bi; green) and antibody deposition (red) demonstrated this area to be a newly forming lesion (Ai and Bi, star) characterised by IgG deposition but little demyelination (Bi, arrow). Areas of demyelination within inflammatory lesions are characterised with marked antibody deposition (B arrows). Scale bars 50 µm.

In order to examine a possible role of autoantibodies in the early cellular stress during the induction phase of AON, the transfer of serum from MOG-immunised into naïve animals was performed. Successful transfer of autoantibodies via serum transfer was confirmed by ELISA for detection of anti-MOG antibodies in recipient animals. Although anti-MOG antibodies persisted for up to 5 days pst (when animals were sacrificed), their levels were found to be considerably lower than those in the MOG-immunised donor animals (Figure 4.21G). Nevertheless, deposition of IgG could be observed in the optic nerve head of animals receiving serum from day 10 p.i. and EAE animals (Figure 4.21E and F respectively). Deposition of IgG could not be observed in the optic nerves of animals that received serum from the sham immunised animals (Figure 4.21D).

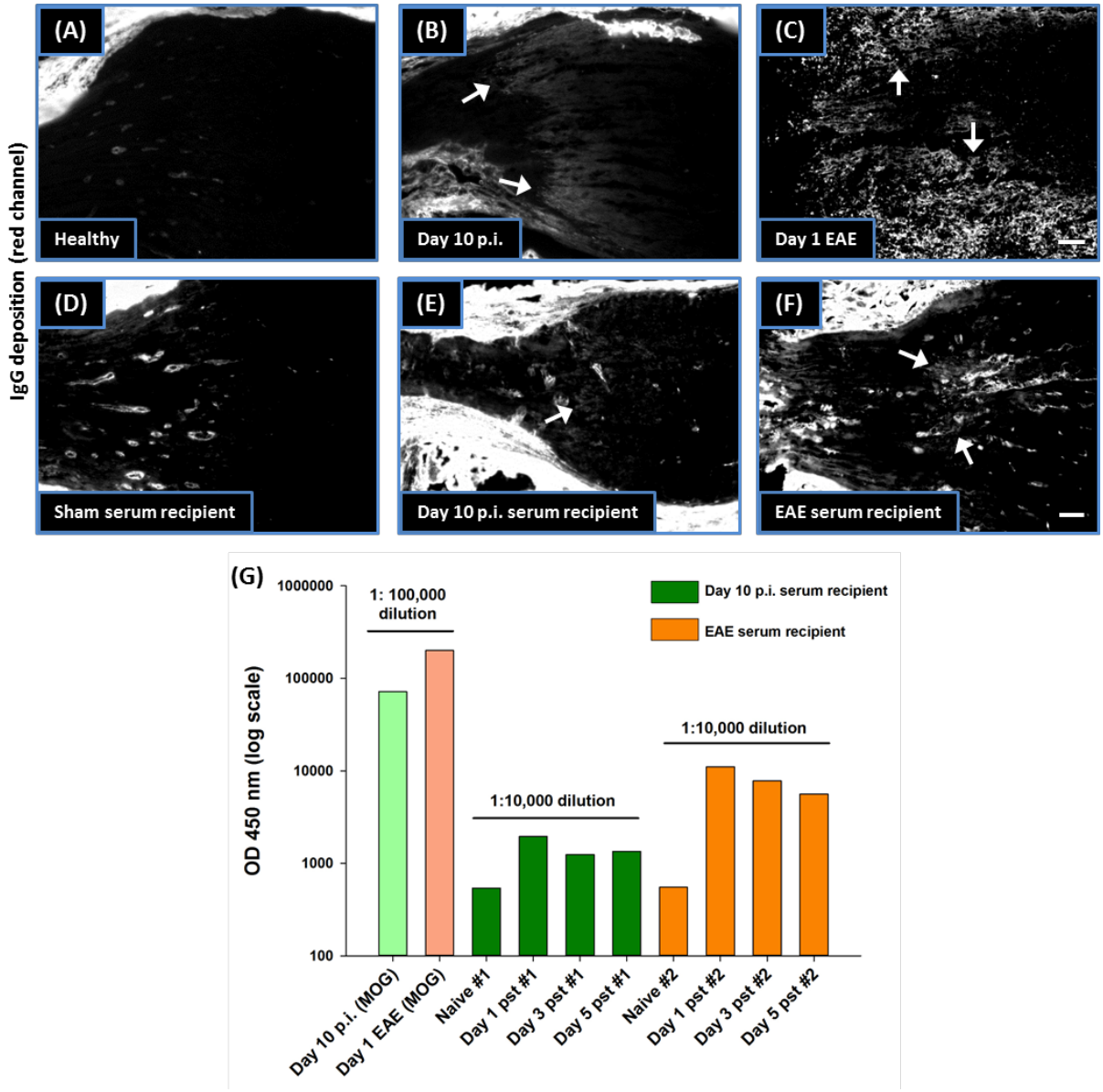

Figure 4.21. Serum transfer from MOG-immunised animals leads to the presence of anti-MOG antibodies in the serum and IgG deposition in the area of the ONH in naïve animals. Example images of the ONH from healthy (A), day 10 p.i. (B) and day 1 of EAE animals stained for IgG deposition (indicated by arrows). (D) There was no antibody deposition in the ONH of animals that received serum from sham-immunised animals. Transfer of serum from day 10 p.i. and animals from the onset of the clinical phase of EAE into naïve animals led to IgG deposition in the ONH (E and F, respectively)**.** (G) Anti-MOG antibodies persist in the serum of recipient animals up to 5 days pst from both day 10 p.i. (green bars) and EAE animals (orange bars). It should be noted that levels of anti-MOG antibodies in the serum of recipient animals are considerably lower than the ones found in MOG-immunised donors, as indicated by the 10-fold difference in sera dilution used to detect them by ELISA – serum dilution for MOG-immunised animals was 1:100,000 and for the recipient animals was 1:10,000. Scale bars 50 µm.

The recipient animals (both those receiving day 10 p.i. or EAE serum) failed to show neurological symptoms characteristic for the clinical phase of the disease (limb weakness/paralysis). Upon investigating optic nerves there were no characteristic signs for the presence of AON – i.e. no myelin/axonal loss or infiltration of macrophages in the tissue of recipient animals (data not shown).

The presence of axonal stress in recipient animals was investigated by examining the integrity of axonal domains and the presence of npNF in the ONH (Figure 4.22A - C). The average length of nodal (1.32 ± 0.03 μm) and paranodal (3.4 ± 0.07 μm) domains in animals that received serum from day 10 p.i. animals did not significantly differ from that observed in healthy animals (nodal length 1.27 ± 0.02 μm; paranodal length 3.23 ± 0.08 μm) or those receiving sham serum (nodal length 1.19 ± 0.05 μm; paranodal length 3.07 ± 0.06 μm). The same was observed in animals that received the EAE serum – the average length of the nodal domain was 1.34 ± 0.04 μm and the average length of the paranodal domain was 3.49 ± 0.09 μm. Similarly, when the presence of npNF was examined – there was no statistical differences in the number of $SMI32^+$ axons in animals that received day 10 p.i. (228.51 ± 27.84 $SMI32^+$ axons/mm^2) or EAE (202.66 ± 8.79 $SMI32^+$ axons/mm^2) serum when compared to healthy (176.53 ± 23.14 $SMI32^+$ axons/mm^2) or sham recipients (122.25 ± 27.73 $SMI32^+$ axons/mm^2).

Considering the observed deposition of IgG in the ONH of recipient animals, the presence of oligodendrocyte stress was investigated with double staining against Olig2 and cryαB. The intensity of cryαB staining associated with $Olig2^+$ nuclei was stronger in animals that received serum from MOG-immunised animals (both day 10 p.i. and EAE serum, Figure 4.22E and F, respectively) when compared with animals that received sham serum (Figure 4.22D). This observation suggests that the low anti-MOG antibody levels achieved could be sufficient to induce oligodendrocyte stress similar to that observed in the induction phase of AON. This is perhaps explained by the fact that the auto-antigen being targeted by the antibodies is present on oligodendrocytes. However, this stress does not then appear to be transmitted to the axons, or to result in structural changes in axonal domains.

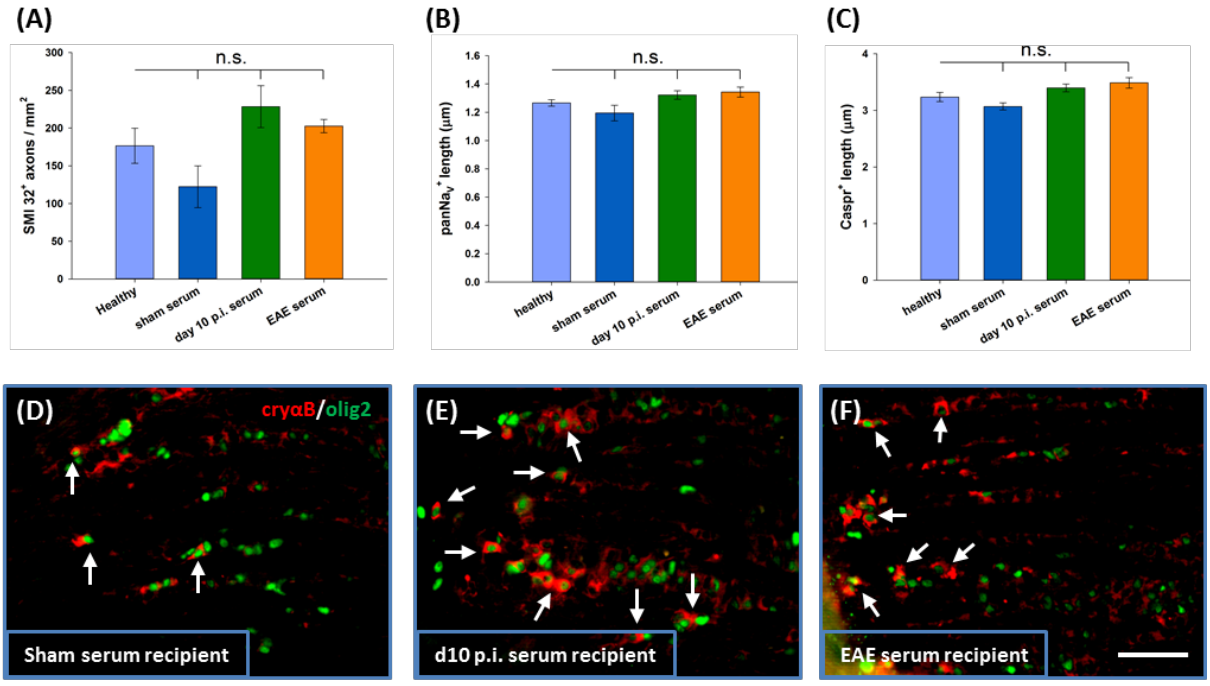

Figure 4.22. Signs of oligodendroglial, but not axonal, stress detected following the transfer of serum from MOG-immunised animals. Transfer of serum from MOG-immunised animals was insufficient to induce axonal stress characteristic for AON. There was no difference in the presence of npNF (A) or in the integrity of nodal (B) or paranodal (C) domains following the serum transfer in recipient animals when compared to healthy animals (n = 6 healthy, 2 sham serum recipients, 3 day 10 p.i. serum recipients and 4 EAE serum recipients). Representative images of the optic nerve head stained with cryαB (red) and Olig2 (green) antibodies in animals that received sham (D), day 10 p.i. (E) and EAE (F) serum (day 5 pst). Increased intensity of cryαB staining associated with oligodendrocytes could be detected in animals that received serum from both day 10 p.i. and animals from the clinical phase of disease (E,F indicated by arrows) when compared to animals that received sera from sham-immunised animals. Scale bar 50 µm.

4.5 Primary retinal insult mimics the axonal stress characteristic of the induction phase of AON

In order to determine whether a primary retinal pathology, such as the one observed early in the induction phase of AON (Fairless et al., 2010) contributes to early signs of stress in axonal and oligodendroglial compartments observed in this study, a model of retinal insult by intravitreal injection of glutamate was employed. Seven days following the injection, animals were sacrificed and optic nerves and retinas were examined for the presence of pathology.

The intravitreal injection of glutamate led to a retinal pathology resembling that observed during the induction phase of AON (Fairless et al., 2012). Seven days following the insult, TUNEL positive cells could be observed in both RGC- and inner nuclear cell layers (Figure 4.23.B). This was accompanied by a significant increase in the numbers of ED1$^+$ microglia (Figure 4.23D and G). An increase in activated microglia could also be observed in the optic nerve compartment. A significant increase in

ED1$^+$ microglia is observed in the ONH (Figure 4.23F and H) and the proximal segments of the nerve (Figure 4.23H). Except for microglial activation, no macroscopic signs of optic nerve injury, such as demyelination and axonal swellings/transections, could be detected following the primary retinal insult (data not shown).

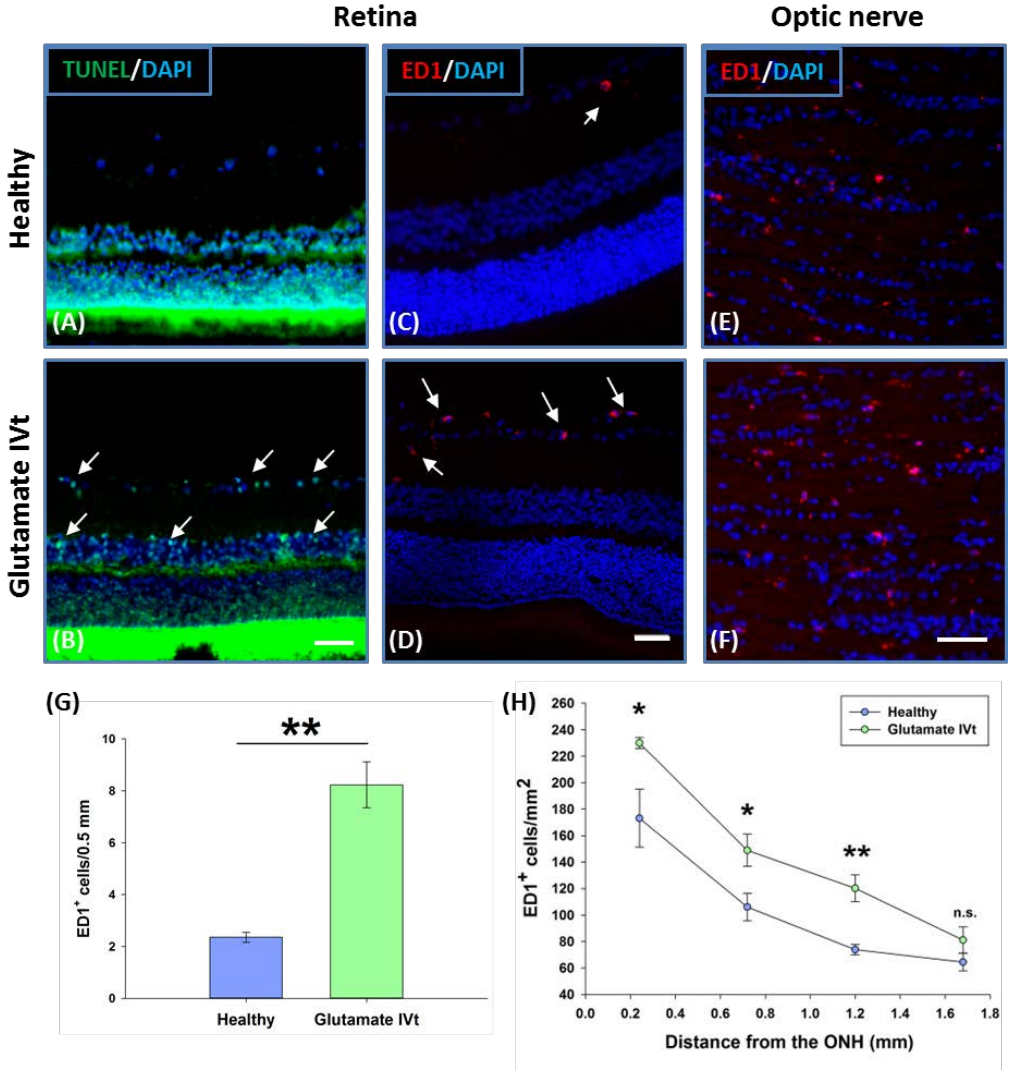

Figure 4.23. Microglial activation and cellular apoptosis are detected following intravitreal injection of glutamate. Representative images of TUNEL assay (green) in healthy (A) and in the retina following the intravitreal injection of glutamate (B, arrows indicate presence of TUNEL$^+$ cells in the RGC and the inner nuclear layer of the retina). Representative images of retinas stained with ED1 antibody (red) for detection of activated microglia in healthy (C) and in retina following glutamate injection (D; arrows indicate ED1$^+$ cells both in C and D). ONH sections from healthy (E) and animals following injection of glutamate (F) stained with ED1 antibody. Intravitreal injection of glutamate led to statistically significant increase in ED1$^+$ cells both in retina (G) and the proximal part of optic nerve (H; * $p < 0.05$ and ** < 0.01 compared to healthy, student's t-test; n = 6 retinas/optic nerves per group). Scale bars 50 µm.

In order to investigate whether the observed retinal pathology is responsible for the axonal stress observed in the late induction phase of AON, optic nerve sections were stained with antibodies

against Caspr and npNF. Measurement of Caspr$^+$ structures following the intravitreal injections revealed a disruption in the paronodal domains in the same manner as observed at day 10 post MOG immunisation (average paranodal length 3.57 ± 0.06 µm; n = 2793 Caspr$^+$ paranodes, p = 0.009 compared to healthy). Similar results were obtained by quantification of npNF. There was a significant increase in the number of SMI32$^+$ axons (367.75 ± 33.69 SMI32$^+$ axons/mm^2, p < 0.001 compared to healthy), being similar to that observed at day 10 post MOG immunisation. Although glutamate injection was successful in mimicking the axonal stress characteristic for the induction phase of AON, it did not lead to the presence of stress in oligodendrocytes, as observed by immunostaining of optic nerves with cryαB (Figure 4.24D)

Taken together, the intravitreal injection experiments showed that a primary retinal insult was sufficient to induce stress in the axonal compartment. This suggests that the RGC loss and retinal changes observed during the early induction phase might be sufficient to induce axonal disruptions observed in the late induction phase of AON.

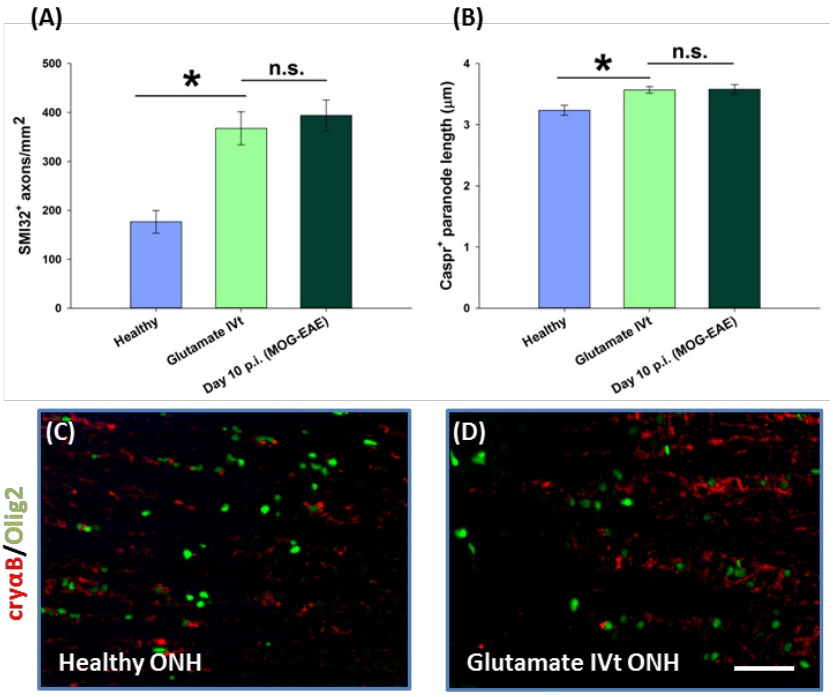

Figure 4.24. Primary retinal insult leads to axonal stress in the optic nerve. Intravitreal injection of glutamate leads to an increase of npNF (A) and disruption in paranodal domains (B) in the axons of the proximal part of the optic nerve in the same manner as observed 10 days post MOG immunisation (* p < 0.01, ANOVA; n = 6 animals per group). However, intravitreal glutamate injection did not cause the presence of oligodendrocyte stress as observed by comparing ONH sections from healthy (C) and glutamate injected (D) animals stained with antibodies against cryαB (red) and Olig2 (green). Scale bars 50 µm.

4.6 Summary

Collectively, data presented in this thesis provide evidence of both a functional and pathological disruption of the optic nerve compartment during the course of AON in MOG-immunised BN rats. During the induction phase of the disease, gross pathological changes (such as demyelination and axonal loss) in the optic nerve were not detected. However impairment in visual function, observed by the decrease in visual acuity by measurement of pVEPs, is detected. This impairment is timed with disruptions in axonal domains (nodes of Ranvier and paranodal domains) involved in saltatory conduction of AP along the axon. Further evidence of stress was observed in both compartments of paranodal axon-glia junctions. In the axonal compartment, an increase of npNF (a stress marker for myelinated axons) was detected and found to correlate with disrupted paranodal domains. Disruption of the parnodal domain is further found to correlate with the presence of activated microglia, particularly in the area of the ONH. In order to determine if microglia mediate these disruptions by the secretion of ROS/RNS, a treatment study with a cocktail of scavengers of these species was performed. However, the treatment failed to prevent signs of axonal stress suggesting a different role for microglia during the induction phase of the disease. In the oligodendroglial compartment, evidence of stress was observed by increased production of cryαB, a small heat shock protein involved in the glial stress response. Oligodendrocyte stress was particularly evident in the ONH, the same area which was characterised by greater disruption of axonal domains, increased numbers of activated microglia and deposition of auto-antibodies during the induction phase of the disease.

Following the onset of the clinical disease phase animals were characterised with greater impairments in visual functions observed by both aberrant fVEP responses and an almost complete loss of visual acuity (as assessed by pVEP). This was accompanied by the presence of inflammatory demyelination and increasing signs of axonal injury in optic nerves. Greater disruption of axonal domains and further increase in npNF are observed at this time point. In addition to increased expression of cryαB, a portion of oligodendrocytes associated with inflammatory lesions underwent the process of apoptosis.

In order to investigate the origins of observed axonal and oligodendroglial stress in the late induction phase two different approaches were made. Firstly, the oligodendrocyte compartment was targeted by auto-antibodies through the transfer of sera from MOG-immunised into naïve animals. This led to deposition of auto-antibodies and the presence of oligodendrocyte stress in the ONH, in a similar manner to that observed in the late induction phase. Secondly, a model of primary retinal injury by intravitreal injection of glutamate was performed and successfully mimicked aspects of the retinal

pathology characteristic of the early induction phase (previously reported in Fairless et al., 2012). This led to the presence of axonal stress in optic nerves in the similar extent to one observed in the late induction phase in MOG-immunised animals. Therefore, it appears that the stress induced from either the oligodendrocyte or the neuronal (axonal) compartments is not transmitted to the other compartment, suggesting that both events might be occurring simultaneously in the disease model of AON.

5 Discussion

The aim of this study was to characterise axonal disruptions during the course of AON in order to gain insight into mechanisms of neurodegeneration and functional deficits of the visual system previously reported in this model (Meyer et al., 2001; Hobom et al., 2004; Fairless et al., 2012; Hoffmann et al., 2013). This study expands on these previous reports by focusing on the optic nerve compartment during the induction phase of the disease and by providing a more detailed histopathological examination, particularly focusing on the axonal domains involved in signal propagation. By combining functional testing (VEPs) and histopathology it was possible to gain further insight into structural correlates of visual impairments associated with optic neuritis. This could be of an importance in human studies where monitoring of optic nerve pathology is limited to *in vivo* imaging (such as MRI) which cannot provide any precise information about the structure of axonal and myelin compartments. In the present study, the observed disruption of nodal and paranodal domains was seen to correlate with timing of the onset of visual impairments in the late induction phase of the disease. This provides a rare report (to the author's knowledge) on how the integrity of axonal domains reflects on visual functions during optic neuritis. In addition to early changes in axons, the presence of stress was also observed in oligodendrocytes, implying that both compartments of the paranodal axon-glia junction are compromised prior to the onset of inflammatory demyelination. Further experiments showed that these compartments could be targeted independently during the induction phase of AON, by mechanisms involving a primary retinal insult and the actions of the humoral immune response. Altogether, the pathological image observed in the induction phase of AON shares great similarities with the pathology of NAWM in MS, in terms of both axonal (Howell et al., 2010) and oligodendroglial stress (Sinclair et al., 2005; Zeis et al., 2008; van Noort et al., 2010), further suggesting that the model of AON is useful for studying degenerative processes in MS.

5.1 AON is associated with impairments in visual function

Measurement of VEPs is a non-invasive technique used in the diagnosis and monitoring of different disorders of the visual pathway. VEPs are electrical potentials generated in the visual cortex in response to visual stimuli (Arroyo et al., 1997; Ridder and Nusinowitz, 2006). They provide information about the signal conduction from the retina to the cortex which gives an estimation of the integrity of the visual (retino-cortical) pathway. Abnormalities in the VEP signal imply the presence of a pathology in the visual pathway. As such, measurements of VEPs have been used in the

MS field for investigating the presence of the optic neuritis for the past 40 years (Halliday et al., 1972; Halliday et al., 1973). The increase in VEP signal latency is considered to result from demyelination which leads to disruption of fast saltatory conduction in axons (You et al., 2011). A decrease in the VEP amplitude is considered to be the functional correlate of axonal injury (You et al., 2011; You et al., 2012). Following an episode of optic neuritis, aberrant VEP responses and decreased visual acuity usually persist for up to one year, with a gradual recovery occurring. During the recovery phase, a shortening of VEP latency is suggestive of regenerative processes (remyelination) in the optic nerve (Brusa et al., 1999; Brusa et al., 2001; Klistorner et al., 2007). Interestingly, altered VEP responses and decreases in visual acuity were also found in some MS patients independent of diagnosis with optic neuritis (Sanders et al., 1985; Van Diemen et al., 1992; Sisto et al., 2005). This could support the hypothesis that diffuse degenerative processes are present in MS within the visual pathway independent of the classical inflammation (such as the defining characteristics of optic neuritis).

The results of fVEP measurements presented in this thesis were found to be in agreement with previous studies (Meyer et al., 2001; Hobom et al., 2004). From the onset of the clinical phase of the disease there was an approximately 2-fold increase in the latency and a similar sized decrease in the signal amplitude (Figure 4.2C, D). The immuno/histopathological examination of the optic nerve showed the presence of extensive demyelinating lesions (Figure 4.4Fi - Giii) and the reduction in axonal densities (Figure 4.6C) along the length of the optic nerve at the onset of the disease. These are considered to be general histopathological correlates of the observed aberrant fVEPs. From the onset of the clinical phase, when a decrease in fVEP amplitude is detected, there is a marked presence of axonal injury, revealed by the presence of many $SMI32^{+}$ axonal ovoids indicative of axonal transections (Figure 4.5C, Ci), and a reduction in axonal density (Figure 4.6C). The inflammatory nature of lesions can also contribute to disruption in visual functions. As it was previously mentioned, inflammatory mediators, such as NO, are shown to be able to cause conduction block and to interfere with normal signal propagation in axons (Redford et al., 1997; Smith et al., 2001). Following the onset of the clinical phase of AON, extensive macrophage infiltration is detected within the lesions in the optic nerve and their presence correlates with both demyelination and axonal injury (Figure 4.5Ai, Bi). A subset of these cells was also positive for iNOS, an enzyme responsible for the production of NO (author's own observation, data not shown).

Despite the early onset of RGC death during the induction phase, there is no macroscopic evidence of optic nerve pathology at this time point (Fairless et al., 2012). Optic nerve axons are still fully myelinated and a reduction in their density is not observed (Figure 4.4Di – Eiii; Figure 4.6B). It could be possible that following the loss of cell bodies, degenerative processes in the axons are initiated

but might take some time to translate into their complete loss. This notion could be supported by ultrastructural signs of axonal injury that are observed already during the induction phase of disease, prior to axonal loss (Fairless et al., 2012). Also, studies of Wallerian degeneration (degeneration of the distal axonal segments following their separation from the cell body) show that the process of anterograde axonal degeneration can take several days to develop. In one such study it was shown that following an intra-retinal axotomy with laser induced injury, marked reduction in axonal density was observed only starting from seven days following the injury (Kanamori et al., 2012). It should be also noted that quantification of axonal loss by histological staining (such as Bielschowsky's sliver staining used in Fairless et al. 2012) might not be sensitive enough to detect a subtle reduction in axonal numbers that could be present already during the induction phase. The absence of major axonal pathology during the induction phase was reflected in the preservation of visual functions assessed by fVEP. The amplitude (Figure 4.2C) and the latency (Figure 4.2D) of the signal were not altered either in in the early (day 5 p.i.) or in the later stage (day 10 p.i.) of the induction phase. This supports the notion that demyelination and axonal loss are the structural correlates of the altered fVEP response observed by increased latency and decreased signal amplitude (You et al., 2011).

Even though the visual evoked response to flash stimuli remained unchanged until the onset of the clinical phase of AON, the decrease of visual acuity, observed by measurement of pVEPs, can already be detected in the late induction phase (at day 10 p.i.; Figure 4.3B). pVEPs are sensitive to contrast modulation, refraction and changes in the spatial frequency allowing more detailed information of the visual acuity to be obtained (Onofrj et al., 1982; Ridder and Nusinowitz, 2006). Measurement of pVEPs is considered to be a more sensitive technique for assessing changes in visual function associated with MS when compared to fVEPs (Halliday and Mushin, 1980). This can also observed in the present study by comparing results from pVEP and fVEP measurements at the onset of the clinical phase of AON. Although at this time point the shape of the response was altered, all animals were able to produce a measurable response when presented with flash stimuli. This was not the case with the pVEP recordings which revealed almost a complete loss of visual acuity (Figure 4.3B). This implies that pVEPs are more sensitive to pathological changes and that they require a more preserved integrity of the visual system in order to produce measurable response. This is opposed to fVEPs which could still be detected (although with an altered signal amplitude and latency) in the presence of demyelination and axonal injury/loss. Therefore the decreased visual acuity observed in the late induction phase of AON, can reflect the presence of more subtle pathological changes in the visual pathway. Such changes have been observed at this time point by ultrastructural changes in optic nerve axons (Fairless et al., 2012) and by disruption of axonal domains observed in this study (further discussed in the chapter 5.2). Although the loss of RGCs during the induction phase of AON did not affect the response to flash stimulus it cannot be excluded as the pathological correlate of

the observed decrease in visual acuity assessed by pVEP recordings. A similar finding was reported in the mouse model of optic neuritis (Matsunaga et al., 2012). In this study, the decrease in visual acuity (assessed by optokinetic head tracking) was observed prior to inflammatory demyelination of the optic nerve and an increase in the fVEP signal latency. The authors suggested that partial disruption of the axonal integrity (observed by irregular patterns of neurofilament staining) and activation of microglial cells in the optic nerve could be the pathological correlates for the early decrease in visual acuity, although it should be noted that they did not investigate a possible involvement of retinal pathology.

5.2 Disruption of axonal domains as a structural correlate of impaired visual functions in AON

Previous studies have shown a correlation between impaired visual function and optic nerve pathology (characterised by demyelination and axonal loss) in different models of optic neuritis (Hobom et al., 2004; Lidster et al., 2013; You et al., 2011; Matsunaga et al., 2012; Aranda et al., 2015). The aim of this study was to closer investigate the integrity of axonal domains involved in signal conduction and how it corresponds to the impairment in visual functions throughout the course of AON. Proper organization of axonal domains is necessary for efficient saltatory conduction (Salzer 2003). This was confirmed by numerous studies with genetically modified animals deficient in nodal and paranodal protein constituents. These animals were characterised as having slower nerve conduction, ataxia, paresis and severe neurological deficits (Bhat et al., 2001; Boyle et al., 2001; Sherman et al., 2005; Zonta et al., 2011).

In the present study, a decrease in visual function, assessed by recording of fVEPs, was observed from the onset of the clinical phase of AON. At this time point, a marked decrease in the number of paranodal domains was detected by immuno-staining with an antibody against Caspr (50% reduction of numbers observed in healthy animals; Figure 4.7F). Furthermore, a significant decrease in the protein levels of both Caspr and Contactin-1 was observed at the same time point by Western blotting (Figure 4.8). This phenomenon cannot be solely explained by the reported loss of axons at the beginning of the clinical disease phase. At this time point, the extent of axonal loss does not reflect the extent of paranodal loss since only a 15% reduction in axonal density was detected at day 1 of EAE (Fairless et al., 2012). In fact, the extent of paranodal loss was found to correspond to the extent of demyelination of the optic nerve (50% demyelination was reported on day 1 of EAE, Fairless et al., 2012). This suggests that the loss of myelin, and therefore the disruption of the axo-glial

contact at the paranodal domain, could play a role in downregulation of the axonal Caspr/Contactin-1 complex. This hypothesis was previously tested by experiments with genetically modified animals where inducible ablation of Nfasc 155 (the oligodendroglial counterpart of the axo-glial junction) in adult mice led to a gradual decrease in Caspr immunoreactivity in the paranodal region (Pillai et al., 2009).

Paranodal domains are considered to act as a physical barrier separating and inhibiting the lateral diffusion of neighbouring nodal and juxtaparanodal components (Rios et al., 2003). This suggests that the absence of paranodal domains would lead to a diffuse distribution of nodal components, such as Na_Vs, along the axons, as has been previously reported in both MS and EAE lesions. Na_V, but also NCX, are found to be diffusely distributed along demyelinated axons of optic nerves and spinal cords in autopsy tissue from SPMS (Craner et al., 2004a). A similar observation was made upon investigation of optic nerves (Craner et al., 2003) and spinal cord tissue (Craner et al., 2004b) following the onset of demyelination in the mouse model of EAE. In the present study, following the onset of the clinical phase of AON and demyelination in the optic nerve, paranodal domains were lost and Na_V were dispersed along demyelinated axons (Figure 4.9I and J), reflecting previous observations from MS tissue and mouse EAE model reported by Craner and colleagues.

Disruption of axonal domains is considered to be an initiating step in the process of demyelination in MS (discussed in chapter 1.7.3). Disrupted axonal domains, characterized by elongated staining patterns of nodal and paranodal components, were detected on the edge of lesions in axons with still preserved myelin sheaths (Wolswijk and Balesar, 2003; Coman et al., 2006; Howell et al., 2006), and also in the NAWM in the absence of inflammatory demyelination (Howell et al., 2010). Upon investigation of axonal domains throughout the course of AON it was discovered that disruption of these domains is an early event, preceding inflammatory demyelination (Figure 4.9B). Both nodal and paranodal domains were found with elongated profiles already at the late induction phase (Figure 4.9G and H). Ultrastructural examination of these axonal domains revealed alterations in the paranodal domains as observed by the detachment of oligodendroglial paranodal loops from axons (Figure 4.9E). Similar pathological features were observed at the onset of the clinical phase of AON. On the lesion edges, axonal domains had elongated profiles similar to those observed in the late induction phase of AON (Figure 4.9C). Detachment of paranodal myelinating loops of oligodendrocytes and unravelling of the myelin sheath was observed through examination of the ultrastructure of such axons with electron microscopy (Figure 4.9F). In contrast, in the lesion centre, complete disruption of axonal domains was characterised by the absence of paranodes and diffuse Na_V expression (Figure 4.10I and J). It should be noted that in axons with disrupted axonal domains (both in the late induction phase and with the onset of the clinical phase of AON) there was no

overlapping staining pattern observed for Caspr and Na_v. This implies that the elongation of the nodal domain (diffusion of Na_V) is secondary to disruption of the paranodal domain. These findings reflect the early pathological events described in MS lesions and imply that similar pathological mechanisms are employed in the model of AON. The nature of these findings further strengthens the hypothesis that the disruption of axonal domains is an early pathological event preceding demyelination.

Proper organization of axonal domains gives rise to the specific electrical properties of the axonal membrane necessary for fast and energetically efficient saltatory conduction (Salzer, 2003). Dense clustering of Na_V in the nodal region allows for energetically efficient propagation of APs since it allows the necessary number of Na^+ ions for membrane depolarisation to be achieved in a smaller area of axonal membrane, without having to depolarise larger areas (requiring more Na^+). Lengthening of the nodal domain increases the number of Na^+ ions required for depolarisation and imposes a greater energy demand for their clearance (discussed in chapter 1.7.2). By employing mathematical modelling of the axonal membrane it was shown that an increase in the nodal surface would lead to an increase in nodal electrical capacitance which would in turn affect the signal conduction by decreasing the amplitude of the AP and conduction velocity of such axons (Babbs and Shi, 2013). A detrimental effect of nodal elongation on signal conduction has been observed in experimental allergic neuritis (EAN), an animal model used for studying Guillain–Barre syndrome, a spectrum of acute peripheral inflammatory neuropathies (Lonigro and Deavux, 2009). Disruption of paranodal domains in EAN also leads to a rearrangement in the juxtaparanodal region as observed by displacement of K_V in the paranodal region. Although this issue was not addressed in the present study, it was reported under similar pathological conditions both in MS and EAE (Howell et al., 2006; Howell et al., 2010). Also, detachment of myelinating loops in the paranodal region could lead to more current flow underneath the myelin sheath which could lead to an aberrant activation of K_V resulting in impaired AP propagation (Arancibia-Carcamo and Attwell, 2014). Considering that morphological changes in axonal domains accompanying these mechanisms are detected during the course of AON, it is plausible that they could be involved in the observed disruption of the visual function. Given that measurement of fVEPs provides information about signal conductance along the visual pathway which consists of great numbers of optic nerve axons, it is not surprising that subtle disruptions, observed only in a portion of axons at the late induction phase of AON, may not be sufficient to alter fVEP responses at the given time point. Following the onset of the clinical phase of AON, the frequency of disrupted axonal domains drastically increases which would, together with diffuse Na_V on demyelinated axons, axonal loss and inflammation-induced conduction block, contribute to aberrant conduction observed by measurement of fVEPs. Although these subtle, “pre-demyelinating” changes in the axonal domains do not lead to alterations in the fVEP response, they

could contribute to decreased visual acuity during the induction phase of AON, as assessed by a more sensitive technique (pVEP).

5.3 Disruption of cytoskeleton as a marker of axonal stress in AON

As previously discussed, the induction phase of AON lacks the signs of the major optic nerve pathology which appear later (discussed in chapter 5.1; Fairless et al., 2012). Upon more detailed examination of the optic nerve axons by employing electron microscopy, subtle alterations in their morphology were detected such as shrunken axons and vacuoles in the peri-axonal space despite normal appearing myelin sheaths (Fairless et al., 2012). Both this finding and the axon-glial paranodal disruption observed in the present study imply that there is a disrupted contact between axons and oligodendrocytes prior to the onset of demyelination. During development, under normal physiological conditions, myelination of axons by oligodendrocytes is required for the proper organization of the axonal cytoskeletal structure and undisrupted axonal transport. This is observed in different studies with dys-myelinating mutant animals which are characterised by disrupted organization of the axonal cytoskeleton and impairment in axonal transport (Griffiths et al., 1998; Brady et al., 1999; Lappe-Siefke et al., 2003).

Neurofilaments (NF) belong to the family of intermediate filaments and together with the microtubule system and microfilaments (actin network) they comprise the cytoskeleton of neurons. NFs are heteropolymers comprised of three different subunits (neurofilament triplets), categorised by their molecular weights – heavy chain NF (NFH, 180 – 200 kDa), medium chain NF (NFM, 130 – 170 kDa) and light chain NF (NFL, 60 – 70 kDa; Fliegner and Liem, 1991). Upon myelination, the axonal calibre increases as a result of heavy phosphorylation of neurofilament chains (particularly NFH) on many KSP (Ser-Lys-Pro) repeats present on their tail domains (Sanchez et al., 1996). Increase of axon calibre leads to an increase in conduction velocity (Arbuthnott et al., 1980) which is particularly important in long axons, such as those found in the optic nerve. Thus, the presence of non-phosphorylated NF (npNF) in myelinated axons is considered to be a sign of stress and has been observed in many neurodegenerative diseases including MS. Axons containing npNF were found in both NAWM in association with activated microglia (Howell et al., 2010) and in MS lesions at various stages of their development (Trapp et al., 1998; Petzold et al., 2008; Schirmer et al., 2011). In the present study, increased levels of npNF were observed already in the late induction phase of the disease (Figure 4.10). At this time point, $SMI32^{+}$ axons were still myelinated (Figure 4.10Ci), further reflecting the previous observation of ultrastructural changes in the absence of demyelination. After the onset of the clinical phase of AON, this phenomenon was more pronounced and the presence of

npNF was detected both in demyelinated and still myelinated axons associated with inflammatory lesions (Figure 4.10Di). Changes in axonal cytoskeletal organization can have deleterious effects on their physiology as they lead to a disruption of axonal transport and subsequent swellings and transections (Trapp et al., 1998). This phenomenon could be observed with the onset of the clinical phase of AON where swollen, $SMI32^+$ axons are detected within demyelinating lesions (Figure 4.5C, Ci).

In the present study, both the significant rise in npNF and disruption of axonal domains are observed at the same time point in the late induction phase of AON (day 10 p.i.). At this time point, double labelling for the paranodal marker Caspr and SMI32 revealed the possible relationship between disruption of axonal domains and changes in the axonal NF cytoskeleton. While paranodal domains not associated with $SMI32^+$ axons appeared normal, ones associated with axons containing npNF were observed with disrupted (elongated) profiles (Figure 4.11). Similar observations have been made upon investigation of disrupted paranodal domains in NAWM MS tissue where disrupted patterns of glial $Nfasc155^+$ staining were observed predominantly on $SMI32^+$ axons (Howell et al., 2010). The relationship between observed disruptions of the axonal cytoskeleton and axonal domains can be drawn from the particular architecture of the axonal cytoskeleton in these domains. In the paranodal domain, transmembrane Caspr protein contains a cytoplasmic domain which binds to the 4.1B protein, a cytoskeletal adaptor protein which stabilises axo-glial junctions by binding to the axonal cytoskeleton (Horresh et al., 2010; Buttermore et al., 2011). 4.1B protein binds to Ankyrin B, αII- and βII- spectrin isoforms that are particularly enriched in the paranodal regions (Ogawa et al., 2006). In nodal regions (and AIS), the localisation of Na_V in the membrane is achieved through its interaction with Nfasc 186 and the cytoskeletal adaptor protein Ankyrin G that is bound to the axonal cytoskeleton through its interaction with βIV-spectrin (Bennett and Gilligan, 1993). β-spectrins serve as a link with the underlying axonal cytoskeleton as they contain binding sites for both actin and NFs (Frappier et al., 1991). Both spectrins and adaptor proteins are necessary for the proper organization of axonal domains. Genetic deletion of 4.1B leads to disrupted paranodal domains (Buttermore et al., 2011) while deletion of βIV-spectrin leads to a disruption in the nodes of Ranvier (observed by elongated Na_V^+ profiles) and alterations in the NF cytoskeleton organization (Yang et al., 2004).

Considering that disruptions in both axonal domains and NFs appear simultaneously at the late induction phase of AON, it is hard to draw a conclusion on causality between these events. Alternatively, it is very plausible that both events share a common driving force, such as an increase in the axonal Ca^{2+} levels. In a recently performed study using Mn^{2+}-enriched MRI, it was shown that the optic nerve compartment contains elevated levels of Ca^{2+} already at the late induction phase of AON (day 10 p.i.; Hoffmann et al., 2013), the same time point when disruptions were observed in the

present study. Increases in Ca^{2+} levels correlated with the activity of the calcium-activated protease calpain, as assessed by the presence of the 147 kDa fragment of spectrin, a cleavage product specifically produced by calpain activity. The particular timing of the observed cleavage of spectrin suggests that this could be the underlying cause in the disruption of the axonal domains in the present study. This hypothesis is strengthened by observations that increased axonal Ca^{2+} levels and calpain activity leads to disruption of axonal domains under different pathological conditions and that pharmacological inhibition of this protease leads to preservation of domain structures (Fu et al., 2009; Schafer et al., 2009; McGonigal et al., 2010; Reeves et al., 2010; Huff et al., 2011; Sun et al., 2012). Dephosphorylation of axonal NF side-arms is mediated by calcineurin, a Ca^{2+}-calmodulin–dependent serine/threonine protein phosphatase (Tanaka et al., 1993). This enzyme is activated by increased Ca^{2+} levels and it has been shown to play a role in axonal injury in models of traumatic brain injury (Okonkwo et al., 1999; Colley et al., 2010) and *in vitro* axonal injury (Staal et al., 2010). Dephosphorylation of NF is considered to be an early step in the axonal injury cascade and it enhances their susceptibility to further degradation in the presence of increased Ca^{2+} levels by calpain-mediated proteolysis (Pant, 1988; Greenwood et al., 1993). This presumably plays a role in the clinical phase of AON when more extensive axonal injury and loss is detected.

The observed disruptions of axonal domains and NF cytoskeleton highlight the important role of Ca^{2+} in the early axonal injury in the model of AON. Hoffmann et al. reported that the increase in Ca^{2+} levels leads to spectrin cleavage by calpain and in the present study a further downstream effect of this cleavage (disruption of axonal domains) can be observed together with dephosphorylation of NF which is also shown to be a Ca^{2+} -mediated process. Further evidence for the role of Ca^{2+} in the early axonal changes characteristic for the late induction phase of AON can be found in studies with the *ex-vivo* rat optic nerve anoxia model (Waxman et al., 1992; Waxman et al., 1994). Here, the authors reported Ca^{2+}-dependent changes on the ultrastructural levels in axons in the similar manner observed in the induction phase of AON (shrunken axons and the vacuoles in the periaxonal space within preserved myelin sheaths, disruption in axonal domains and changes in the axonal cytoskeleton) as well as an impairment of AP propagation.

5.4 Oxidative stress does not play a role in axonal disruptions during the induction phase of AON

Microglia play an important role in the pathogenesis of MS. The activation of residential microglial cells has been observed in all lesion types, starting from the early stages of their development

(discussed in chapters 1.4 and 1.7.1). In the EAE model, it has been shown that microglial cells are mobilized to the sites of early BBB disruptions prior to the onset of peripheral immune cell infiltration and the onset of inflammatory demyelination (Davalos et al., 2012). Their activation results from the leakage of blood-borne proteins which leads to axonal injury mediated by the production of ROS (Adams et al., 2007; Davalos et al., 2012). In the model of AON, activation of residential microglial cells was observed during the induction phase, prior to infiltration of inflammatory cells from the periphery. In the retina, an increase in the numbers of activated microglia coincides with the disruption of the blood-retinal barrier and the loss of RGCs which suggests their potential role in the process of neurodegeneration. Similar observations were made in the optic nerve compartment where an increase in activated microglia was also detected during the induction phase, particularly in the region of the ONH which is characterised by a permeable BBB (Fairless et al., 2012).

In the present study, the integrity of axonal domains was investigated with respect to the early activation of microglial cells. In the late induction phase of AON, disruption of paranodal domains showed a strong correlation with the distribution of $ED1^+$ microglia (Figure 4.17) suggesting their involvement in the early disruption of axonal domains. This result is in agreement with a previous report that showed a correlation between disrupted axonal domains and activated microglia in the MS-NAWM (Howell et al., 2010). This same study showed the disruption of axonal domains and axonal injury (assessed by the presence of npNF in axons) in the spinal cord of mice induced with MOG-EAE during the pre-clinical phase. Since activated residential microglial cells were observed in this tissue, they were subsequently inhibited by minocycline treatment, leading to a reduction in axonal injury, further strengthening the case for their role in early axonal disruptions.

One of the mechanisms by which activated microglia can induce CNS damage is through the production of ROS/RNS (Block et al., 2007). The deleterious effects of these species could be observed through the presence of oxidized lipids and DNA in oligodendrocytes and neurons/axons within MS lesions (Vladimirova et al., 1998; Haider et al., 2011). Elevated levels of ROS/RNS are also detected in inflammatory lesions of EAE animals (Ruuls et al., 1995; Nikic et al., 2011; Davalos et al., 2012). The direct effect of ROS/RNS on axonal integrity was shown by employing in vivo imaging of the spinal cord axons in the mouse model of MOG-EAE (Nikic et al., 2011). The authors showed elevated levels of ROS/RNS in inflammatory lesions with extensive axonal damage. In addition, scavenging of reactive species was sufficient to reverse this observed axonal pathology. Furthermore, they showed that application of ROS/RNS donors to the spinal cord of a naïve animal was sufficient to cause axonal damage comparable to that observed in EAE animals in the absence of demyelination, confirming a direct role of these species in axonal pathology. Oxidative stress is also known to contribute to neurodegeneration following stroke (Allen and Bayraktutan, 2009) and

traumatic brain injury (Cornelius et al., 2013) which are also characterised by the activation of residential microglial cells following the initial injury. In this present study, a greater disruption of paranodal domains in the late induction phase of AON was observed in the close vicinity of activated microglia (Figure 4.18) suggesting a possible role for secreted disruptive mediators from activated microglia. However, a treatment study with a cocktail of ROS/RNS scavengers failed to prevent both the disruption of paranodal domains and the presence of npNF in axons implying that these species do not play a role in the early axonal injury observed in the induction phase of AON (Figure 4.19).

Another possible mechanism of how microglia could induce paranodal disruptions and axonal injury is by glutamate-mediated damage. Elevated glutamate levels are found associated with both NAWM and MS lesions (Srinivasan et al., 2005). Microglia and macrophages with increased glutaminase expression (an enzyme involved in the synthesis of glutamate) are found in MS lesions associated with dystrophic, $SMI32^{+}$ axons (Werner et al., 2001). In the model of AON, increased levels of glutamate are found in the retina starting from the induction phase of the disease and coinciding with RGC death (Maier et al., 2007). In this study, inhibition of microglial activity with minocycline led to a decrease in glutamate levels and preservation of RGCs. An *in vivo*/*ex vivo* imaging study with the application of glutamate on exposed spinal cords resulted in axonal disruptions (Fu et al., 2009), similar to those observed in this and previous studies of AON. The authors showed that exogenous application of glutamate led to a retraction of paranodal myelin in a Ca^{2+}/calpain-mediated manner. Furthermore, disruption of paranodal domains led to a subsequent Ca^{2+} influx in the axons implying their secondary degeneration. Following paranodal disruption, axonal Ca^{2+} signals were first detected in the paranodal region, subsequently spreading along the axon. This highlights the importance of an undisrupted paranodal domain for axonal viability. Although this study shows great similarities with observations presented in this thesis and previous work in the AON model (Hoffmann et al., 2013), further work is needed to investigate a possible role of glutamate in the early axonal disruptions and elevated Ca^{2+} levels observed during the induction phase of AON.

Under neuroinflammatory conditions, microglia show great plasticity in their response which is orchestrated by signals from surrounding tissue, coming from both residential CNS cells and infiltrating lymphocytes (concept reviewed in Bogie et al., 2014; Cherry et., 2014). In addition to the deleterious role of microglia (characterised by the expression of receptors involved in antigen presentation, production of ROS/RNS, and secretion of pro-inflammatory cytokines and chemokines) they can also acquire a beneficial phenotype characterised by their role in immune-suppression and tissue remodelling. This heterogeneity of microglial responses is reflected in MS-NAWM where both pro-inflammatory (Zeis et al., 2008; Howell et al., 2010) and immune-suppressive (Melief et al., 2013) microglia have been observed in different studies. Taking this into consideration, the activation of

microglia in the induction phase of AON could also be a consequence rather than a cause of axonal disruptions. This can also be supported by the observation that the expression of iNOS was only detected following the onset of the clinical phase of AON on $ED1^+$ cells with macrophage-like morphology (author's observation, data not shown). Also the area of ONH, where axonal disruption and microglia activation was most prominent, is also characterised with an increased presence of cryαB, an oligodendroglial stress protein which was shown to modulate the response of microglia in preactive MS lesion towards immune-suppression and tissue repair (van Noort et al., 2010; Bsibsi et al., 2013; discussed further in chapter 5.6). Taking this into consideration, further characterisation of the microglial phenotype is needed to reveal their role during the induction phase of AON.

5.5 Disruption of axonal domains is not a consequence of oligodendrocyte apoptosis

In addition to extensive demyelination, MS lesions are frequently characterised by the presence of oligodendrocyte death (Ozawa et al., 1994; Lucchinetti et al., 2000). In some cases the apoptosis of oligodendrocytes is considered to be an early event in lesion formation as it can be observed prior to myelin degradation and its phagocytosis by macrophages (Barnett and Prineas, 2004). Oligodendrocytes are particularly sensitive to inflammatory mediators commonly present in MS lesions as they express receptors for glutamate (McDonald et al., 1998), TNF-α (Selmaj et al., 1988), INF-γ (Vartanian et al., 1995) and Fas receptor (Dowling et al., 1996). Activation of these receptors in an inflammatory setting can lead to caspase-dependent apoptosis of oligodendrocytes (Cudrici et al., 2006). This phenomenon, as well as the particular sensitivity of potentially regenerative OPCs to inflammation (Baerwald et al., 1998; Bernardo et al., 2003), can lead to impairment in tissue regeneration, represented as the lack of remyelinating processes in such lesions (Lucchinetti et al., 2000).

As previously discussed, myelination of axons by oligodendrocytes provides the basis for the fast and energetically efficient signal propagation which is crucial for the proper functioning of the CNS. The oligodendrocyte-axon interaction also provides metabolic coupling between the two compartments which is necessary for the long term viability of axons (concept reviewed in Simons and Nave, 2015). This suggests that an insult to oligodendrocytes alone could lead to deleterious effects in axons. In fact, this has been shown using different experimental models resulting in primary oligodendrocyte death, where targeted ablation of oligodendrocytes leads to pathological axonal changes. For example, in a toxin-induced model of demyelination, primary death of oligodendrocytes leads to

demyelination in different regions of the brain of animals on a cuprizone diet (Praet et al., 2014). In this model, axonal pathology is detected already in early stages of demyelination (Sun et al., 2006; Crawford et al., 2009). In a transgenic model with mice that have human diphtheria toxin (DT) receptor expressed under the MBP promotor, ablation of mature oligodendrocytes can be induced with a single DT injection. This leads to a disruption of axonal domains and the presence of axonal injury (as assessed by APP accumulation) in the absence of demyelination (Oluich et al., 2012). In this present study, axonal injury in the late induction phase of AON could not be attributed to oligodendrocyte death as their apoptosis could not be detected prior to the onset of the clinical phase of the disease. Instead, $TUNEL^+$ oligodendrocytes were only observed associated with inflammatory lesions following the onset of the clinical phase of AON (Figure 4.12) confirming their susceptibility to inflammatory-mediated apoptosis.

5.6 CryαB as a marker of oligodendrocyte stress in the course of AON

Although apoptosis of oligodendrocytes could not be detected prior to the onset of inflammatory demyelination, signs of early oligodendrocyte stress, as assessed by the increased production of cryαB, were detected already in the late induction phase of AON (Figure 4.17). CryαB is a small heat shock protein expressed in various cell types in different tissues where it exerts anti-apoptotic activity under different stress conditions (Klemenz et al., 1991; Goldbaum and Richter-Landsberg, 2004; Mao et al., 2004; Kamradt et al., 2005; Liu et al., 2007). In the CNS, increased expression of cryαB is detected both in glial cells (oligodendrocytes and astrocytes) and neurons under different neurodegenerative conditions (Iwaki et al., 1992; Zabel et al., 2006). This protein has a particularly interesting role in MS as it was found to be the most prominent protein found in lesions (Chabas et al., 2001; Han et al., 2008). Furthermore, cryαB has also been identified as a T cell autoantigen in MS (van Noort et al., 1995; Bajramovic et al., 2000). Increased cryαB expression has been detected in glial cells at different stages of lesion development (Bajramovic et al., 1997; Sinclair et al., 2005). In preactive MS lesions, accumulation of cryαB was detected in oligodendrocytes coinciding with appearance of activated $HLA\text{-}DR^+$ microglia nodules in the absence of demyelination and leukocyte infiltration (van Noort et al., 2010). In this, and subsequent studies, the authors showed that in such lesions cryαB, produced and secreted by stressed oligodendrocytes, modulates the activity of the surrounding microglia/macrophages by binding to its receptors (CD14 and Toll-like receptors 1 and 2), shifting their phenotype towards one of immune-suppression and tissue repair (van Noort et al., 2010; Bsibsi et al., 2013). These studies showed the importance of oligodendrocyte stress for

orchestrating the innate immune response during lesion formation. Further studies showed that this pathway can be re-programed under the stetting of lymphocyte inflammation in active lesions. For example, INF-γ secreted by invading T cells can re-programme cryαB-sensitised microglia to release pro-inflammatory cytokines (TNF-α, IL-6, IL-12, IL-1β), ROS/RNS and chemokines (Bsibsi et al., 2014). This mechanism presents a self-feeding, vicious cycle of demyelination and tissue destruction in MS lesions where an initially beneficial oligodendroglial stress response that suppresses innate immune activity becomes detrimental following lymphocyte invasion.

Increased expression of cryαB in the present study was detected already in the late induction phase of AON in the optic nerve compartment (Figure 4.15E). Double staining with different glial cell markers revealed that, at this time point, increased expression of cryαB was associated with oligodendrocytes, particularly in the ONH area (Figure 4.15B). As previously discussed, this area is characterized as having a permeable BBB and shows signs of axonal paranodal disruptions and microglial activation (discussed in chapter 5.4). This reflects the previously discussed observation from preactive MS lesions where up-regulation of cryαB in oligodendrocytes was observed in areas with activated microglia (van Noort et al., 2010). Following the onset of the clinical phase of AON, increased cryαB expression in oligodendrocytes was more widespread and was associated with inflammatory demyelinating lesions (Figure 4.16A and B).

Collectively, it is possible that blood-borne stress molecules which can penetrate through the permeable BBB in the late induction phase of AON could inflict sub-lethal stress on oligodendrocytes (as observed by the increased expression of cryαB and the lack of apoptotic oligodendrocytes at this time point). When the BBB is finally broken down and infiltration of inflammatory cells into the optic nerve occurs, the capacity of oligodendrocytes to defend against pro-apoptotic, inflammatory mediators fails, as observed by the later appearance of $TUNEL^+$ oligodendrocytes associated with inflammatory lesions. Increased cryαB expression in surviving oligodendrocytes within such lesions might contribute to further demyelination and tissue degradation by mechanisms as previously described in MS lesions (Bsibsi et al., 2014). In later stages of the clinical phase of AON, reactive astrocytes may also contribute to the increased cryαB expression, as confirmed by its presence in hypertrophic $GFAP^+$ processes (Figure 4.16D, Di).

5.7 Autoantibodies in AON – a role in early oligodendrocyte stress?

The ONH area seems to play an important role in the pathology of the optic nerve compartment in the model of AON. Previous studies have reported that the BBB is incomplete in this area (Tso et al.,

1975; Hu et al., 1998; Fairless et al., 2012) and that activation of residential microglia precedes BBB breakdown and infiltration of immune cells from the periphery (Fairless et al., 2012). In this study, the presence of both axonal and oligodendroglial stress was found to be more pronounced in this area during the late induction phase of AON, further implying its particular vulnerability and potential role in pathogenesis. Furthermore, at the onset of the clinical phase of AON, the first inflammatory lesions are also observed extending from the ONH (author's observation, data not shown) implying that this area is the first entry point for invading inflammatory cells from the periphery.

Immunisation of BN rats with MOG elicits a strong humoral immune response as observed by the production of anti-MOG antibodies (Stefferl et al., 1999; Fairless et al., 2012). Elevated levels of anti-MOG antibodies have been detected in the serum of animals from day 10 p.i. (Fairless et al., 2012), the same time point as when signs of both axonal and oligodendroglial stress have been reported in this study. Furthermore, at this time point, deposition of IgG was detected in the area of the ONH suggesting the possible role of autoantibodies in inducing early cellular stress (Figure 4.21.B; Fairless et al., 2012). Following the onset of AON, extensive IgG deposition has been observed in areas with reduced MBP staining intensity (Figure 4.20B). This reflects the pathological image of a type II white matter MS lesion, characterised by antibody-mediated demyelination (Lucchinetti et al., 2000). Interestingly, strong antibody deposition was also observed in newly forming lesions characterized by very little demyelination (Figure 4.20Bi) and an increased expression of cryαB (Figure 422Ai). These results suggested that the deposition of auto-reactive (MOG) antibodies might induce a stress response in oligodendrocytes at an early stage of lesion development. Considering that in the late induction phase of AON areas of IgG deposition and oligodendrocyte stress coincide within the area of the ONH, this could also be the underlying mechanism for early oligodendrocyte stress prior to the onset of inflammatory demyelination.

5.8 Different compartments of the axon-glia junction might be targeted independently during the induction phase of AON

Paranodal domains are the anchoring regions for myelinating oligodendrocytes to axons. Considering that signs of stress were observed in both axonal and glial compartments simultaneously, as well as in the paranodal domains themselves, it is hard to draw a conclusion on the origins of these disruptions, particularly due to the possibility that stress might be translated from one compartment to the other. In order to investigate the contribution of the individual compartments to the disrupted axonal-glial junction at the paranodal domain during the induction phase of AON, two different

experimental approaches were performed. The aim was to determine whether oligodendrocyte stress (perhaps mediated by sublytic autoantibody binding) or neuronal stress (perhaps mediated by retinal disturbances present early in the induction phase of AON) were responsible for the observations made.

The potential disruptive role of anti-MOG antibodies in AON was addressed by transferring sera from MOG-immunised animals into naïve animals. The pathological role of anti-MOG antibodies was previously investigated in different studies through the use of both *in vivo* and in *in vitro* models. Transfer of anti-MOG antibodies into different EAE models where a humoral response is absent or minimal, leads to an exacerbated disease course (Zhou et al., 2006; Lee et al., 2012). Also the injection of anti-MOG antibodies, isolated from patients suffering from neuromyelitis optica (syndrome characterized by inflammatory demyelination of the optic nerve and spinal cord), into the mouse brain, led to transient episodes of demyelination and the loss of axonal domains in the absence of inflammation (Saadoun et al., 2014). In the cultured rat telencephalon, application of anti-MOG antibodies together with complement led to demyelination and a strong increase of cryαB expression in oligodendrocytes and astrocytes (Duvanel et al., 2004). Collectively, these studies provide evidence of the demyelinating potential of anti-MOG antibodies and their involvement in pathological processes in neuroinflammation. In addition, studies that examined a broader effect of these antibodies on oligodendrocyte integrity have been performed in order to investigate the possibility of additional disruptive mechanisms. In such cell-based assays, application of anti-MOG antibodies was sufficient to induce sub-lethal alterations in oligodendrocyte morphology. This was observed by internalisation of oligodendroglial membrane compartments and retraction of their processes (Marta et al., 2005a, b), and also a disruption in their cytoskeletal organization (Dale et al., 2014).

The loss of RGCs, accompanied by a disruption of the blood-retinal barrier and activation of microglia in the retina, are the early pathological signs characteristic of the induction phase of AON (Fairless et al., 2012). Considering that these retinal events precede the observed changes in optic nerve axonal domains and the cytoskeleton (being observed from as early as day 5 p.i.) they could be the underlying cause of axonal stress in the late induction phase. In order to investigate this hypothesis, a model of primary retinal insult was employed. Intravitreal injection of glutamate is a model often used for studying pathological mechanisms in the retina as it leads to the death of RGCs and other neurons within the inner retinal layers (Sisk et al., 1985; Schori et al., 2001; Zhou et al., 2007). As previously mentioned, elevated glutamate levels are found in the retina during the induction phase of AON, coinciding with RGC death (Maier et al., 2007). Also the blockade of NMDA glutamate receptors in AON led to RGC protection, even during the induction phase (Sühs et al., 2014). These

studies provide evidence for glutamate-mediated RGC death in the early stages of AON. Furthermore, they provide justification for employing intravitreal glutamate injections as a model for studying the effects of RGC loss on optic nerve axons. Although models of both glutamate- and NMDA-induced degeneration have been widely used for studying retinal pathology, there are only a few studies that have investigated the integrity of the axonal compartment following primary RGC death. In one study, intravitreal injection of NMDA led to post-chiasmal neuronal degeneration and astrocytic activation in the contralateral LGN (Ito et al., 2008). Another study focused on the integrity of axonal transport and axonal viability itself in the optic nerve following intravitreal NMDA injection (Kuribayashi et al., 2010). The authors reported a decrease in axonal counts and a reduction in kinesin (a protein involved in axonal transport) in the absence of demyelination 72h following the intravitreal injection. Such studies could be highly relevant in the field of MS research in light of recent reports of a primary retinal pathology in MS patients in the absence of optic neuritis (Fisher et al., 2006; Pulicken et al., 2007; Henderson et al., 2008; Saidha et al., 2011).

5.8.1 Transfer of serum from MOG-immunised animals supports the role of autoantibodies in early oligodendrocyte stress in AON

In this present study, transfer of serum from MOG-immunised animals into naïve animals was performed in order to determine the role anti-MOG antibodies may have in inducing the early signs of stress that were seen. Levels of anti-MOG antibodies in recipient animals were considerably lower than in MOG-immunised donors (Figure 4.21G) but nevertheless, their deposition could be observed in the ONH of recipient animals (Figure 4.23E, F). Although the transfer of serum from MOG-immunised animals did not induce demyelination and axonal injury (Figure 4.22A - C), it was sufficient to induce oligodendrocyte stress in the ONH, as observed by an increased expression of cryαB (Figure 4.22E and F). Lack of demyelination and axonal disruptions in the optic nerve is probably owed to low levels of anti-MOG antibodies in the serum of recipient animals considering that previous studies were able to observe such phenotype upon direct injection of anti-MOG antibodies into the brain (Saadoun et al., 2014). These results suggest that even the low levels of anti-MOG antibodies, such as those observed in the late induction phase of AON, are sufficient to induce oligodendrocyte stress independently of demyelination.

5.8.2 Primary retinal insult is sufficient to induce axonal disruptions in the induction phase of AON

A single intravitreal injection of glutamate into a naïve animal was sufficient to mimic aspects of the retinal pathology reported during the induction phase of AON as observed by the presence of $TUNEL^+$ cells in the RGC and inner nuclear layer (Figure 4.23B) and the increased presence of activated microglial cells in the retina (Figure 4.23D and G). Although there was no evidence of macroscopic changes in the optic nerve compartment (such as the axonal loss reported by Kuribayashi and colleagues) subtle changes in axons could be detected. The utilization of the glutamate-mediated model of a primary retinal insult alone was sufficient to induce an axonal injury in the optic nerve, similar to that observed during the induction phase of AON, characterised by disruption of axonal domains (Figure 4.24B) and changes in the NF phosphorylation status (Figure 4.24A). Interestingly, increased microglial activation was also observed in the optic nerve (Figure 4.23H), in a similar manner to that observed during the induction phase of AON. This strengthens the possibility that activation of microglia during the induction phase of AON could be a consequence, rather than a cause, of the observed axonal stress. The lack of oligodendrocyte stress, demyelination and large-scale inflammation in the optic nerve imply that the observed axonal disruptions are caused by the primary insult in the retinal compartment. Although the precise mechanisms of these disruptions were not addressed, they are likely to involve impaired metabolic/energetic support from the compromised RGC body. The notion that axonal injury could be a consequence of a compromised neuronal cell body in the absence of the inflammatory demyelination is also suggested in MS. One study employing MRI showed that diffuse axonal injury in NAWM is found to correlate with the presence of cortical lesions rather than with inflammatory lesions in the white matter (Mistry et al., 2014).

In conclusion, by employing these two models it was possible to gain further insight into the origins of axonal and oligodendroglial stress observed in the induction phase of AON. In both instances signs of stress were not translated from one compartment to the other, although it should be noted that in the case of serum transfer, the low concentrations of anti-MOG antibodies achieved in recipient animals could explain the lack of demyelination and disruption in axonal domains. This hurdle could be overstepped by transferring purified anti-MOG antibodies (either commercial or isolated from sera of immunised animals) in order to achieve higher concentrations in recipient animals. An alternative possibility is that the observed stresses seen in both in axonal and oligodendroglial compartments during the late induction phase of AON might result from two separate stimuli occurring simultaneously such as a still unclear retinal pathology and circulating (anti-MOG) autoantibodies. Further work is needed to determine the relevance of these findings to the human

condition, but observations of retinal degeneration and impaired visual functions in the absence of clinically-defined optic neuritis suggest that there may be common mechanisms at work.

References

- Abbott N.J., Patabendige A.A., Dolman D.E., Yusof S.R. and Begley DJ. (2010) Structure and function of the blood-brain barrier. Neurobiol Dis. 37(1):13-25.
- Adams R.A., Bauer J., Flick M.J., Sikorski S.L., Nuriel T., Lassmann H., Degen J.L. and Akassoglou K. (2007) The fibrin-derived gamma377-395 peptide inhibits microglia activation and suppresses relapsing paralysis in central nervous system autoimmune disease. J Exp Med. 204(3):571-82.
- Alberts B., Bray D., Lewis J., Raff M., Roberts K. and Watson J.D. (1998) The cells of the nervous system: an overview of their structure and function. In: Molecular biology of the cell. 2nd edn. New York: Garland p. 1059–63.
- Allen C.L. and Bayraktutan U. (2009) Oxidative stress and its role in the pathogenesis of ischaemic stroke. Int J Stroke 4(6):461-70.
- Alonso A. and Hernán M.A. (2008) Temporal trends in the incidence of multiple sclerosis: a systematic review. Neurology 71(2):129-35.
- Arancibia-Carcamo I.L. and Attwell D. (2014) The node of Ranvier in CNS pathology. Acta Neuropathol. 128(2):161-75.
- Aranda M.L., Dorfman D., Sande P.H. and Rosenstein R.E. (2015) Experimental optic neuritis induced by the microinjection of lipopolysaccharide into the optic nerve. Exp Neurol. 266:30-41.
- Arbuthnott E.R., Boyd I.A. and Kalu K.U. (1980) Ultrastructural dimensions of myelinated peripheral nerve fibres in the cat and their relation to conduction velocity. J Physiol. 308:125-57.
- Arnett H.A., Mason J., Marino M., Suzuki K., Matsushima G.K. and Ting J.P. (2001) TNF alpha promotes proliferation of oligodendrocyte progenitors and remyelination. Nat Neurosci. 4(11):1116-22
- Arnold A.C. (2005) Evolving management of optic neuritis and multiple sclerosis. Am J Ophthalmol. 139(6):1101-8.
- Arroyo S., Lesser R.P., Poon W.T., Webber W.R. and Gordon B. (1997) Neuronal generators of visual evoked potentials in humans: visual processing in the human cortex. Epilepsia. 38(5):600-10.
- Babbe H., Roers A., Waisman A., Lassmann H., Goebels N., Hohlfeld R., Friese M., Schröder R., Deckert M., Schmidt S., Ravid R. and Rajewsky K. (2000) Clonal expansions of CD8(+) T cells

dominate the T cell infiltrate in active multiple sclerosis lesions as shown by micromanipulation and single cell polymerase chain reaction. J Exp Med. 192(3):393-404.

- Babbs C.F. and Shi R. (2013) Subtle paranodal injury slows impulse conduction in a mathematical model of myelinated axons. PLoS One 8(7):e67767.
- Baerwald K.D. and Popko B. (1998) Developing and mature oligodendrocytes respond differently to the immune cytokine interferon-gamma. J Neurosci Res. 52(2):230-9.
- Bajramović J.J., Lassmann H. and van Noort JM. (1997) Expression of alphaB-crystallin in glia cells during lesional development in multiple sclerosis. J Neuroimmunol. 78(1-2):143-51.
- Bajramović J.J., Plomp A.C., Goes Av., Koevoets C., Newcombe J., Cuzner M.L. and van Noort J.M. (2000) Presentation of alpha B-crystallin to T cells in active multiple sclerosis lesions: an early event following inflammatory demyelination. J Immunol. 164(8):4359-66.
- Bakshi R., Czarnecki D., Shaikh Z.A., Priore R.L., Janardhan V., Kaliszky Z. and Kinkel P.R. (2000) Brain MRI lesions and atrophy are related to depression in multiple sclerosis. Neuroreport 11(6):1153-8.
- Barnett M.H. and Prineas J.W. (2004) Relapsing and remitting multiple sclerosis: pathology of the newly forming lesion. Ann Neurol. 55(4):458-68.
- Bechtold D.A., Kapoor R. and Smith K.J. (2004) Axonal protection using flecainide in experimental autoimmune encephalomyelitis. Ann Neurol. 55(5):607-16.
- Bechtold D.A., Miller S.J., Dawson A.C., Sun Y., Kapoor R., Berry D. and Smith K.J. (2006) Axonal protection achieved in a model of multiple sclerosis using lamotrigine. J Neurol. 253(12):1542-51.
- Beck R.W., Trobe J.D., Moke P.S., Gal R.L., Xing D., Bhatti M.T., Brodsky M.C., Buckley E.G., Chrousos G.A., Corbett J., Eggenberger E., Goodwin J.A., Katz B., Kaufman D.I., Keltner J.L., Kupersmith M.J., Miller N.R., Nazarian S., Orengo-Nania S., Savino P.J., Shults W.T., Smith C.H., Wall M., Optic Neuritis Study Group. (2003) High- and low-risk profiles for the development of multiple sclerosis within 10 years after optic neuritis: experience of the optic neuritis treatment trial. Arch Ophthalmol. 121(7):944-9.
- Bellen H.J., Lu Y., Beckstead R. and Bhat M.A. (1998) Neurexin IV, caspr and paranodin–novel members of the neurexin family: encounters of axons and glia. Trends Neurosci. 21, pp. 444–449.
- Ben-Nun A., Wekerle H. and Cohen I.R. (1981) The rapid isolation of clonable antigen-specific T lymphocyte lines capable of mediating autoimmune encephalomyelitis. Eur J Immunol. 11(3):195-9.
- Bennett V. and Gilligan D.M. (1993) The spectrin-based membrane skeleton and micron-scale organization of the plasma membrane. Annu Rev Cell Biol. 9:27-66.

- Berghs S., Aggujaro D., Dirkx R., Maksimova E., Stabach P., Hermel J.M., Zhang J.P., Philbrick W., Slepnev V., Ort T. and Solimena, M. (2000) betaIV spectrin, a new spectrin localized at axon initial segments and nodes of ranvier in the central and peripheral nervous system. J. Cell Biol. 151, pp. 985–1002.
- Bernardo A., Greco A., Levi G. and Minghetti L. (2003) Differential lipid peroxidation, Mn superoxide, and bcl-2 expression contribute to the maturation-dependent vulnerability of oligodendrocytes to oxidative stress. J. Neuropathol. Exp. Neurol. 62, 509–519.
- Bhat M.A., Rios J.C., Lu Y., Garcia-Fresco G.P., Ching W., St Martin M., Li J., Einheber S., Chesler M., Rosenbluth J., Salzer J.L. and Bellen H.J. (2001) Axon-glia interactions and the domain organization of myelinated axons requires neurexin IV/Caspr/Paranodin. Neuron 30(2):369-83.
- Bitsch A., Schuchardt J., Bunkowski S., Kuhlmann T. and Brück W. (2000) Acute axonal injury in multiple sclerosis. Correlation with demyelination and inflammation. Brain 123 (Pt 6): 1174-83.
- Bjartmar C., Kidd G., Mörk S., Rudick R. and Trapp B.D. (2000) Neurological disability correlates with spinal cord axonal loss and reduced N-acetyl aspartate in chronic multiple sclerosis patients. Ann Neurol. 48(6):893-901.
- Bjartmar C., Kinkel R.P., Kidd G., Rudick R.A. and Trapp B.D. (2001) Axonal loss in normal-appearing white matter in a patient with acute MS. Neurology ;57(7):1248-52.
- Black J.A., Newcombe J., Trapp B.D. and Waxman S.G. (2007a) Sodium channel expression within chronic multiple sclerosis plaques. J Neuropathol Exp Neurol. 66(9):828-37.
- Black J.A., Liu S, Carrithers M., Carrithers L.M., Waxman S.G. (2007b) Exacerbation of experimental autoimmune encephalomyelitis after withdrawal of phenytoin and carbamazepine. Ann Neurol. 62(1):21-33.
- Block M.L., Zecca L. and Hong J.S. (2007) Microglia-mediated neurotoxicity: uncovering the molecular mechanisms. Nat Rev Neurosci. 8(1):57-69.
- Bogie J.F., Stinissen P. and Hendriks J.J. (2014) Macrophage subsets and microglia in multiple sclerosis. Acta Neuropathol. 128(2):191-213.
- Boiko T., Rasband M.N., Levinson S.R., Caldwell J.H., Mandel G., Trimmer J.S. and Matthews G. (2001) Compact myelin dictates the differential targeting of two sodium channel isoforms in the same axon. Neuron 30, pp. 91–104.
- Boiko T., Van Wart A., Caldwell J.H., Levinson S.R., Trimmer J.S. and Matthews G. (2003) Functional specialization of the axon initial segment by isoform-specific sodium channel targeting. J. Neurosci. 23, pp. 2306–2313.

- Boretius S., Gadjanski I., Demmer I., Bähr M., Diem R., Michaelis T. and Frahm J. (2008) MRI of optic neuritis in a rat model. Neuroimage 41(2):323-34.
- Bourquin C., Schubart A., Tobollik S., Mather I., Ogg S., Liblau R. and Linington C. (2003) Selective unresponsiveness to conformational B cell epitopes of the myelin oligodendrocyte glycoprotein in H-2b mice. J Immunol. 171(1):455-61.
- Bouzidi M., Tricaud N., Giraud P., Kordeli E., Caillol G., Deleuze C., Couraud F. and Alcaraz G. (2002) Interaction of the Nav1.2a subunit of the voltage-dependent sodium channel with nodal ankyrinG. In vitro mapping of the interacting domains and association in synaptosomes. J Biol Chem. 277(32):28996-9004.
- Boyle E.A. and McGeer P.L. (1990) Cellular immune response in multiple sclerosis plaques. Am J Pathol. 137(3):575-84.
- Boyle M.E., Berglund E.O., Murai K.K., Weber L., Peles E. and Ranscht B. (2001) Contactin orchestrates assembly of the septate-like junctions at the paranode in myelinated peripheral nerve. Neuron. 30(2):385-97.
- Bö L, Dawson TM, Wesselingh S, Mörk S, Choi S, Kong PA, Hanley D and Trapp BD. (1994) Induction of nitric oxide synthase in demyelinating regions of multiple sclerosis brains. Ann Neurol. 36(5):778-86.
- Bö L., Peterson J.W., Mørk S., Hoffman P.A., Gallatin W.M., Ransohoff R.M. and Trapp B.D. (1996) Distribution of immunoglobulin superfamily members ICAM-1, -2, -3, and the beta 2 integrin LFA-1 in multiple sclerosis lesions. J Neuropathol Exp Neurol. 55(10):1060-72.
- Bö L., Vedeler C.A., Nyland H., Trapp B.D. and Mörk S.J. (2003) Intracortical multiple sclerosis lesions are not associated with increased lymphocyte infiltration. Mult Scler. 9(4):323-31.
- Brady S.T., Witt A.S., Kirkpatrick L.L., de Waegh S.M., Readhead C., Tu P.H. and Lee V.M. (1999) Formation of compact myelin is required for maturation of the axonal cytoskeleton. J Neurosci. 19(17):7278-88.
- Brownell B. and Hughes J.T. (1962) The distribution of plaques in the cerebrum in multiple sclerosis. J Neurol Neurosurg Psychiatry 25:315-20.
- Brusa A., Jones S.J., Kapoor R., Miller D.H. and Plant GT. (1999) Long-term recovery and fellow eye deterioration after optic neuritis, determined by serial visual evoked potentials. J Neurol. 246(9):776-82.
- Brusa A., Jones S.J. and Plant G.T. (2001) Long-term remyelination after optic neuritis: A 2-year visual evoked potential and psychophysical serial study. Brain. 124(Pt 3):468-79.
- Brück W., Porada P., Poser S., Rieckmann P., Hanefeld F., Kretzschmar H.A. and Lassmann H. (1995) Monocyte/macrophage differentiation in early multiple sclerosis lesions. Ann Neurol. 38(5):788-96.

- Brück W (2005) The pathology of multiple sclerosis is the result of focal inflammatory demyelination with axon damage J Neurol. 252 Suppl 5:v3-9.
- Bsibsi M., Holtman I.R., Gerritsen W.H., Eggen B.J., Boddeke E., van der Valk P., van Noort J.M. and Amor S. (2013) Alpha-B-crystallin induces an immune-regulatory and antiviral microglial response in preactive multiple sclerosis lesions. J Neuropathol Exp Neurol. 72(10):970-9.
- Bsibsi M., Peferoen L.A., Holtman I.R., Nacken P.J., Gerritsen W.H., Witte M.E., van Horssen J., Eggen B.J., van der Valk P., Amor S. and van Noort J.M. (2014) Demyelination during multiple sclerosis is associated with combined activation of microglia/macrophages by IFN-γ and alpha B-crystallin. Acta Neuropathol. 128(2):215-29.
- Buckle G.J. (2005) Functional magnetic resonance imaging and multiple sclerosis: the evidence for neuronal plasticity. J Neuroimaging. 15(4 Suppl):82S-93S.
- Buttermore E.D., Dupree J.L., Cheng J., An X., Tessarollo L. and Bhat M.A. (2011) The cytoskeletal adaptor protein band 4.1B is required for the maintenance of paranodal axoglial septate junctions in myelinated axons. J Neurosci. 31(22):8013-24.
- Calabrese M., Poretto V., Favaretto A., Alessio S., Bernardi V., Romualdi C., Rinaldi F., Perini P. and Gallo P. (2012) Cortical lesion load associates with progression of disability in multiple sclerosis. Brain 135(Pt 10):2952-61.
- Calabrese M., Romualdi C., Poretto V., Favaretto A., Morra A., Rinaldi F., Perini P. and Gallo P. (2013) The changing clinical course of multiple sclerosis: a matter of grey matter. Ann Neurol. 74(1):76-83.
- Calabrese M., Magliozzi R., Ciccarelli O., Geurts J.J., Reynolds R. and Martin R. (2015) Exploring the origins of grey matter damage in multiple sclerosis. Nat Rev Neurosci. 16(3):147-58.
- Carbone F., De Rosa V., Carrieri P.B., Montella S., Bruzzese D., Porcellini A., Procaccini C., La Cava A. and Matarese G. (2014) Regulatory T cell proliferative potential is impaired in human autoimmune disease. Nat Med. 20(1):69-74.
- Catterall W.A. (2000) From ionic currents to molecular mechanisms: the structure and function of voltage-gated sodium channels. Neuron 26, pp. 13–25.
- Chabas D., Baranzini S.E., Mitchell D., Bernard C.C., Rittling S.R., Denhardt D.T., Sobel R.A., Lock C., Karpuj M., Pedotti R., Heller R., Oksenberg J.R. and Steinman L. (2001) The influence of the proinflammatory cytokine, osteopontin, on autoimmune demyelinating disease. Science 294(5547):1731-5.
- Charcot M., (1868) Histologie de la sclerose en plaques. Gaz Hosp. 141 554-5,-557-8.

- Chard DT, Griffin CM, Parker GJ, Kapoor R, Thompson AJ and Miller DH. (2002) Brain atrophy in clinically early relapsing-remitting multiple sclerosis. Brain 125(Pt 2):327-37.
- Charles P., Tait S., Faivre-Sarrailh C., Barbin G., Gunn-Moore F., Denisenko-Nehrbass N., Guennoc A.M., Girault J.A., Brophy P.J. and Lubetzki, C. (2002) Neurofascin is a glial receptor for the paranodin/Caspr-contactin axonal complex at the axoglial junction. Curr. Biol. 12, pp. 217–220.
- Cherry J.D., Olschowka J.A. and O'Banion M.K. (2014) Neuroinflammation and M2 microglia: the good, the bad, and the inflamed. J Neuroinflammation 11:98.
- Chinnery H.R., Ruitenberg M.J. and McMenamin P.G. (2010) Novel characterization of monocyte-derived cell populations in the meninges and choroid plexus and their rates of replenishment in bone marrow chimeric mice. J Neuropathol Exp Neurol. 69(9):896-909.
- Colley B.S., Phillips L.L. and Reeves T.M. (2010) The effects of cyclosporin-A on axonal conduction deficits following traumatic brain injury in adult rats. Exp Neurol. 224(1):241-51.
- Coman I., Aigrot M.S., Seilhean D., Reynolds R., Girault J.A., Zalc B. and Lubetzki C. (2006) Nodal, paranodal and juxtaparanodal axonal proteins during demyelination and remyelination in multiple sclerosis. Brain 129(Pt 12):3186-95.
- Compston A. and Coles A. (2002) Multiple sclerosis. Lancet 359(9313):1221-31.
- Compston A. and Coles A. (2008) Multiple sclerosis. Lancet 372(9648):1502-17.
- Confavreux C. and Vukusic S. (2006) Age at disability milestones in multiple sclerosis. Brain 129(Pt 3):595-605.
- Cornelius C., Crupi R., Calabrese V., Graziano A., Milone P., Pennisi G., Radak Z., Calabrese E.J. and Cuzzocrea S. (2013) Traumatic brain injury: oxidative stress and neuroprotection. Antioxid Redox Signal. 19(8):836-53.
- Costello F., Coupland S., Hodge W., Lorello G.R., Koroluk J., Pan Y.I., Freedman M.S., Zackon D.H. and Kardon R.H. (2006) Quantifying axonal loss after optic neuritis with optical coherence tomography. Ann Neurol. 59(6):963-9.
- Craner M.J., Lo A.C., Black J.A. and Waxman S.G. (2003) Abnormal sodium channel distribution in optic nerve axons in a model of inflammatory demyelination. Brain 126(Pt 7):1552-61.
- Craner M.J., Newcombe J., Black J.A., Hartle C., Cuzner M.L. and Waxman S.G. (2004a) Molecular changes in neurons in multiple sclerosis: altered axonal expression of Nav1.2 and Nav1.6 sodium channels and Na+/Ca2+ exchanger. Proc Natl Acad Sci U S A. 101(21):8168-73.
- Craner M.J., Hains B.C., Lo A.C., Black J.A. and Waxman S.G. (2004b) Co-localization of sodium channel Nav1.6 and the sodium-calcium exchanger at sites of axonal injury in the spinal cord in EAE. Brain 127(Pt 2):294-303.

- Craner M.J., Damarjian T.G., Liu S., Hains B.C., Lo A.C., Black J.A., Newcombe J., Cuzner M.L. and Waxman S.G. (2005) Sodium channels contribute to microglia/macrophage activation and function in EAE and MS. Glia 49(2):220-9.
- Crawford D.K., Mangiardi M., Xia X., López-Valdés H.E. and Tiwari-Woodruff S.K. (2009) Functional recovery of callosal axons following demyelination: a critical window. Neuroscience 164(4):1407-21.
- Cross A.H., Stark J.L., Lauber J., Ramsbottom M.J. and Lyons J.A. (2006) Rituximab reduces B cells and T cells in cerebrospinal fluid of multiple sclerosis patients. J Neuroimmunol. 180(1-2):63-70.
- Cudrici C., Niculescu T., Niculescu F., Shin M.L. and Rus H. (2006) Oligodendrocyte cell death in pathogenesis of multiple sclerosis: Protection of oligodendrocytes from apoptosis by complement. J Rehabil Res Dev. 43(1):123-32.
- Cunnea P., Mháille A.N., McQuaid S., Farrell M., McMahon J. and FitzGerald U. (2011) Expression profiles of endoplasmic reticulum stress-related molecules in demyelinating lesions and multiple sclerosis. Mult Scler. 17(7):808-18.
- Dale R.C., Tantsis E.M., Merheb V., Kumaran R.Y., Sinmaz N., Pathmanandavel K., Ramanathan S., Booth D.R., Wienholt L.A., Prelog K., Clark D.R., Guillemin G.J., Lim C.K., Mathey E.K. and Brilot F. (2014) Antibodies to MOG have a demyelination phenotype and affect oligodendrocyte cytoskeleton. Neurol Neuroimmunol Neuroinflamm. 1(1):e12.
- Davalos D., Ryu J.K., Merlini M., Baeten K.M., Le Moan N., Petersen M.A., Deerinck T.J., Smirnoff D.S., Bedard C., Hakozaki H., Gonias Murray S., Ling J.B., Lassmann H., Degen J.L., Ellisman M.H. and Akassoglou K. (2012) Fibrinogen-induced perivascular microglial clustering is required for the development of axonal damage in neuroinflammation. Nat Commun. 3:1227.
- Detels R., Visscher B.R., Malmgren R.M., Coulson A.H., Lucia M.V. and Dudley J.P. (1977) Evidence for lower susceptibility to multiple sclerosis in Japanese-Americans. Am J Epidemiol. 105(4):303-10.
- De Groot C.J., Bergers E., Kamphorst W., Ravid R., Polman C.H., Barkhof F., van der Valk P. (2001) Post-mortem MRI-guided sampling of multiple sclerosis brain lesions: increased yield of active demyelinating and (p)reactive lesions. Brain 124(Pt 8):1635-45.
- DeLuca G.C., Alterman R., Martin J.L., Mittal A., Blundell S., Bird S., Beale H., Hong L.S. and Esiri M.M. (2013) Casting light on multiple sclerosis heterogeneity: the role of HLA-DRB1 on spinal cord pathology. Brain 136(Pt 4):1025-34.

- Diem R., Sättler M.B., Merkler D, Demmer I., Maier K., Stadelmann C., Ehrenreich H. and Bähr M. (2005) Combined therapy with methylprednisolone and erythropoietin in a model of multiple sclerosis. Brain 128(Pt 2):375-85.
- van Diemen H.A., Lanting P., Koetsier J.C., Strijers R.L., van Walbeek H.K. and Polman CH. (1992) Evaluation of the visual system in multiple sclerosis: a comparative study of diagnostic tests. Clin Neurol Neurosurg. 94(3):191-5.
- Disanto G., Morahan J.M., Barnett M.H., Giovannoni G. and Ramagopalan S.V. (2012) The evidence for a role of B cells in multiple sclerosis. Neurology 78(11):823-32.
- Dragunow M. (2013) Meningeal and choroid plexus cells--novel drug targets for CNS disorders. Brain Res. 1501:32-55.
- Derfuss T., Parikh K., Velhin S., Braun M., Mathey E., Krumbholz M., Kümpfel T., Moldenhauer A., Rader C., Sonderegger P., Pöllmann W., Tiefenthaller C., Bauer J., Lassmann H., Wekerle H., Karagogeos D., Hohlfeld R., Linington C. and Meinl E. (2009) Contactin-2/TAG-1-directed autoimmunity is identified in multiple sclerosis patients and mediates gray matter pathology in animals. Proc Natl Acad Sci U S A 106(20):8302-7.
- Dong X.X., Wang Y. and Qin Z.H. (2009) Molecular mechanisms of excitotoxicity and their relevance to pathogenesis of neurodegenerative diseases. Acta Pharmacol Sin. 30(4):379-87. doi: 10.1038/aps.2009.24.
- Dowling P., Shang G., Raval S., Menonna J., Cook S. and Husar W. (1996) Involvement of the CD95 (APO-1/Fas) receptor/ligand system in multiple sclerosis brain. J Exp Med. 184(4):1513-8.
- Dunn S.E. and Steinman L. (2013) The gender gap in multiple sclerosis: intersection of science and society. JAMA Neurol. 70(5):634-5.
- Dutta R., McDonough J., Yin X., Peterson J., Chang A., Torres T., Gudz T., Macklin W.B., Lewis D.A., Fox R.J., Rudick R., Mirnics K. and Trapp B.D. (2006) Mitochondrial dysfunction as a cause of axonal degeneration in multiple sclerosis patients. Ann Neurol. 59(3):478-89.
- Dutta R. and Trapp B.D. (2011) Mechanisms of neuronal dysfunction and degeneration in multiple sclerosis. Prog Neurobiol. 93(1):1-12.
- Duvanel C.B., Monnet-Tschudi F., Braissant O., Matthieu J.M. and Honegger P. (2004) Tumor necrosis factor-alpha and alphaB-crystallin up-regulation during antibody-mediated demyelination in vitro: a putative protective mechanism in oligodendrocytes. J Neurosci Res. 78(5):711-22.
- Dyment D.A., Ebers G.C. and Sadovnick A.D. (2004) Genetics of multiple sclerosis. Lancet Neurol. 3(2):104-10.

- Ebers G.C., Yee I.M., Sadovnick A.D. and Duquette P. (2000) Conjugal multiple sclerosis: population-based prevalence and recurrence risks in offspring. Canadian Collaborative Study Group. Ann Neurol. 48(6):927-31.
- Ellwardt E. and Zipp F. (2014) Molecular mechanisms linking neuroinflammation and neurodegeneration in MS. Exp Neurol. 262 Pt A:8-17.
- Engelhardt B. (2006) Molecular mechanisms involved in T cell migration across the blood-brain barrier. J Neural Transm. 113(4):477-85.
- Eugster H.P., Frei K., Bachmann R., Bluethmann H., Lassmann H. and Fontana A. (1999) Severity of symptoms and demyelination in MOG-induced EAE depends on TNFR1. Eur J Immunol. 29(2):626-32.
- Fairless R., Williams S.K., Hoffmann D.B., Stojic A., Hochmeister S., Schmitz F., Storch M.K. and Diem R. (2012) Preclinical retinal neurodegeneration in a model of multiple sclerosis. J Neurosci. 32(16):5585-97.
- Fairless R., Williams S.K. and Diem R. (2014) Dysfunction of neuronal calcium signalling in neuroinflammation and neurodegeneration. Cell Tissue Res. 357(2):455-62.
- Ferguson B., Matyszak M.K., Esiri M.M. and Perry V.H. (1997) Axonal damage in acute multiple sclerosis lesions. Brain 120 (Pt 3):393-9.
- Fisher J.B., Jacobs D.A., Markowitz C.E., Galetta S.L., Volpe N.J., Nano-Schiavi M.L., Baier M.L., Frohman E.M., Winslow H., Frohman T.C., Calabresi P.A., Maguire M.G., Cutter G.R. and Balcer L.J. (2006) Relation of visual function to retinal nerve fiber layer thickness in multiple sclerosis. Ophthalmology 113(2):324-32.
- Fisniku L.K., Brex P.A., Altmann D.R., Miszkiel K.A., Benton C.E., Lanyon R., Thompson A.J. and Miller D.H. (2008) Disability and T2 MRI lesions: a 20-year follow-up of patients with relapse onset of multiple sclerosis. Brain 131(Pt 3):808-17.
- Fliegner K.H. and Liem R.K. (1991) Cellular and molecular biology of neuronal intermediate filaments. Int Rev Cytol. 131:109-67.
- Foroozan R., Buono L.M., Savino P.J. and Sergott R.C. (2002) Acute demyelinating optic neuritis. Curr Opin Ophthalmol. 13(6):375-80.
- Frappier T., Stetzkowski-Marden F., Pradel L.A. (1991) Interaction domains of neurofilament light chain and brain spectrin. Biochem J. 275 (Pt 2):521-7.
- Frederiksen J.L., Madsen H.O., Ryder L.P., Larsson H.B., Morling N. and Svejgaard A. (1997) HLA typing in acute optic neuritis. Relation to multiple sclerosis and magnetic resonance imaging findings. Arch Neurol. 54(1):76-80.
- Freedman M.S., Thompson E.J., Deisenhammer F., Giovannoni G., Grimsley G., Keir G., Ohman S., Racke M.K., Sharief M., Sindic C.J., Sellebjerg F. and Tourtellotte W.W. (2005)

Recommended standard of cerebrospinal fluid analysis in the diagnosis of multiple sclerosis: a consensus statement. Arch Neurol. 62(6):865-70.

- Friese M.A. and Fugger L. (2005) Autoreactive CD8+ T cells in multiple sclerosis: a new target for therapy? Brain 128(Pt 8):1747-63.
- Frischer J.M., Bramow S., Dal-Bianco A., Lucchinetti C.F., Rauschka H., Schmidbauer M., Laursen H., Sorensen P.S. and Lassmann H. (2009) The relation between inflammation and neurodegeneration in multiple sclerosis brains. Brain. 132(Pt 5):1175-89.
- Fu Y., Sun W., Shi Y., Shi R. and Cheng JX. (2009) Glutamate excitotoxicity inflicts paranodal myelin splitting and retraction. PLoS One 4(8):e6705.
- Fujino M., Funeshima N., Kitazawa Y., Kimura H., Amemiya H., Suzuki S. and Li X.K. (2003) Amelioration of experimental autoimmune encephalomyelitis in Lewis rats by FTY720 treatment. J Pharmacol Exp Ther. 305(1):70-7.
- Furley A.J., Morton S.B., Manalo D., Karagogeos D., Dodd J. and Jessell T.M. (1990) The axonal glycoprotein TAG-1 is an immunoglobulin superfamily member with neurite outgrowth-promoting activity. Cell 61, pp. 157–170.
- Fujimoto J.G., Pitris C., Boppart S.A. and Brezinski M.E. (2000) Optical coherence tomography: an emerging technology for biomedical imaging and optical biopsy. Neoplasia 2(1-2):9-25.
- Gale C.R. and Martyn C.N. (1995) Migrant studies in multiple sclerosis. Prog Neurobiol. 47(4-5):425-48.
- Ganter P, Prince C and Esiri MM. (1999) Spinal cord axonal loss in multiple sclerosis: a post-mortem study. Neuropathol Appl Neurobiol. 25(6):459-67.
- Gasser D.L., Newlin C.M., Palm J. and Gonatas N.K. (1973) Genetic control of susceptibility to experimental allergic encephalomyelitis in rats. Science 181(4102):872-3.
- Gavrieli Y., Sherman Y. and Ben-Sasson S.A. (1992) Identification of programmed cell death in situ via specific labeling of nuclear DNA fragmentation. J Cell Biol. 119(3):493-501.
- Gilligan D.M. and Bennett V. (1993) The junctional complex of the membrane skeleton. Semin Hematol. 30(1):74-83.
- Gilmore C.P., Donaldson I., Bö L., Owens T., Lowe J. and Evangelou N. (2008) Regional variations in the extent and pattern of grey matter demyelination in multiple sclerosis: a comparison between the cerebral cortex, cerebellar cortex, deep grey matter nuclei and the spinal cord. J Neurol Neurosurg Psychiatry 80(2):182-7.
- Gilmore C.P., DeLuca G.C., Bö L., Owens T., Lowe J., Esiri M.M. and Evangelou N. (2009) Spinal cord neuronal pathology in multiple sclerosis. Brain Pathol. 19(4):642-9.

- Ginhoux F., Lim S., Hoeffel G., Low D. and Huber T. (2013) Origin and differentiation of microglia. Front Cell Neurosci. 7:45.
- Gobin S.J., Montagne L., Van Zutphen M., Van Der Valk P., Van Den Elsen P.J. and De Groot C.J. (2001) Upregulation of transcription factors controlling MHC expression in multiple sclerosis lesions. Glia 36(1):68-77.
- van der Goes A., Boorsma W., Hoekstra K., Montagne L., de Groot C.J. and Dijkstra C.D. (2005) Determination of the sequential degradation of myelin proteins by macrophages. J Neuroimmunol. 161(1-2):12-20.
- Goldin, A.L. (2001) Resurgence of sodium channel research. Annu. Rev. Physiol. 63, pp. 871–894.
- Goldbaum O. and Richter-Landsberg C. (2001) Stress proteins in oligodendrocytes: differential effects of heat shock and oxidative stress. J Neurochem. 78(6):1233-42.
- Goldbaum O. and Richter-Landsberg C. (2004) Proteolytic stress causes heat shock protein induction, tau ubiquitination, and the recruitment of ubiquitin to tau-positive aggregates in oligodendrocytes in culture. J Neurosci. 24(25):5748-57.
- Goverman J., Woods A., Larson L., Weiner L.P., Hood L. and Zaller D.M. (1993) Transgenic mice that express a myelin basic protein-specific T cell receptor develop spontaneous autoimmunity. Cell 72(4):551-60.
- Gray E., Thomas T.L., Betmouni S., Scolding N. and Love S. (2008) Elevated matrix metalloproteinase-9 and degradation of perineuronal nets in cerebrocortical multiple sclerosis plaques. J Neuropathol Exp Neurol. 67(9):888-99.
- Green A.J., McQuaid S., Hauser S.L., Allen I.V. and Lyness R. (2010) Ocular pathology in multiple sclerosis: retinal atrophy and inflammation irrespective of disease duration. Brain. 133(Pt 6):1591-601.
- Greenwood J.A., Troncoso J.C., Costello A.C. and Johnson G.V. (1993) Phosphorylation modulates calpain-mediated proteolysis and calmodulin binding of the 200-kDa and 160-kDa neurofilament proteins. J Neurochem. 61(1):191-9.
- Griffiths I., Klugmann M., Anderson T., Yool D., Thomson C., Schwab M.H., Schneider A., Zimmermann F., McCulloch M., Nadon N. and Nave K.A. (1998) Axonal swellings and degeneration in mice lacking the major proteolipid of myelin. Science 280(5369):1610-3.
- Guinamard R., Demion M. and Launay P. (2010) Physiological roles of the TRPM4 channel extracted from background currents. Physiology (Bethesda) 25(3):155-64.
- Guo F., Maeda Y., Ko E.M., Delgado M., Horiuchi M., Soulika A., Miers L., Burns T., Itoh T., Shen H., Lee E., Sohn J. and Pleasure D. (2012) Disruption of NMDA receptors in

oligodendroglial lineage cells does not alter their susceptibility to experimental autoimmune encephalomyelitis or their normal development. J Neurosci. 32(2):639-45. doi: 10.1523

- Haahr S., Plesner A.M., Vestergaard B.F. and Höllsberg P. (2004) A role of late Epstein-Barr virus infection in multiple sclerosis. Acta Neurol Scand. 109(4):270-5.
- Hafler D.A., International Multiple Sclerosis Genetics Consortium, Compston A., Sawcer S., Lander E.S., Daly M.J., De Jager P.L., de Bakker P.I., Gabriel S.B., Mirel D.B., Ivinson A.J., Pericak-Vance M.A., Gregory S.G., Rioux J.D., McCauley J.L., Haines J.L., Barcellos L.F., Cree B., Oksenberg J.R., Hauser .SL. (2007) Risk alleles for multiple sclerosis identified by a genomewide study. N Engl J Med. 357(9):851-62.
- Haider L, Fischer MT, Frischer JM, Bauer J, Höftberger R, Botond G, Esterbauer H, Binder CJ, Witztum JL and Lassmann H. (2011) Oxidative damage in multiple sclerosis lesions. Brain 134(Pt 7):1914-24.
- Haider L., Simeonidou C., Steinberger G., Hametner S., Grigoriadis N., Deretzi G., Kovacs G.G., Kutzelnigg A., Lassmann H. and Frischer J.M. (2014) Multiple sclerosis deep grey matter: the relation between demyelination, neurodegeneration, inflammation and iron. J Neurol Neurosurg Psychiatry 85(12):1386-95.
- Halliday A.M., McDonald W.I. and Mushin J. (1972) Delayed visual evoked response in optic neuritis. Lancet. 1(7758):982-5.
- Halliday A.M., McDonald W.I. and Mushin J. (1973) Visual evoked response in diagnosis of multiple sclerosis. Br Med J. 4(5893):661-4.
- Halliday A.M. and Mushin J. (1980) The visual evoked potential in neuroophthalmology. Int Ophthalmol Clin. 20(1):155-83.
- Han M.H., Hwang S.I., Roy D.B., Lundgren D.H., Price J.V., Ousman S.S., Fernald G.H., Gerlitz B., Robinson W.H., Baranzini S.E., Grinnell B.W., Raine C.S., Sobel R.A., Han D.K. and Steinman L. (2008) Proteomic analysis of active multiple sclerosis lesions reveals therapeutic targets. Nature 451(7182):1076-81.
- Hauser S.L. and Oksenberg J.R. (2006) The neurobiology of multiple sclerosis: genes, inflammation, and neurodegeneration. Neuron 52(1):61-76.
- Hauser S.L., Waubant E., Arnold D.L., Vollmer T., Antel J., Fox R.J., Bar-Or A., Panzara M., Sarkar N., Agarwal S., Langer-Gould A., Smith C.H., HERMES Trial Group. (2008) B-cell depletion with rituximab in relapsing-remitting multiple sclerosis. N Engl J Med. 358(7):676-88.
- Hedström A.K., Bäärnhielm M., Olsson T. and Alfredsson L. (2009) Tobacco smoking, but not Swedish snuff use, increases the risk of multiple sclerosis. Neurology 73(9):696-701.

- Henderson A.P., Barnett M.H., Parratt J.D. and Prineas J.W. (2009) Multiple sclerosis: distribution of inflammatory cells in newly forming lesions. Ann Neurol. 66(6):739-53.
- Hein K., Gadjanski I., Kretzschmar B., Lange K., Diem R., Sättler M.B. and Bähr M. (2012) An optical coherence tomography study on degeneration of retinal nerve fiber layer in rats with autoimmune optic neuritis. Invest Ophthalmol Vis Sci. 53(1):157-63.
- Henderson A.P., Trip S.A., Schlottmann P.G., Altmann D.R., Garway-Heath D.F., Plant G.T. and Miller D.H. (2008) An investigation of the retinal nerve fibre layer in progressive multiple sclerosis using optical coherence tomography. Brain. 131(Pt 1):277-87.
- Hobom M., Storch M.K., Weissert R., Maier K., Radhakrishnan A., Kramer B., Bähr M. and Diem R. (2004) Mechanisms and time course of neuronal degeneration in experimental autoimmune encephalomyelitis. Brain Pathol. 14(2):148-57.
- Hoffmann D.B., Williams S.K., Bojcevski J., Müller A., Stadelmann C., Naidoo V., Bahr B.A., Diem R. and Fairless R. (2013) Calcium influx and calpain activation mediate preclinical retinal neurodegeneration in autoimmune optic neuritis. J Neuropathol Exp Neurol. 72(8):745-57.
- Hofman F.M., Hinton D.R., Johnson K. and Merrill J.E. (1989) Tumor necrosis factor identified in multiple sclerosis brain. J Exp Med. 170(2):607-12.
- Hofstetter H.H., Shive C.L. and Forsthuber T.G. (2002) Pertussis toxin modulates the immune response to neuroantigens injected in incomplete Freund's adjuvant: induction of Th1 cells and experimental autoimmune encephalomyelitis in the presence of high frequencies of Th2 cells. J Immunol. 169(1):117-25.
- Hohlfeld R (1997) Biotechnological agents for the immunotherapy of multiple sclerosis. Principles, problems and perspectives. Brain 120 (Pt 5):865-916.
- Honce J.M. (2013) Gray Matter Pathology in MS: Neuroimaging and Clinical Correlations. Mult Scler Int. 2013:627870.
- Horresh I., Bar V., Kissil J.L. and Peles E. (2010) Organization of myelinated axons by Caspr and Caspr2 requires the cytoskeletal adapter protein 4.1B. J Neurosci. 30(7):2480-9.
- Houtchens M.K., Benedict R.H., Killiany R., Sharma J., Jaisani Z., Singh B., Weinstock-Guttman B., Guttmann C.R. and Bakshi R. (2007) Thalamic atrophy and cognition in multiple sclerosis. Neurology 69(12):1213-23.
- Howell O.W., Palser A., Polito A., Melrose S., Zonta B., Scheiermann C., Vora A.J., Brophy P.J. and Reynolds R. (2006) Disruption of neurofascin localization reveals early changes preceding demyelination and remyelination in multiple sclerosis. Brain 129(Pt 12):3173-85.
- Howell O.W., Rundle J.L., Garg A., Komada M., Brophy PJ and Reynolds R. (2010) Activated microglia mediate axoglial disruption that contributes to axonal injury in multiple sclerosis. J Neuropathol Exp Neurol. 69(10):1017-33.

- Howell O.W., Reeves C.A., Nicholas R., Carassiti D., Radotra B., Gentleman S.M., Serafini B., Aloisi F., Roncaroli F., Magliozzi R. and Reynolds R. (2011) Meningeal inflammation is widespread and linked to cortical pathology in multiple sclerosis. Brain 134(Pt 9):2755-71.
- Höftberger R., Aboul-Enein F., Brueck W., Lucchinetti C., Rodriguez M., Schmidbauer M., Jellinger K. and Lassmann H. (2004) Expression of major histocompatibility complex class I molecules on the different cell types in multiple sclerosis lesions. Brain Pathol. 14(1):43-50.
- Hu P, Pollard J, Hunt N, Taylor J, Chan-Ling T (1998) Microvascular and cellular responses in the optic nerve of rats with acute experimental allergic encephalomyelitis (EAE). Brain Pathol 8:475– 486.
- Huan J., Culbertson N., Spencer L., Bartholomew R., Burrows G.G., Chou Y.K., Bourdette D., Ziegler S.F., Offner H. and Vandenbark A.A. (2005) Decreased FOXP3 levels in multiple sclerosis patients. J Neurosci Res. 81(1):45-52.
- Huff T.B., Shi Y., Sun W., Wu W., Shi R. and Cheng J.X. (2011) Real-time CARS imaging reveals a calpain-dependent pathway for paranodal myelin retraction during high-frequency stimulation. PLoS One 6(3):e17176.
- Huitinga I., Erkut Z.A., van Beurden D. and Swaab D.F. (2004) Impaired hypothalamus-pituitary-adrenal axis activity and more severe multiple sclerosis with hypothalamic lesions. Ann Neurol. 55(1):37-45.
- Huizinga R, van der Star BJ, Kipp M, Jong R, Gerritsen W, Clarner T, Puentes F, Dijkstra CD, van der Valk P and Amor S. (2011) Phagocytosis of neuronal debris by microglia is associated with neuronal damage in multiple sclerosis. Glia 60(3):422-31.
- Huizinga R., van der Star B.J., Kipp M., Jong R., Gerritsen W., Clarner T., Puentes F., Dijkstra C.D., van der Valk P. and Amor S. (2012) Phagocytosis of neuronal debris by microglia is associated with neuronal damage in multiple sclerosis. Glia 60(3):422-31.
- Ignacio R.J., Patrucco L. and Cristiano E. (2010) Oligoclonal bands and MRI in clinically isolated syndromes: predicting conversion time to multiple sclerosis. J Neurol. 257(7):1188-91.
- Ito Y., Shimazawa M., Inokuchi Y., Fukumitsu H., Furukawa S., Araie M. and Hara H. (2008) Degenerative alterations in the visual pathway after NMDA-induced retinal damage in mice. Brain Res. 1212:89-101.
- Itoyama Y., Webster H.D., Sternberger N.H., Richardson E.P. Jr, Walker D.L., Quarles R.H. and Padgett B.L. (1982) Distribution of papovavirus, myelin-associated glycoprotein, and myelin basic protein in progressive multifocal leukoencephalopathy lesions. Ann Neurol. 11(4):396-407.

- Iwaki T., Wisniewski T., Iwaki A., Corbin E., Tomokane N., Tateishi J. and Goldman J.E. (1992) Accumulation of alpha B-crystallin in central nervous system glia and neurons in pathologic conditions. Am J Pathol. 140(2):345-56.
- Jadidi-Niaragh F. and Mirshafiey A. (2011) Th17 cell, the new player of neuroinflammatory process in multiple sclerosis. Scand J Immunol. 74(1):1-13.
- Jin Y., de Pedro-Cuesta J., Söderström M., Stawiarz L. and Link H. (2000) Seasonal patterns in optic neuritis and multiple sclerosis: a meta-analysis. J Neurol Sci.; 181(1-2):56-64.
- Kamradt M.C., Lu M., Werner M.E., Kwan T., Chen F., Strohecker A., Oshita S., Wilkinson J.C., Yu C., Oliver P.G., Duckett C.S., Buchsbaum D.J., LoBuglio A.F., Jordan V.C. and Cryns V.L. (2005) The small heat shock protein alpha B-crystallin is a novel inhibitor of TRAIL-induced apoptosis that suppresses the activation of caspase-3. J Biol Chem. 280(12):11059-66.
- Kanamori A., Catrinescu M.M., Belisle J.M., Costantino S. and Levin LA. (2012) Retrograde and Wallerian axonal degeneration occur synchronously after retinal ganglion cell axotomy. Am J Pathol. 181(1):62-73.
- Kapoor R., Davies M., Blaker P.A., Hall S.M. and Smith K.J. (2003) Blockers of sodium and calcium entry protect axons from nitric oxide-mediated degeneration. Ann Neurol. 53(2):174-80.
- Kapoor R., Furby J., Hayton T., Smith K.J., Altmann D.R., Brenner R., Chataway J., Hughes R.A. and Miller D.H. (2010) Lamotrigine for neuroprotection in secondary progressive multiple sclerosis: a randomised, double-blind, placebo-controlled, parallel-group trial. Lancet Neurol. 9(7):681-8.
- Kappos L., Radue E.W., O'Connor P., Polman C., Hohlfeld R., Calabresi P., Selmaj K., Agoropoulou C., Leyk M., Zhang-Auberson L., Burtin P.; FREEDOMS Study Group. (2010) A placebo-controlled trial of oral fingolimod in relapsing multiple sclerosis. N Engl J Med. 362(5):387-401.
- Káradóttir R, Cavelier P, Bergersen LH and Attwell D. (2005) NMDA receptors are expressed in oligodendrocytes and activated in ischaemia. Nature 438(7071):1162-6.
- Kierdorf K., Erny D., Goldmann T., Sander V., Schulz C., Perdiguero E.G., Wieghofer P., Heinrich A., Riemke P., Hölscher C., Müller D.N., Luckow B., Brocker T., Debowski K., Fritz G., Opdenakker G., Diefenbach A., Biber K., Heikenwalder M., Geissmann F., Rosenbauer F. and Prinz M. (2013) Microglia emerge from erythromyeloid precursors via Pu.1- and Irf8-dependent pathways. Nat Neurosci. 16(3):273-80.
- Kipp M., van der Valk P. and Amor S. (2012) Pathology of multiple sclerosis. CNS Neurol Disord Drug Targets 11(5):506-17.

- Klemenz R., Fröhli E., Steiger R.H., Schäfer R. and Aoyama A. (1991) Alpha B-crystallin is a small heat shock protein. Proc Natl Acad Sci U S A. 88(9):3652-6.
- Klistorner A., Graham S., Fraser C., Garrick R., Nguyen T., Paine M., O'Day J., Grigg J., Arvind H. and Billson F.A. (2007) Electrophysiological evidence for heterogeneity of lesions in optic neuritis. Invest Ophthalmol Vis Sci. 48(10):4549-56.
- Kluver H. and Barrera E. (1953) A method for the combined staining of cells and fibers in the nervous system. J Neuropathol Exp Neurol. 12(4):400-3.
- Koch-Henriksen N. and Sørensen P.S. (2010) The changing demographic pattern of multiple sclerosis epidemiology. Lancet Neurol. 9(5):520-32.
- Kolappan M., Henderson A.P., Jenkins T.M., Wheeler-Kingshott C.A., Plant G.T., Thompson A.J. and Miller D.H. (2009) Assessing structure and function of the afferent visual pathway in multiple sclerosis and associated optic neuritis. J Neurol. 256(3):305-19.
- Komada M. and Soriano P. (2002) IV-spectrin regulates sodium channel clustering through ankyrin-G at axon initial segments and nodes of Ranvier. J. Cell Biol. 156, pp. 337–348 [Beta].
- Koritschoner R.S. and Schweinburg F. (1925) Induktion von Paralyse und Rückenmarksentzündung durch Immunisierung von Kaninchen mit menschlichem Rückenmarksgewebe. Z Immunitätsf Exp Therapie 1925; 42: 217–83.
- Kornek B., Storch M.K., Weissert R., Wallstroem E., Stefferl A., Olsson T., Linington C., Schmidbauer M. and Lassmann H. (2000) Multiple sclerosis and chronic autoimmune encephalomyelitis: a comparative quantitative study of axonal injury in active, inactive, and remyelinated lesions. Am J Pathol. 157(1):267-76.
- Kornek B., Storch M.K., Bauer J., Djamshidian A., Weissert R., Wallstroem E., Stefferl A., Zimprich F., Olsson T., Linington C., Schmidbauer M. and Lassmann H. (2001) Distribution of a calcium channel subunit in dystrophic axons in multiple sclerosis and experimental autoimmune encephalomyelitis. Brain 124(Pt 6):1114-24.
- Körner H., Riminton D.S., Strickland D.H., Lemckert F.A., Pollard J.D. and Sedgwick J.D. (1997) Critical points of tumor necrosis factor action in central nervous system autoimmune inflammation defined by gene targeting. J Exp Med. 186(9):1585-90.
- Krishnamoorthy G., Lassmann H., Wekerle H. and Holz A. (2006) Spontaneous opticospinal encephalomyelitis in a double-transgenic mouse model of autoimmune T cell/B cell cooperation. J Clin Invest. 116(9):2385-92.
- Krishnamoorthy G. and Wekerle H. (2009) EAE: an immunologist's magic eye. Eur J Immunol. 39(8):2031-5.

- Kuhle J, Leppert D, Petzold A, Regeniter A, Schindler C, Mehling M, Anthony DC, Kappos L and Lindberg RL. (2011) Neurofilament heavy chain in CSF correlates with relapses and disability in multiple sclerosis. Neurology 76(14):1206-13.
- Kuhle J., Disanto G., Dobson R., Adiutori R., Bianchi L., Topping J., Bestwick J.P., Meier U.C., Marta M., Costa G.D., Runia T., Evdoshenko E., Lazareva N., Thouvenot E., Iaffaldano P., Direnzo V., Khademi M., Piehl F., Comabella M., Sombekke M., Killestein J., Hegen H., Rauch S., D'Alfonso S., Alvarez-Cermeño J.C., Kleinová P., Horáková D., Roesler R., Lauda F., Llufriu S., Avsar T., Uygunoglu U., Altintas A., Saip S., Menge T., Rajda C., Bergamaschi R., Moll N., Khalil M., Marignier R., Dujmovic I., Larsson H., Malmestrom C., Scarpini E., Fenoglio C., Wergeland S., Laroni A., Annibali V., Romano S., Martínez A.D., Carra A., Salvetti M., Uccelli A., Torkildsen Ø., Myhr K.M., Galimberti D., Rejdak K., Lycke J., Frederiksen J.L., Drulovic J., Confavreux C., Brassat D., Enzinger C., Fuchs S., Bosca I., Pelletier J., Picard C., Colombo E., Franciotta D., Derfuss T., Lindberg R., Yaldizli Ö., Vécsei L., Kieseier B.C., Hartung H.P., Villoslada P., Siva A., Saiz A., Tumani H., Havrdová E., Villar L.M., Leone M., Barizzone N., Deisenhammer F., Teunissen C., Montalban X., Tintoré M., Olsson T., Trojano M., Lehmann S., Castelnovo G., Lapin S., Hintzen R., Kappos L., Furlan R., Martinelli V., Comi G., Ramagopalan S.V. and Giovannoni G. (2015) Conversion from clinically isolated syndrome to multiple sclerosis: A large multicentre study. Mult Scler. 21(8):1013-24.
- Kuhlmann T., Lingfeld G., Bitsch A., Schuchardt J. and Brück W. (2002) Acute axonal damage in multiple sclerosis is most extensive in early disease stages and decreases over time. Brain 125(Pt 10):2202-12.
- Kuribayashi J., Kitaoka Y., Munemasa Y. and Ueno S. (2010) Kinesin-1 and degenerative changes in optic nerve axons in NMDA-induced neurotoxicity. Brain Res. 1362:133-40.
- Kutzelnigg A, Lucchinetti CF, Stadelmann C, Brück W, Rauschka H, Bergmann M, Schmidbauer M, Parisi JE and Lassmann H. (2005) Cortical demyelination and diffuse white matter injury in multiple sclerosis. Brain 128(Pt 11):2705-12.
- Kutzelnigg A. and Lassmann H. (2005) Cortical lesions and brain atrophy in MS. J Neurol Sci. 233(1-2):55-9.
- Lambert S., Davis J.Q. and Bennett V. (1997) Morphogenesis of the node of ranvier: co-clusters of ankyrin and ankyrin-binding integral proteins define early developmental intermediates. J Neurosci. 17:7025-36.
- Lappe-Siefke C, Goebbels S, Gravel M, Nicksch E, Lee J, Braun PE, Griffiths IR and Nave KA. (2003) Disruption of Cnp1 uncouples oligodendroglial functions in axonal support and myelination. Nat Genet. 33(3):366-74.

- Larochelle C., Alvarez J.I. and Prat A. (2011) How do immune cells overcome the blood-brain barrier in multiple sclerosis? FEBS Lett. 585(23):3770-80.
- Lassmann H. (2005) Multiple sclerosis pathology: evolution of pathogenetic concepts. Brain Pathol. 15(3):217-22.
- Lassmann H. and van Horssen J. (2011) The molecular basis of neurodegeneration in multiple sclerosis. FEBS Lett. 585(23):3715-23.
- Lee D.H. and Linker R.A. (2012) The role of myelin oligodendrocyte glycoprotein in autoimmune demyelination: a target for multiple sclerosis therapy? Expert Opin Ther Targets 16(5):451-62.
- The Lenercept MS study group. (1999) TNF neutralization in MS: results of a randomized, placebo-controlled multicenter study. The Lenercept Multiple Sclerosis Study Group and The University of British Columbia MS/MRI Analysis Group. Neurology 53(3):457-65.
- Leuenberger T., Paterka M., Reuter E., Herz J., Niesner R.A., Radbruch H., Bopp T., Zipp F. and Siffrin V. (2013) The role of CD8+ T cells and their local interaction with CD4+ T cells in myelin oligodendrocyte glycoprotein35-55-induced experimental autoimmune encephalomyelitis. J Immunol. 191(10):4960-8.
- Li C, Tropak MB, Gerlai R, Clapoff S, Abramow-Newerly W, Trapp B, Peterson A and Roder J. (1994) Myelination in the absence of myelin-associated glycoprotein. Nature 369(6483):747-50.
- Lidster K., Jackson S.J., Ahmed Z., Munro P., Coffey P., Giovannoni G., Baker M.D. and Baker D. (2013) Neuroprotection in a novel mouse model of multiple sclerosis. PLoS One 8(11):e79188.
- Linthicum D.S., Munoz J.J. and Blaskett A. (1982) Acute experimental autoimmune encephalomyelitis in mice. I. Adjuvant action of Bordetella pertussis is due to vasoactive amine sensitization and increased vascular permeability of the central nervous system. Cell Immunol. 73(2):299-310.
- Liu J.S., Zhao ML, Brosnan CF and Lee SC. (2001) Expression of inducible nitric oxide synthase and nitrotyrosine in multiple sclerosis lesions. Am J Pathol. 158(6):2057-66.
- Liu J., Liu M.C. and Wang K.K. (2008) Calpain in the CNS: from synaptic function to neurotoxicity. Sci Signal. 1(14):re1.
- Liu S., Li J., Tao Y. and Xiao X. (2007) Small heat shock protein alphaB-crystallin binds to p53 to sequester its translocation to mitochondria during hydrogen peroxide-induced apoptosis. Biochem Biophys Res Commun. 354(1):109-14.

- Lo A.C., Saab C.Y., Black J.A. and Waxman SG. (2003) Phenytoin protects spinal cord axons and preserves axonal conduction and neurological function in a model of neuroinflammation in vivo. J Neurophysiol 90:3566-71.
- Lonigro A. and Devaux J.J. (2009) Disruption of neurofascin and gliomedin at nodes of Ranvier precedes demyelination in experimental allergic neuritis. Brain 132(Pt 1):260-73.
- Lovas G, Szilágyi N, Majtényi K, Palkovits M and Komoly S. (2000) Axonal changes in chronic demyelinated cervical spinal cord plaques. Brain 123 (Pt 2):308-17.
- Lovato L., Willis S.N., Rodig S.J., Caron T., Almendinger S.E., Howell O.W., Reynolds R., O'Connor K.C. and Hafler D.A. (2011) Related B cell clones populate the meninges and parenchyma of patients with multiple sclerosis. Brain 134(Pt 2):534-41.
- Lublin F.D. and Reingold S.C. (1996) Defining the clinical course of multiple sclerosis: results of an international survey. National Multiple Sclerosis Society (USA) Advisory Committee on Clinical Trials of New Agents in Multiple Sclerosis. Neurology 46(4):907-11.
- Lublin F.D., Reingold S.C., Cohen J.A., Cutter G.R., Sørensen P.S., Thompson A.J., Wolinsky J.S., Balcer L.J., Banwell B., Barkhof F., Bebo B. Jr, Calabresi P.A., Clanet M., Comi G., Fox R.J., Freedman M.S., Goodman A.D., Inglese M., Kappos L., Kieseier B.C., Lincoln J.A., Lubetzki C., Miller A.E., Montalban X., O'Connor P.W., Petkau J., Pozzilli C., Rudick R.A., Sormani M.P., Stüve O., Waubant E. and Polman C.H. (2014) Defining the clinical course of multiple sclerosis: the 2013 revisions. Neurology 83(3):278-86.
- Lucas R.M., Hughes A.M., Lay M.L., Ponsonby A.L., Dwyer D.E., Taylor B.V. and Pender MP. (2011) Epstein-Barr virus and multiple sclerosis. J Neurol Neurosurg Psychiatry. 82(10):1142-8.
- Lucchinetti C., Brück W., Parisi J., Scheithauer B., Rodriguez M. and Lassmann H. (2000) Heterogeneity of multiple sclerosis lesions: implications for the pathogenesis of demyelination. Ann Neurol. 47(6):707-17.
- Lucchinetti C., Popescu B.F., Bunyan R.F., Moll N.M., Roemer S.F., Lassmann H., Brück W., Parisi J.E., Scheithauer B.W., Giannini C., Weigand S.D., Mandrekar J. and Ransohoff R.M. (2011) Inflammatory cortical demyelination in early multiple sclerosis. N Engl J Med. 365(23):2188-97.
- Lumsden C.E. (1970) The neuropathology of multiple sclerosis. In Handbook of Clinical Neurology, ed. PJ Vinken, GW Bruyn, pp. 217–309. New York: Elsevier
- Lund F.E. and Randall T.D. (2010) Effector and regulatory B cells: modulators of CD4+ T cell immunity. Nat Rev Immunol. 10(4):236-47.
- Ludwin S.K. and Johnson E.S. (1981) Evidence for a "dying-back" gliopathy in demyelinating disease. Ann Neurol. 9(3):301-5.

- MacDonald B.K., Cockerell O.C., Sander J.W. and Shorvon S.D. The incidence and lifetime prevalence of neurological disorders in a prospective community-based study in the UK. Brain. 123 (Pt 4):665-76.
- Madsen L.S., Andersson E.C., Jansson L., krogsgaard M., Andersen C.B., Engberg J., Strominger J.L., Svejgaard A., Hjorth J.P., Holmdahl R., Wucherpfennig K.W. and Fugger L. (1999) A humanized model for multiple sclerosis using HLA-DR2 and a human T-cell receptor. Nat Genet. 23(3):343-7.
- Magliozzi R., Howell O., Vora A., Serafini B., Nicholas R., Puopolo M., Reynolds R. and Aloisi F. (2007) Meningeal B-cell follicles in secondary progressive multiple sclerosis associate with early onset of disease and severe cortical pathology. Brain 130(Pt 4):1089-104.
- Magliozzi R., Howell O.W., Reeves C., Roncaroli F., Nicholas R., Serafini B., Aloisi F. and Reynolds R. (2010) A Gradient of neuronal loss and meningeal inflammation in multiple sclerosis. Ann Neurol. 68(4):477-93.
- Maier K., Merkler D., Gerber J., Taheri N., Kuhnert A.V., Williams S.K., Neusch C., Bähr M. and Diem R. (2007) Multiple neuroprotective mechanisms of minocycline in autoimmune CNS inflammation. Neurobiol Dis. 25(3):514-25.
- Mao Y.W., Liu J.P., Xiang H. and Li D.W. (2004) Human alphaA- and alphaB-crystallins bind to Bax and Bcl-X(S) to sequester their translocation during staurosporine-induced apoptosis. Cell Death Differ. 11(5):512-26.
- Marta C.B., Oliver A.R., Sweet R.A., Pfeiffer S.E. and Ruddle N.H. (2005a) Pathogenic myelin oligodendrocyte glycoprotein antibodies recognize glycosylated epitopes and perturb oligodendrocyte physiology. Proc Natl Acad Sci U S A 102(39):13992-7.
- Marta C.B., Montano M.B., Taylor C.M., Taylor A.L., Bansal R. and Pfeiffer S.E. (2005b) Signaling cascades activated upon antibody cross-linking of myelin oligodendrocyte glycoprotein: potential implications for multiple sclerosis. J Biol Chem. 280(10):8985-93.
- del Pilar Martin M., Cravens P.D., Winger R., Frohman E.M., Racke M.K., Eagar T.N., Zamvil S.S., Weber M.S., Hemmer B., Karandikar N.J., Kleinschmidt-DeMasters B.K. and Stüve O. (2008) Decrease in the numbers of dendritic cells and CD4+ T cells in cerebral perivascular spaces due to natalizumab. Arch Neurol. 65(12):1596-603.
- Martínez-Lapiscina E.H., Sanchez-Dalmau B., Fraga-Pumar E., Ortiz-Perez S., Tercero-Uribe A.I., Torres-Torres R. and Villoslada P. (2014) The visual pathway as a model to understand brain damage in multiple sclerosis. Mult Scler. 20(13):1678-85.
- Masjuan J., Alvarez-Cermeño J.C., García-Barragán N., Díaz-Sánchez M., Espiño M., Sádaba M.C., González-Porqué P., Martínez San Millán J. and Villar L.M. (2006) Clinically isolated

syndromes: a new oligoclonal band test accurately predicts conversion to MS. Neurology 66(4):576-8.

- Mathey E.K., Derfuss T., Storch M.K., Williams K.R., Hales K., Woolley D.R., Al-Hayani A., Davies S.N., Rasband M.N., Olsson T., Moldenhauer A., Velhin S., Hohlfeld R., Meinl E. and Linington C. (2007) Neurofascin as a novel target for autoantibody-mediated axonal injury. J Exp Med. 204(10):2363-72.
- Matloubian M., Lo C.G., Cinamon G., Lesneski M.J., Xu Y., Brinkmann V., Allende M.L., Proia R.L. and Cyster J.G. (2004) Lymphocyte egress from thymus and peripheral lymphoid organs is dependent on S1P receptor 1. Nature 427(6972):355-60.
- Matsunaga Y., Kezuka T., An X., Fujita K., Matsuyama N., Matsuda R., Usui Y., Yamakawa N., Kuroda M. and Goto H. (1992) Visual functional and histopathological correlation in experimental autoimmune optic neuritis. Invest Ophthalmol Vis Sci. 53(11):6964-71.
- Matute C, Alberdi E, Domercq M, Pérez-Cerdá F, Pérez-Samartín A and Sánchez-Gómez MV. (2001) The link between excitotoxic oligodendroglial death and demyelinating diseases. Trends Neurosci. 24(4):224-30.
- McDonald J.W., Althomsons S.P., Hyrc K.L., Choi D.W. and Goldberg M.P. (1998) Oligodendrocytes from forebrain are highly vulnerable to AMPA/kainate receptor-mediated excitotoxicity. Nat Med. 4(3):291-7.
- McGonigal R., Rowan E.G., Greenshields K.N., Halstead S.K., Humphreys P.D., Rother R.P., Furukawa K. and Willison H.J. (2010) Anti-GD1a antibodies activate complement and calpain to injure distal motor nodes of Ranvier in mice. Brain 133(Pt 7):1944-60.
- Melief J., Schuurman K.G., van de Garde M.D., Smolders J., van Eijk M., Hamann J. and Huitinga I. (2013) Microglia in normal appearing white matter of multiple sclerosis are alerted but immunosuppressed. Glia 61(11):1848-61.
- Menegoz M., Gaspar P., Bert M.L., Galvez T., Burgaya F., Palfrey C., Ezan P., Arnos F. and Girault, J.A. (1997) Paranodin, a glycoprotein of neuronal paranodal membranes. Neuron 19, pp. 319–331.
- Mendel I., Kerlero de Rosbo N. and Ben-Nun A. (1995) A myelin oligodendrocyte glycoprotein peptide induces typical chronic experimental autoimmune encephalomyelitis in H-2b mice: fine specificity and T cell receptor V beta expression of encephalitogenic T cells. Eur J Immunol. 25(7):1951-9.
- Merrill J.E., Kono D.H., Clayton J., Ando D.G., Hinton D.R. and Hofman F.M. (1992) Inflammatory leukocytes and cytokines in the peptide-induced disease of experimental allergic encephalomyelitis in SJL and B10.PL mice. Proc Natl Acad Sci U S A. 89(2):574-8.

- Mews I, Bergmann M, Bunkowski S, Gullotta F and Brück W. (1998) Oligodendrocyte and axon pathology in clinically silent multiple sclerosis lesions. Mult Scler. 4(2):55-62.
- Meyer R., Weissert R., Diem R., Storch M.K., de Graaf K.L., Kramer B. and Bahr M. (2001) Acute neuronal apoptosis in a rat model of multiple sclerosis. J Neurosci. 21(16):6214-20.
- Micu I, Jiang Q, Coderre E, Ridsdale A, Zhang L, Woulfe J, Yin X, Trapp BD, McRory JE, Rehak R, Zamponi GW, Wang W and Stys PK. (2006) NMDA receptors mediate calcium accumulation in myelin during chemical ischaemia. Nature 439(7079):988-92.
- Miller D.H. and Leary S.M. (2007) Primary-progressive multiple sclerosis. Lancet Neurol. 6(10):903-12.
- Miller D.H., Chard D.T. and Ciccarelli O. (2012) Clinically isolated syndromes. Lancet Neurol. 11(2):157-69.
- Mistry N., Abdel-Fahim R., Mougin O., Tench C., Gowland P. and Evangelou N. (2014) Cortical lesion load correlates with diffuse injury of multiple sclerosis normal appearing white matter. Mult Scler. 20(2):227-33.
- Moll N.M., Rietsch A.M., Thomas S., Ransohoff A.J., Lee J.C., Fox R., Chang A., Ransohoff R.M. and Fisher E. (2011) Multiple sclerosis normal-appearing white matter: pathology-imaging correlations. Ann Neurol. 70(5):764-73.
- Munger K.L., Levin L.I., Hollis B.W., Howard N.S. and Ascherio A. (2006) Serum 25-hydroxyvitamin D levels and risk of multiple sclerosis. JAMA. 296(23):2832-8.
- Naismith R.T., Piccio L., Lyons J.A., Lauber J., Tutlam N.T., Parks B.J., Trinkaus K., Song S.K. and Cross A.H. (2010) Rituximab add-on therapy for breakthrough relapsing multiple sclerosis: a 52-week phase II trial. Neurology 74(23):1860-7.
- Neema M., Arora A., Healy B.C., Guss Z.D., Brass S.D., Duan Y., Buckle G.J., Glanz B.I., Stazzone L., Khoury S.J., Weiner H.L., Guttmann C.R. and Bakshi R. (2009) Deep gray matter involvement on brain MRI scans is associated with clinical progression in multiple sclerosis. J Neuroimaging 19(1):3-8.
- Neumann H., Medana I.M., Bauer J. and Lassmann H. (2002) Cytotoxic T lymphocytes in autoimmune and degenerative CNS diseases. Trends Neurosci. 25(6):313-9.
- Nikić I, Merkler D, Sorbara C, Brinkoetter M, Kreutzfeldt M, Bareyre FM, Brück W, Bishop D, Misgeld T and Kerschensteiner M. (2011) A reversible form of axon damage in experimental autoimmune encephalomyelitis and multiple sclerosis. Nat Med. 17(4):495-9.
- Nitsch R., Pohl E.E., Smorodchenko A., Infante-Duarte C., Aktas O. and Zipp F. (2004) Direct impact of T cells on neurons revealed by two-photon microscopy in living brain tissue. J Neurosci. 24(10):2458-64.

- van Noort J.M., van Sechel A.C., Bajramovic J.J., el Ouagmiri M., Polman C.H., Lassmann H. and Ravid R. (1995) The small heat-shock protein alpha B-crystallin as candidate autoantigen in multiple sclerosis. Nature 375(6534):798-801.
- van Noort J.M., Bsibsi M., Gerritsen W.H., van der Valk P., Bajramovic J.J., Steinman L. and Amor S. (2010) Alphab-crystallin is a target for adaptive immune responses and a trigger of innate responses in preactive multiple sclerosis lesions. J Neuropathol Exp Neurol. 69(7):694-703.
- van Noort J.M. (2013) Autoimmunity in multiple sclerosis need not be abnormal. Mult Scler. 20(8):1030-1032.
- Noseworthy J.H., Lucchinetti C., Rodriguez M. and Weinshenker B.G. (2000) Multiple sclerosis. N Engl J Med. 343(13):938-52.
- O'Brien E.T., Salmon E.D. and Erickson H.P. (1997). How calcium causes microtubule depolymerization. Cell Motil. Cystoskeleton 36,125–135.
- O'Connor K.C., Appel H., Bregoli L., Call M.E., Catz I., Chan J.A., Moore N.H., Warren K.G., Wong S.J., Hafler D.A. and Wucherpfennig KW. (2005) Antibodies from inflamed central nervous system tissue recognize myelin oligodendrocyte glycoprotein. J Immunol. 175(3):1974-82.
- O'Gorman C., Lucas R. and Taylor B. (2012) Environmental risk factors for multiple sclerosis: a review with a focus on molecular mechanisms. Int J Mol Sci. 13(9):11718-52.
- Odeberg J., Piao J.H., Samuelsson E.B., Falci S. and Akesson E. (2005) Low immunogenicity of in vitro-expanded human neural cells despite high MHC expression. J Neuroimmunol. 161(1-2):1-11.
- Ogawa Y., Schafer D.P., Horresh I., Bar V., Hales K., Yang Y., Susuki K., Peles E., Stankewich M.C. and Rasband M.N. (2006) Spectrins and ankyrinB constitute a specialized paranodal cytoskeleton. J Neurosci. 26(19):5230-9.
- Okonkwo D.O., Büki A., Siman R. and Povlishock J.T. (1999) Cyclosporin A limits calcium-induced axonal damage following traumatic brain injury. Neuroreport. 10(2):353-8.
- Okuda D.T., Mowry E.M., Beheshtian A., Waubant E., Baranzini S.E., Goodin D.S., Hauser S.L. and Pelletier D. (2009) Incidental MRI anomalies suggestive of multiple sclerosis: the radiologically isolated syndrome. Neurology 72(9):800-5.
- Oluich L.J., Stratton J.A., Xing Y.L., Ng S.W., Cate H.S., Sah P., Windels F., Kilpatrick T.J. and Merson T.D. (2012) Targeted ablation of oligodendrocytes induces axonal pathology independent of overt demyelination. J Neurosci. 32(24):8317-30.
- Onofrj M., Bodis-Wollner I. and Bobak P. (1982) Pattern visual evoked potentials in the rat. Physiol Behav. 28(2):227-30.

- Optic Neuritis Study Group (1991) The clinical profile of optic neuritis. Experience of the Optic Neuritis Treatment Trial. Arch Ophthalmol. 109(12):1673.
- Optic Neuritis Study Group (2008) Multiple sclerosis risk after optic neuritis: final optic neuritis treatment trial follow-up. Arch Neurol. 65(6):727-32.
- Owens T., Bechmann I. and Engelhardt B. (2008) Perivascular spaces and the two steps to neuroinflammation. J Neuropathol Exp Neurol. 67(12):1113-21.
- Owens G.P., Bennett J.L., Lassmann H., O'Connor K.C., Ritchie A.M., Shearer A., Lam C., Yu X., Birlea M., DuPree C., Williamson R.A., Hafler D.A., Burgoon M.P. and Gilden D. (2009) Antibodies produced by clonally expanded plasma cells in multiple sclerosis cerebrospinal fluid. Ann Neurol. 65(6):639-49.
- Ozawa K., Suchanek G., Breitschopf H., Brück W., Budka H., Jellinger K. and Lassmann H. (1994) Patterns of oligodendroglia pathology in multiple sclerosis. Brain 117 (Pt 6):1311-22.
- Pacher P, Beckman JS and Liaudet L. (2007) Nitric oxide and peroxynitrite in health and disease. Physiol Rev. 87(1):315-424.
- Pant H.C. (1988) Dephosphorylation of neurofilament proteins enhances their susceptibility to degradation by calpain. Biochem J. 256(2):665-8.
- Pantano P., Mainero C. and Caramia F. (2006) Functional brain reorganization in multiple sclerosis: evidence from fMRI studies. J Neuroimaging. 16(2):104-14.
- Paterson P.Y. (1960) Transfer of allergic encephalomyelitis in rats by means of lymph node cells. J Exp Med. 111:119-36.
- Paty D.W. and Li D.K. (1993) Interferon beta-1b is effective in relapsing-remitting multiple sclerosis. II. MRI analysis results of a multicenter, randomized, double-blind, placebo-controlled trial. UBC MS/MRI Study Group and the IFNB Multiple Sclerosis Study Group. Neurology 43(4):662-7.
- Paul C and Bolton C. (2002) Modulation of blood-brain barrier dysfunction and neurological deficits during acute experimental allergic encephalomyelitis by the N-methyl-D-aspartate receptor antagonist memantine. J Pharmacol Exp Ther. 302(1):50-7.
- Pearce J.M.S., (2005) Historical descriptions of multiple sclerosis. Eur Neurol. 54:49-53.
- Peles E., Nativ M., Lustig M., Grumet M., Schilling J., Martinez R., Plowman G.D. and Schlessinger J. (1997) Identification of a novel contactin-associated transmembrane receptor with multiple domains implicated in protein-protein interactions. EMBO J. 16, pp. 978–988.
- Petereit H.F., Moeller-Hartmann W., Reske D. and Rubbert A. (2008) Rituximab in a patient with multiple sclerosis--effect on B cells, plasma cells and intrathecal IgG synthesis. Acta Neurol Scand. 117(6):399-403.

- Peterson J.W., Bö L., Mörk S., Chang A. and Trapp B.D. (2001) Transected neurites, apoptotic neurons, and reduced inflammation in cortical multiple sclerosis lesions. Ann Neurol. 50(3):389-400.
- Petzold A., Gveric D., Groves M., Schmierer K., Grant D., Chapman M., Keir G., Cuzner L. and Thompson E.J. (2008) Phosphorylation and compactness of neurofilaments in multiple sclerosis: indicators of axonal pathology. Exp Neurol. 213(2):326-35.
- Pillai A.M., Thaxton C., Pribisko A.L., Cheng J.G., Dupree J.L. and Bhat M.A. (2009) Spatiotemporal ablation of myelinating glia-specific neurofascin (Nfasc NF155) in mice reveals gradual loss of paranodal axoglial junctions and concomitant disorganization of axonal domains. J Neurosci Res. 87(8):1773-93.
- Pitt D., Werner P. and Raine C.S. (2000) Glutamate excitotoxicity in a model of multiple sclerosis. Nat Med. 6(1):67-70.
- Poliak S., Gollan L., Martinez R., Custer A., Einheber S., Salzer J.L., Trimmer J.S., Shrager P. and Peles E. (1999) Caspr2, a new member of the neurexin superfamily, is localized at the juxtaparanodes of myelinated axons and associates with K+ channels. Neuron 24, pp. 1037–1047.
- Poliak S., Gollan L., Salomon D., Berglund E.O., Ohara R., Ranscht B. and Peles E. (2001) Localization of Caspr2 in myelinated nerves depends on axon-glia interactions and the generation of barriers along the axon. J. Neurosci. 21, pp. 7568–7575.
- Poliak S., Salomon D., Elhanany H., Sabanay H., Kiernan B., Pevny L., Stewart C.L., Xu X., Chiu S.-Y., Shrager P., Furley A.J. and Peles E. (2003) Juxtaparanodal clustering of Shaker-like K+ channels in myelinated axons depends on Caspr2 and TAG-1. J. Cell Biol. 162, pp. 1149–1160.
- Polman C.H., Reingold S.C., Banwell B., Clanet M., Cohen J.A., Filippi M., Fujihara K., Havrdova E., Hutchinson M., Kappos L., Lublin F.D., Montalban X., O'Connor P., Sandberg-Wollheim M., Thompson A.J., Waubant E., Weinshenker B. and Wolinsky J.S. (2011) Diagnostic criteria for multiple sclerosis: 2010 revisions to the McDonald criteria. Ann Neurol. 69(2):292-302.
- Popescu B.F., Bunyan R.F., Parisi J.E., Ransohoff R.M. and Lucchinetti C.F. (2011) A case of multiple sclerosis presenting with inflammatory cortical demyelination. Neurology 76(20):1705-10.
- Porciatti V. Pizzorusso T. and Maffei L. (1999) The visual physiology of the wild type mouse determined with pattern VEPs. Vision Res. 39(18):3071-81.
- Pöllinger B., Krishnamoorthy G., Berer K., Lassmann H., Bösl M.R., Dunn R., Domingues H.S., Holz A., Kurschus F.C. and Wekerle H. (2009) Spontaneous relapsing-remitting EAE in the SJL/J mouse: MOG-reactive transgenic T cells recruit endogenous MOG-specific B cells. J Exp Med. 206(6):1303-16.

- Praet J., Guglielmetti C., Berneman Z., Van der Linden A. and Ponsaerts P. (2014) Cellular and molecular neuropathology of the cuprizone mouse model: clinical relevance for multiple sclerosis. Neurosci Biobehav Rev. 47:485-505.
- Prinz M. (2014) Microglia and monocytes: molecularly defined. Acta Neuropathol. 128(3):317-8.
- Pugliatti M., Sotgiu S. and Rosati G. (2002) The worldwide prevalence of multiple sclerosis. Clin Neurol Neurosurg. 104(3):182-91.
- Pulicken M., Gordon-Lipkin E., Balcer L.J., Frohman E., Cutter G. and Calabresi P.A. (2007) Optical coherence tomography and disease subtype in multiple sclerosis. Neurology 69(22):2085-92.
- Redford E.J., Kapoor R. and Smith K.J. (1997) Nitric oxide donors reversibly block axonal conduction: demyelinated axons are especially susceptible. Brain 120 (Pt 12):2149-57.
- Reeves T.M., Greer J.E., Vanderveer A.S. and Phillips L.L. (2010) Proteolysis of submembrane cytoskeletal proteins ankyrin-G and αII-spectrin following diffuse brain injury: a role in white matter vulnerability at Nodes of Ranvier. Brain Pathol. 20(6):1055-68.
- Ridder W.H. 3rd and Nusinowitz S. (2006) The visual evoked potential in the mouse--origins and response characteristics. Vision Res. 46(6-7):902-13. Epub 2005 Oct 20.
- Rios J.C., Rubin M., St Martin M., Downey R.T., Einheber S., Rosenbluth J., Levinson S.R., Bhat M. and Salzer J.L. (2003) Paranodal interactions regulate expression of sodium channel subtypes and provide a diffusion barrier for the node of Ranvier. J Neurosci. 23(18):7001-11.
- Rhodes K.J., Strassle B.W., Monaghan M.M., Bekele-Arcuri A., Matos M.F. and Trimmer J.S. (1997) Association and colocalization of the Kvß1 and Kvß2 β-subunits with Kv1 α-subunits in mammalian brain K+ channels complexes. J. Neurosci. 17, pp. 8246–8258.
- Rodriguez M. (1995) Virus-induced demyelination in mice: "dying back" of oligodendrocytes. Mayo Clin Proc. 60(7):433-8.
- Ruuls S.R., Bauer J., Sontrop K., Huitinga I., 't Hart B.A. and Dijkstra C.D. (1995) Reactive oxygen species are involved in the pathogenesis of experimental allergic encephalomyelitis in Lewis rats. J Neuroimmunol. 56(2):207-17.
- Saadoun S., Waters P., Owens G.P., Bennett J.L., Vincent A. and Papadopoulos M.C. (2014) Neuromyelitis optica MOG-IgG causes reversible lesions in mouse brain. Acta Neuropathol Commun. 2:35.
- Saidha S., Syc S.B., Ibrahim M.A., Eckstein C., Warner C.V., Farrell S.K., Oakley J.D., Durbin M.K., Meyer S.A., Balcer L.J., Frohman E.M., Rosenzweig J.M., Newsome S.D., Ratchford J.N., Nguyen Q.D. and Calabresi P.A. (2011) Primary retinal pathology in multiple sclerosis as detected by optical coherence tomography. Brain 134(Pt 2):518-33.

- Salzer J.L. (2003) Polarized domains of myelinated axons. Neuron. 40(2):297-318.
- Sanders E.A., Reulen J.P., Hogenhuis L.A. and van der Velde EA. (1985) Electrophysiological disorders in multiple sclerosis and optic neuritis. Can J Neurol Sci. 12(4):308-13.
- Sánchez I, Hassinger L, Paskevich PA, Shine HD and Nixon RA. (1996) Oligodendroglia regulate the regional expansion of axon caliber and local accumulation of neurofilaments during development independently of myelin formation. J Neurosci. 16(16):5095-105.
- Sättler M.B., Merkler D., Maier K., Stadelmann C., Ehrenreich H., Bähr M. and Diem R. (2004) Neuroprotective effects and intracellular signaling pathways of erythropoietin in a rat model of multiple sclerosis. Cell Death Differ. 11 Suppl 2:S181-92.
- Sawcer S., International Multiple Sclerosis Genetics Consortium, Wellcome Trust Case Control Consortium. (2011) Genetic risk and a primary role for cell-mediated immune mechanisms in multiple sclerosis. Nature 476(7359):214-9.
- Schafer D.P., Jha S., Liu F., Akella T., McCullough L.D. and Rasband M.N. (2009) Disruption of the axon initial segment cytoskeleton is a new mechanism for neuronal injury. J Neurosci. 29(42):13242-54.
- Selmaj K., Raine C.S. and Cross A.H. (1991) Anti-tumor necrosis factor therapy abrogates autoimmune demyelination. Ann Neurol. 30(5):694-700.
- Selmaj K., Walczak A., Mycko M., Berkowicz T., Kohno T. and Raine CS. (1998) Suppression of experimental autoimmune encephalomyelitis with a TNF binding protein (TNFbp) correlates with down-regulation of VCAM-1/VLA-4. Eur J Immunol. 28(6):2035-44.
- Serafini B., Rosicarelli B., Magliozzi R., Stigliano E. and Aloisi F. (2004) Detection of ectopic B-cell follicles with germinal centers in the meninges of patients with secondary progressive multiple sclerosis. Brain Pathol. 14(2):164-74.
- Schattling B., Steinbach K., Thies E., Kruse M., Menigoz A., Ufer F., Flockerzi V., Brück W., Pongs O., Vennekens R., Kneussel M., Freichel M., Merkler D. and Friese MA. (2012) TRPM4 cation channel mediates axonal and neuronal degeneration in experimental autoimmune encephalomyelitis and multiple sclerosis. Nat Med. 18(12):1805-11.
- Schirmer L., Antel J.P., Brück W. and Stadelmann C. (2011) Axonal loss and neurofilament phosphorylation changes accompany lesion development and clinical progression in multiple sclerosis. Brain Pathol. 21(4):428-40.
- Schori H., Kipnis J., Yoles E., WoldeMussie E., Ruiz G., Wheeler L.A. and Schwartz, M. (2001) Vaccination for protection of retinal ganglion cells against death from glutamate cytotoxicity and ocular hypertension: Implications for glaucoma. Proc. Natl. Acad. Sci. U.S.A. 98, 3398–3403.

- Sharief M.K. and Hentges R. (1991) Association between tumor necrosis factor-alpha and disease progression in patients with multiple sclerosis. N Engl J Med. 325(7):467-72.
- Sharma R., Narayana P.A. and Wolinsky J.S. (2001) Grey matter abnormalities in multiple sclerosis: proton magnetic resonance spectroscopic imaging. Mult. Scler. 7:221–26.
- Sherman D.L., Tait S., Melrose S., Johnson R., Zonta B., Court F.A., Macklin W.B., Meek S., Smith A.J., Cottrell D.F. and Brophy P.J. (2005) Neurofascins are required to establish axonal domains for saltatory conduction. Neuron 48(5):737-42.
- Sherman D.L. and Brophy P.J. (2005) Mechanisms of axon ensheathment and myelin growth. Nat Rev Neurosci. 6:683-90.
- Shields D.C., Schaecher K.E., Saido T.C. and Banik N.L. (1999) A putative mechanism of demyelination in multiple sclerosis by a proteolytic enzyme, calpain. Proc Natl Acad Sci U S A. 96(20):11486-91.
- Siffrin V., Radbruch H., Glumm R., Niesner R., Paterka M., Herpez J., Leuenberger T., Lehmann S.M., Luenstedt S., Rinnenthal J.L., Laube G., Luche H., Lehnardt S., Fehling H.J., Griesbeck O. and Zipp F. (2010) In vivo imaging of partially reversible th17 cell-induced neuronal dysfunction in the course of encephalomyelitis. Immunity. 24;33(3):424-36.
- Simone De R., Giampaolo A., Giometto B., Gallo P., Levi G., Peschle C. and Aloisi F. (1995) The costimulatory molecule B7 is expressed on human microglia in culture and in multiple sclerosis acute lesions. J Neuropathol Exp Neurol. 54(2):175-87.
- Simons M and Nave K.A. (2015) Oligodendrocytes: Myelination and Axonal Support. Cold Spring Harb Perspect Biol. pii: a020479.
- Sinclair C., Mirakhur M., Kirk J., Farrell M. and McQuaid S. (2005) Up-regulation of osteopontin and alphaBeta-crystallin in the normal-appearing white matter of multiple sclerosis: an immunohistochemical study utilizing tissue microarrays. Neuropathol Appl Neurobiol. 31(3):292-303.
- Singh S, Metz I, Amor S, van der Valk P, Stadelmann C and Brück W. (2013) Microglial nodules in early multiple sclerosis white matter are associated with degenerating axons. Acta Neuropathol. 125(4):595-608.
- Sisk D.R. and Kuwabara T. (1985) Histologic changes in the inner retina of albino rats following intravitreal injection of monosodium L-glutamate. Graefes Arch Clin Exp Ophthalmol. 223(5):250-8.
- Sisto D., Trojano M., Vetrugno M., Trabucco T., Iliceto G. and Sborgia C. (2005) Subclinical visual involvement in multiple sclerosis: a study by MRI, VEPs, frequency-doubling perimetry, standard perimetry, and contrast sensitivity. Invest Ophthalmol Vis Sci. 46(4):1264-8.

- Smith K.J., Kapoor R, Hall SM and Davies M. (2001) Electrically active axons degenerate when exposed to nitric oxide. Ann Neurol. 49(4):470-6.
- Sobel R.A., Mitchell M.E. and Fondren G. (1990) Intercellular adhesion molecule-1 (ICAM-1) in cellular immune reactions in the human central nervous system. Am J Pathol. 136(6):1309-16
- Soilu-Hänninen M., Airas L., Mononen I., Heikkilä A., Viljanen M. and Hänninen A. (2005) 25-Hydroxyvitamin D levels in serum at the onset of multiple sclerosis. Mult Scler. 11(3):266-71.
- Srinivasan R, Sailasuta N, Hurd R, Nelson S and Pelletier D. (2005) Evidence of elevated glutamate in multiple sclerosis using magnetic resonance spectroscopy at 3 T. Brain 128(Pt 5):1016-25.
- Steinman L. (2007) A brief history of T(H)17, the first major revision in the T(H)1/T(H)2 hypothesis of T cell-mediated tissue damage. Nat Med. 13(2):139-45.
- Staal J.A., Dickson T.C., Gasperini R., Liu Y., Foa L. and Vickers JC. (2010) Initial calcium release from intracellular stores followed by calcium dysregulation is linked to secondary axotomy following transient axonal stretch injury. J Neurochem. 112(5):1147-55.
- Stashenko P., Nadler L.M., Hardy R. and Schlossman S.F. (1980) Characterization of a human B lymphocyte-specific antigen. J Immunol. 125(4):1678-85.
- Stefferl A., Brehm U., Storch M., Lambracht-Washington D., Bourquin C., Wonigeit K., Lassmann H. and Linington C. (1999) Myelin oligodendrocyte glycoprotein induces experimental autoimmune encephalomyelitis in the "resistant" Brown Norway rat: disease susceptibility is determined by MHC and MHC-linked effects on the B cell response. J Immunol. 163(1):40-9.
- Storch M.K., Stefferl A., Brehm U., Weissert R., Wallström E., Kerschensteiner M., Olsson T., Linington C. and Lassmann H. (1998) Autoimmunity to myelin oligodendrocyte glycoprotein in rats mimics the spectrum of multiple sclerosis pathology. Brain Pathol. 8(4):681-94.
- Stüve O., Marra C.M., Jerome K.R., Cook L., Cravens P.D., Cepok S., Frohman E.M., Phillips J.T., Arendt G., Hemmer B., Monson N.L. and Racke M.K. (2006) Immune surveillance in multiple sclerosis patients treated with natalizumab. Ann Neurol. 59(5):743-7.
- Stys P.K., Lehning E., Saubermann A.J. and LoPachin RM Jr. (1997) Intracellular concentrations of major ions in rat myelinated axons and glia: calculations based on electron probe X-ray microanalyses. J Neurochem. 68(5):1920-8.
- Stys P.K. (2004) White matter injury mechanisms. Curr Mol Med. 4(2):113-30.
- Sundqvist E., Sundström P., Lindén M., Hedström A.K., Aloisi F., Hillert J., Kockum I., Alfredsson L. and Olsson T. (2012) Epstein-Barr virus and multiple sclerosis: interaction with HLA. Genes Immun. 13(1):14-20.

- Sun S.W., Liang H.F., Trinkaus K., Cross A.H., Armstrong R.C. and Song S.K. (2006) Noninvasive detection of cuprizone induced axonal damage and demyelination in the mouse corpus callosum. Magn Reson Med. 55(2):302-8.
- Sun W., Fu Y., Shi Y., Cheng J.X., Cao P. and Shi R. (2012) Paranodal myelin damage after acute stretch in Guinea pig spinal cord. J Neurotrauma. 2012 Feb 10;29(3):611-9.
- Sühs K.W., Fairless R., Williams S.K., Heine K., Cavalié A. and Diem R. (2014) N-methyl-D-aspartate receptor blockade is neuroprotective in experimental autoimmune optic neuritis. J Neuropathol Exp Neurol. 73(6):507-18.
- Tait S., Gunn-Moore F., Collinson J.M., Huang J., Lubetzki C., Pedraza L., Sherman D.L., Colman D.R. and Brophy P.J. (2000) An oligodendrocyte cell adhesion molecule at the site of assembly of the paranodal axo-glial junction. J. Cell Biol. 150, pp. 657–666.
- Tanaka T., Takeda M., Niigawa H., Hariguchi S. and Nishimura T. (1993) Phosphorylated neurofilament accumulation in neuronal perikarya by cyclosporin A injection in rat brain. Methods Find Exp Clin Pharmacol. 15(2):77-87.
- Tekkök S.B. and Goldberg M.P. (2001) Ampa/kainate receptor activation mediates hypoxic oligodendrocyte death and axonal injury in cerebral white matter. J Neurosci. 21(12):4237-48.
- Toosy A.T., Mason D.F. and Miller D.H. (2014) Optic neuritis. Lancet Neurol. 13(1):83-99.
- Traka M., Goutebroze L., Denisenko N., Nifli A., Havaki S., Iwakura Y., Fukamauchi F., Watanabe K., Soliven B., Girault J.A. and Karagogeos D. (2003) Association of TAG-1 with Caspr2 is essential for the molecular organization of juxtaparanodal regions of myelinated fibers. J. Cell Biol. 162, pp. 1161–1172.
- Trapp B.D., Peterson J., Ransohoff R.M., Rudick R., Mörk S. and Bö L. (1998) Axonal transection in the lesions of multiple sclerosis. N Engl J Med. 338(5):278-85.
- Trapp B.D., Ransohoff R. and Rudick R. (1999) Axonal pathology in multiple sclerosis: relationship to neurologic disability. Curr Opin Neurol. 12(3):295-302.
- Trapp B.D. and Kidd G.J. (2000) Axo-glial septate junctions. The maestro of nodal formation and myelination? J Cell Biol. 150(3):F97-F100.
- Trapp B.D. and Nave K.A. (2008) Multiple sclerosis: an immune or neurodegenerative disorder? Annu Rev Neurosci. 31:247-69.
- Trapp B.D. and Stys P.K. (2009) Virtual hypoxia and chronic necrosis of demyelinated axons in multiple sclerosis. Lancet Neurol. 8(3):280-91.
- Tremlett H., Paty D. and Devonshire V. (2005) The natural history of primary progressive MS in British Columbia, Canada. Neurology 65(12):1919-23.

- Trip S.A., Schlottmann P.G., Jones S.J., Altmann D.R., Garway-Heath D.F., Thompson A.J., Plant G.T. and Miller D.H. (2005) Retinal nerve fiber layer axonal loss and visual dysfunction in optic neuritis. Ann Neurol. 58(3):383-91.
- Tso M.O., Shih C.Y. and McLean I.W. (1975) Is there a blood-brain barrier at the optic nerve head? Arch Ophthalmol 93:815– 825.
- van der Valk P. and Amor S. (2009) Preactive lesions in multiple sclerosis. Curr Opin Neurol. 22(3):207-13.
- Vartanian T., Li Y., Zhao M. and Stefansson K. (1995) Interferon-gamma-induced oligodendrocyte cell death: implications for the pathogenesis of multiple sclerosis. Mol Med. 1(7):732-43.
- Vercellino M., Plano F., Votta B., Mutani R., Giordana M.T. and Cavalla P. (2005) Grey matter pathology in multiple sclerosis. J Neuropathol Exp Neurol. 64(12):1101-7.
- Vercellino M., Merola A., Piacentino C., Votta B., Capello E., Mancardi G.L., Mutani R., Giordana M.T. and Cavalla P. (2007) Altered glutamate reuptake in relapsing-remitting and secondary progressive multiple sclerosis cortex: correlation with microglia infiltration, demyelination, and neuronal and synaptic damage. J Neuropathol Exp Neurol. 66(8):732-9.
- Vercellino M., Masera S., Lorenzatti M., Condello C., Merola A., Mattioda A., Tribolo A., Capello E., Mancardi G.L., Mutani R., Giordana M.T. and Cavalla P. (2009) Demyelination, inflammation, and neurodegeneration in multiple sclerosis deep grey matter. J Neuropathol Exp Neurol. 68(5):489-502.
- Vergo S., Craner M.J., Etzensperger R., Attfield K., Friese M.A., Newcombe J., Esiri M. and Fugger L. (2011) Acid-sensing ion channel 1 is involved in both axonal injury and demyelination in multiple sclerosis and its animal model. Brain 134(Pt 2):571-84.
- Vladimirova O., O'Connor J., Cahill A., Alder H., Butunoi C. and Kalman B. (1998) Oxidative damage to DNA in plaques of MS brains. Mult Scler. 4(5):413-8.
- Vogt J., Paul F., Aktas O., Müller-Wielsch K., Dörr J., Dörr S., Bharathi B.S., Glumm R., Schmitz C., Steinbusch H., Raine C.S., Tsokos M., Nitsch R. and Zipp F. (2009) Lower motor neuron loss in multiple sclerosis and experimental autoimmune encephalomyelitis. Ann Neurol. 66(3):310-22.
- Wallström E., Diener P., Ljungdahl A., Khademi M., Nilsson C.G. and Olsson T. (1996) Memantine abrogates neurological deficits, but not CNS inflammation, in Lewis rat experimental autoimmune encephalomyelitis. J Neurol Sci. 137(2):89-96.
- Warren K.G. and Catz I. (1993) Autoantibodies to myelin basic protein within multiple sclerosis central nervous system tissue. J Neurol Sci. 115(2):169-76

- Washington R., Burton J., Todd R.F. 3rd, Newman W., Dragovic L. and Dore-Duffy P. (1994) Expression of immunologically relevant endothelial cell activation antigens on isolated central nervous system microvessels from patients with multiple sclerosis. Ann Neurol. 35(1):89-97.
- Waxman S.G., Black J.A., Stys P.K. and Ransom B.R. (1992) Ultrastructural concomitants of anoxic injury and early post-anoxic recovery in rat optic nerve. Brain Res. 574(1-2):105-19.
- Waxman S.G., Black J.A., Ransom B.R. and Stys P.K. (1994) Anoxic injury of rat optic nerve: ultrastructural evidence for coupling between Na+ influx and Ca(2+)-mediated injury in myelinated CNS axons. Brain Res. 644(2):197-204.
- Webb M., Tham C.S., Lin F.F., Lariosa-Willingham K., Yu N., Hale J., Mandala S., Chun J. and Rao T.S. (2004) Sphingosine 1-phosphate receptor agonists attenuate relapsing-remitting experimental autoimmune encephalitis in SJL mice. J Neuroimmunol. 153(1-2):108-21.
- Werner P., Pitt D. and Raine C.S. (2001) Multiple sclerosis: altered glutamate homeostasis in lesions correlates with oligodendrocyte and axonal damage. Ann Neurol. (2):169-80.
- Wikström J., Poser S. and Ritter G. (1980) Optic neuritis as an initial symptom in multiple sclerosis. Acta Neurol Scand. 61(3):178-85.
- Williams S.K., Fairless R., Weise J., Kalinke U., Schulz-Schaeffer W. and Diem R. (2011) Neuroprotective effects of the cellular prion protein in autoimmune optic neuritis. Am J Pathol. 178(6):2823-31. doi: 10.1016/j.ajpath.2011.02.046.
- Williams S.K., Maier O., Fischer R., Fairless R., Hochmeister S., Stojic A., Pick L., Haar D., Musiol S., Storch M.K., Pfizenmaier K. and Diem R. (2014) Antibody-mediated inhibition of TNFR1 attenuates disease in a mouse model of multiple sclerosis. PLoS One 9(2):e90117.
- Wolswijk G. and Balesar R. (2003) Changes in the expression and localization of the paranodal protein Caspr on axons in chronic multiple sclerosis. Brain 126(Pt 7):1638-49.
- World Health Organization (2008) Atlas: Multiple Sclerosis Resources in the World
- Yang Y., Lacas-Gervais S., Morest D.K., Solimena M. and Rasband M.N. (2004) BetaIV spectrins are essential for membrane stability and the molecular organization of nodes of Ranvier. J Neurosci. 24(33):7230-40.
- Ye ZC, Wyeth MS, Baltan-Tekkok S and Ransom BR. (2003) Functional hemichannels in astrocytes: a novel mechanism of glutamate release. J Neurosci. 23(9):3588-96.
- Yednock T.A., Cannon C., Fritz L.C., Sanchez-Madrid F., Steinman L. and Karin N. (1992) Prevention of experimental autoimmune encephalomyelitis by antibodies against alpha 4 beta 1 integrin. Nature 356(6364):63-6.

- Yermolaieva O., Leonard A.S., Schnizler M.K., Abboud F.M. and Welsh M.J. (2004) Extracellular acidosis increases neuronal cell calcium by activating acid-sensing ion channel 1a. Proc Natl Acad Sci U S A. 101(17):6752-7.
- Yin X, Crawford TO, Griffin JW, Tu Ph, Lee VM, Li C, Roder J and Trapp BD. (1998) Myelin-associated glycoprotein is a myelin signal that modulates the caliber of myelinated axons. J Neurosci. 18(6):1953-62.
- You Y., Klistorner A., Thie J. and Graham S.L. (2011) Latency delay of visual evoked potential is a real measurement of demyelination in a rat model of optic neuritis. Invest Ophthalmol Vis Sci. 52(9):6911-8.
- You Y., Klistorner A., Thie J., Gupta V.K. and Graham S.L. (2012) Axonal loss in a rat model of optic neuritis is closely correlated with visual evoked potential amplitudes using electroencephalogram-based scaling. Invest Ophthalmol Vis Sci. 53(7):3662.
- Youl B.D., Turano G., Miller D.H., Towell A.D., MacManus D.G., Moore S.G., Jones S.J., Barrett G., Kendall B.E., Moseley I.F., et al. (1991) The pathophysiology of acute optic neuritis. An association of gadolinium leakage with clinical and electrophysiological deficits. Brain. 114 (Pt 6):2437-50.
- Yu F.H. and Catterall W.A. (2003) Overview of the voltage-gated sodium channel family. Genome Biol. 4, p. 207.
- Zabel C., Sagi D., Kaindl A.M., Steireif N., Kläre Y., Mao L., Peters H., Wacker M.A., Kleene R. and Klose J. (2006) Comparative proteomics in neurodegenerative and non-neurodegenerative diseases suggest nodal point proteins in regulatory networking. J Proteome Res. 5(8):1948-58.
- Zeis T., Graumann U., Reynolds R. and Schaeren-Wiemers N. (2008) Normal-appearing white matter in multiple sclerosis is in a subtle balance between inflammation and neuroprotection. Brain 131(Pt 1):288-303.
- Zeis T., Probst A., Steck A.J., Stadelmann C., Brück W. and Schaeren-Wiemers N. (2009) Molecular changes in white matter adjacent to an active demyelinating lesion in early multiple sclerosis. Brain Pathol. 19(3):459-66.
- Zhou D., Srivastava R., Nessler S., Grummel V., Sommer N., Brück W., Hartung H.P., Stadelmann C. and Hemmer B. (2006) Identification of a pathogenic antibody response to native myelin oligodendrocyte glycoprotein in multiple sclerosis. Proc Natl Acad Sci U S A 103(50):19057-62.
- Zhou R.H., Yan H., Wang B.R., Kuang F., Duan X.L. and Xu Z. (2007) Role of extracellular signal-regulated kinase in glutamate-stimulated apoptosis of rat retinal ganglion cells. Curr Eye Res. 32(3):233-9.

- Zonta B., Desmazieres A., Rinaldi A., Tait S., Sherman D.L., Nolan M.F. and Brophy P.J. (2011) A critical role for Neurofascin in regulating action potential initiation through maintenance of the axon initial segment. Neuron 69(5):945-56.
- Zozulya A.L. and Wiendl H. (2008) The role of regulatory T cells in multiple sclerosis. Nat Clin Pract Neurol. 4(7):384-98.

Abbreviations

AIS	Axon initial segment
AMPA	α-amino-3-hydroxy-5-methyl-4-isoxazolepropionic acid
ANOVA	Analysis of variance
AON	Autoimmune optic neuritis
AP	Action potential
APP	Amyloid precursor protein
ASIC	Acid-sensing ion channels
ATP	Adenosine triphosphate
BBB	Blood-brain barrier
BCA	Bicinchoninic acid
bFGF	Basic fibroblast growth factor
BN	Brown Norway
BRB	Blood-retinal barrier
BSA	Bovine serum albumin
CAM	Cellular adhesion molecules
Ca_V	Voltage-gated calcium channels
CD	Cluster of differentiation
CDMS	Clinically definite multiple sclerosis
CFA	Complete Freund's adjuvant
CIS	Clinically isolated syndrome
CNPase	2',3'-cyclic-nucleotide 3'-phosphodiesterase
CNS	Central nervous system
CNTF	Ciliary neurotrophic factor
CRT	Cathode ray tube
CryαB	Alpha-B crystallin
CSF	Cerebrospinal fluid
DAPI	4',6-diamidino-2-phenylindole
DMSO	Dimethyl sulfoxide
DNA	Deoxyribonucleic acid
DT	Diphtheria toxin
dUTP	Deoxyuridine triphosphate
EAE	Experimental autoimmune encephalomyelitis
EAN	Experimental allergic neuritis

EBV	Epstein-Barr virus
ELISA	Enzyme-linked immunosorbent assay
FCS	Fetal calf serum
FeTPPS	5,10,15,20-Tetrakis(4-sulfonatophenyl)porphyrinato Iron (III), Chloride
GAPDH	Glyceraldehyde-3-Phosphate Dehydrogenase
GFAP	Glial fibrillary acidic protein
HLA	Human leukocyte antigen
HRP	Horseradish peroxidase
i.p.	Intraperitoneal
IgG	Immunoglobulin G
INFγ	Interferon gamma
iNOS	Inducible nitric oxide synthase
K_V	Voltage-gated potassium channels
LED	Light-emitting diode
LFB	Luxol fast blue
LGN	Lateral geniculate nucleus
MAG	Myelin-associated glycoprotein
MBP	Myelin basic protein
MG2	Neural/glial antigen 2
MHC	Major Histocompatibility complex
MOG	Myelin oligodendrocyte glycoprotein
MRI	Magnetic resonance imaging
MS	Multiple sclerosis
Na_V	Voltage-gated sodium channels
NAWM	Normal-appearing white matter
NCX	Sodium-calcium exchanger
NF	Neurofilament
NGS	Normal goat serum
NMDA	N-Methyl-D-aspartate
nNOS	Neuronal nitric oxide synthase
NO	Nitric oxide
npNF	Non-phosphorylated neurofilaments
NRS	Normal rabbit serum
OCT	Optical coherence tomography
ONH	Optic nerve head

OPC	Oligodendrocyte progenitor cell
PBN	N-tert-butyl-α-phenylnitrone
PBS	Phosphate-buffered saline
PBS-T	Phosphate-buffered saline - Tween 20
PBS-Tr	Phosphate-buffered saline – Triton X-100
PDGF	Platelet-derived growth factor
PFA	Paraformaldehyde
PLL	Poly-L-lysine
PLP	Proteolipid protein
PPMS	Primary-progressive multiple sclerosis
PRMS	Primary-relapsing multiple sclerosis
pst	Post serum transfer
PVDF	Polyvinylidene fluoride
RGC	Retinal ganglion cells
RNFL	Retinal nerve fiber layer
RNS	Reactive nitrogen species
ROS	Reactive oxygen species
RPMI	Roswell Park Memorial Institute
RRMS	Relapsing-remitting multiple sclerosis
RT	Room temperature
SD	Sprague Dawley
SDS-PAGE	Sodium dodecyl sulfate polyacrylamide gel electrophoresis
SPMS	Secondary-progressive multiple sclerosis
T3	Triiodothyronine
TBS	Tris-buffered saline
TBS-T	Tris-buffered saline – Tween 20
TBS-Tr	Tris-buffered saline – Triton x-100
TCR	T cell receptor
TdT	Terminal deoxynucleotidyl transferase
TMB	3,3’,5,5’-Tetramethylbenzidine
TNFα	Tumor necrosis factor alpha
TRP	Transient receptor potential
TUNEL	Terminal deoxynucleotidyl transferase dUTP nick end labeling
VEP	Visual evoked potential